Palladium(II) Complex Bearing a Pyrazolyl-1,2,3-Triazolyl Hybrid Ligand for C-H Bond Activation Toward N-Substituted Carbazole Synthesis

Rishi Raj, Bhawana Shekhawat, Rinkle Agarwal, Puneet Singh Gahlaut, Sumitra Saini, Abhineet Verma and Barun Jana*

Supporting Information

Contents

1. General Information

All the solvents (DMSO, Acetone, Methanol and N,N-Dimethylformamide) used in the synthesis of [bppp] alkyne, [bbppmt] ligand (L1), Pd(II) complex and catalytic reactions were purified *via* distillation under an argon atmosphere, and were stored over 4Å molecular sieves. All other reagents and chemicals were purchased from commercially available sources and were used without further purification. Analytical TLC test was performed using a Merck 60 F254 silica gel plate of 0.25 mm thickness. Column chromatographic separation was performed using Merck 60 silica gel of 230-400 mesh. For drying and concentrating all the solvents, DLAB Rotavapor RE-100-S was used. UV/vis absorption measurements were conducted at room temperature on a SHIMADZU UV-19000l UV/vis spectrophotometer. The melting point of ligand and complex were determined on an analog melting point apparatus. IR spectra were recorded on a FTIR-03130 Shimadzu Spectrophotometer. Fluorescence spectra were recorded on RF-6000 Shimadzu Fluorophotometer. The NMR spectra were collected in JEOL ECS-400 (400 MHz) spectrometer using tetramethyl silane (TMS) as the internal

reference. Q-TOF mass spectrometer (serial no. YA 263) was used for HRMS analysis. All the catalytic reactions were performed under ambient atmosphere. Benzyl azide was synthesized following a literature procedure.[1]

2. Synthesis and characterization data of ligand (L1) and catalyst ($L1PdCl_2PdCl_2$)

Synthesis of 5-benzyl-3-phenyl-1H-pyrazole

Firstly, dimer of ethynylbenzene was synthesized from ethynylbenzene and used as the precursor for the synthesis of 3,5-disubstituted pyrazole, following the procedure reported in literature.[2] A reaction flask was charged with ethynylbenzene (0.6 mmol), CuI (5 mol%, 5.7 mg), and DMSO (3.0 mL). The reaction mixture was stirred on magnetic stirrer at 90 °C for 8 hours and then was cooled to room temperature. The reaction mixture was worked up, and the product was extracted with ethyl acetate (10 mL × 3). The combined organic layers were washed with brine (10 mL × 2) and dried over anhydrous Na_2SO_4. The solvent was removed under reduced pressure and the residue obtained was purified *via* silica gel chromatography (eluent: hexane, yield).

In the second step, 3,5-disubstituted pyrazole was synthesized from the obtained 1,4-diphenylbuta-1,3-diyne *via* a Cope-type hydroamination, following the reported literature procedure.[2] In a 25 mL round-bottom flask, 1,4-diphenylbuta-1,3-diyne (0.4 mmol) and aqueous hydrazine solution (50 wt%, 3.0 equiv., 76.9 mg) were mixed in 3.0 mL of DMSO. The reaction mixture was sealed and stirred at 60 °C for 20 hours and then was cooled to room temperature. Water (10 mL) was added to the resultant mixture. The product was extracted with ethyl acetate (10 mL × 3), and the combined organic layers were washed with brine (10 mL × 2) and dried over Na_2SO_4. The solvent was removed under reduced pressure, and the residue obtained was purified *via* silica gel chromatography (eluent: hexane/ethyl acetate = 80:20, yield) to afford 5-benzyl-3-phenyl-1H-pyrazole.

Synthesis of 5-benzyl-3-phenyl-1-(prop-2-yn-1-yl)-1H-pyrazole [bppp]

After successful preparation of 3,5-disubstituted pyrazole, the ligand precursor [bppp] was synthesized. A reaction flask was charged with 5-benzyl-3-phenyl-1H-pyrazole (0.5 mmol), K_2CO_3 (345.5 mg, 2.5 mmol), and acetone (2 mL). The mixture was stirred at room temperature for 10 minutes, after which propargyl bromide (1.5 mmol) was added dropwise. The reaction was then allowed to stir at room temperature for 16 hours. The reaction mixture was worked up and the product was extracted with ethyl acetate (10 mL × 3) and dried over Na_2SO_4. The solvent was removed under reduced pressure, and the residue obtained was purified *via* silica gel chromatography (eluent: hexane/ethyl acetate = 96:4, yield). ^{1}H NMR (400 MHz, CHLOROFORM-*D*) δ 7.71 – 7.66 (m, 2H), 7.29 – 7.24 (m, 3H), 7.23 – 7.14 (m, 5H), 6.25 (s, 1H), 4.72 (d, *J* = 2.4 Hz, 2H), 4.04 (s, 2H), 2.31 (t, *J* = 2.4 Hz, 1H). ^{13}C NMR (101 MHz, CHLOROFORM-*D*) δ 149.7, 141.7, 136.0, 127.8, 127.7, 127.6, 127.6, 127.5, 127.5, 127.4, 126.6, 125.9, 124.5, 124.5, 103.2, 72.7, 38.5, 30.8. IR υ_{max}.(cm^{-1}):2127(m, C≡C strech), 3280(s, C_{sp}–H stretch).

Synthesis of 1-benzyl-4-((5-benzyl-3-phenyl-1H-pyrazol-1-yl)methyl)-1H-1,2,3-triazole [bbppmt] (L1)

In a reaction flask, bppp (0.2 mmol) and $Cu(OAc)_2$ (5 mol%) were dissolved in methanol and stirred for 10 minutes at room temperature. Subsequently, benzyl azide (0.21 mmol) was added drop-wise with continuous stirring. The resulting mixture was then stirred at room temperature for 24 hours.To the reaction mixture, 20 mL of water was added, and the product was extracted with ethyl acetate and dried over Na_2SO_4. The solvent was removed under reduced pressure, and the residue obtained was purified *via* silica gel chromatography (eluent: hexane/ethyl acetate = 80:20 to 75:25, yield). ^{1}H NMR (400 MHz, DMSO-D_6) δ 7.95 (s, 1H), 7.74 – 7.70 (m, 2H), 7.38 – 7.21 (m, 13H), 6.42 (s, 1H), 5.54 (s, 2H), 5.38 (s, 2H), 4.16 (s, 2H). ^{13}C NMR (101 MHz, DMSO-D_6) δ 149.2, 143.4, 143.4, 138.0, 136.0, 133.3, 128.8, 128.7, 128.6, 128.2, 128.0, 127.4, 126.5, 125.0, 123.6, 103.0, 52.8, 44.5, 31.0. IR υ_{max}.(cm^{-1}): 1550 (m, N=N stretch), 3118 (w, triazole C_{sp2}–H stretch). HRMS (ESI$^+$) *m/z* calculated for $C_{26}H_{24}N_5^+$ [M+H$^+$] = 406.2026; found 406.1671. m.p: 98-100 °C.

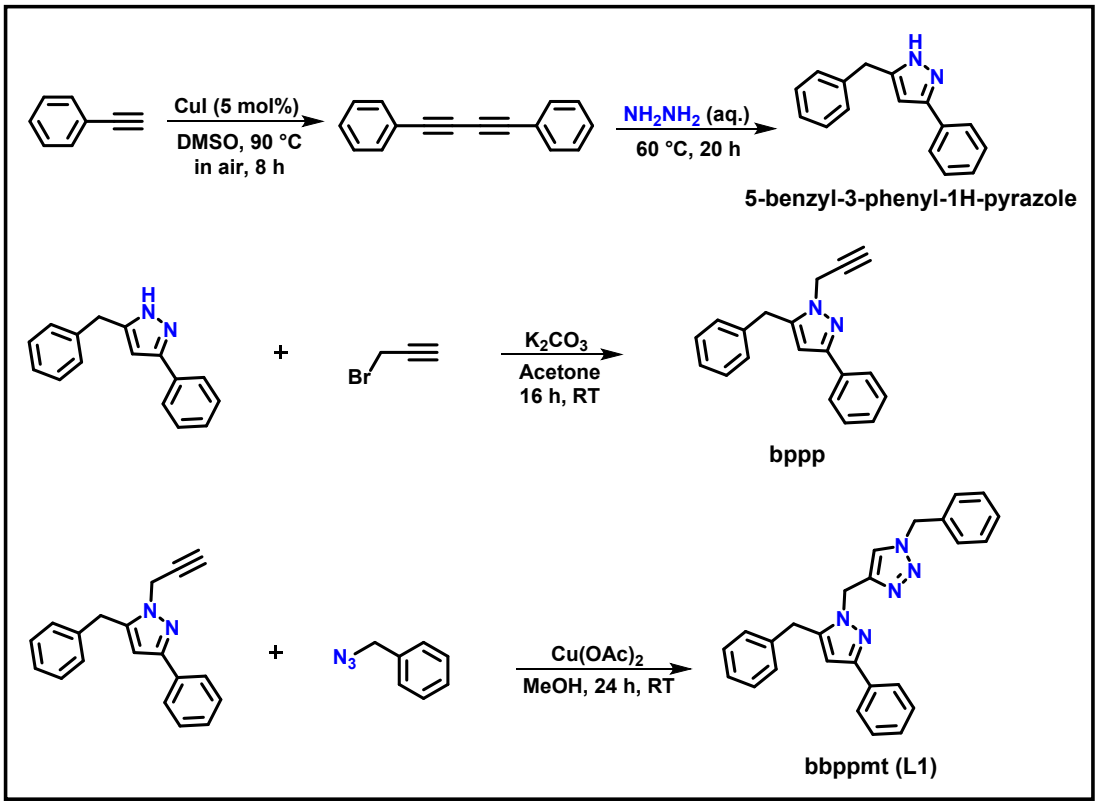

Scheme S1: The step-wise synthesis of ligand [bbppmt] (L1)

Synthesis of L1$PdCl_2PdCl_2$ complex

In a 25 mL round-bottom flask, ligand L1 (0.25 mmol) was dissolved in 3 mL of chloroform at room temperature. To this solution, $Pd(CH_3CN)_2Cl_2$ (2.0 equiv) was added, and the reaction mixture was stirred at room temperature for 1 hour. Upon completion of the reaction, a pale yellow precipitate formed, which was filtered and washed twice with chloroform to remove any remaining ligand. The solid product was then dried

and collected. Analytically pure compound was obtained as a pale yellow solid in 87% yield (Scheme S1). Initially, the complexation reaction was performed using an equimolar ratio (1:1) of ligand L1 and $Pd(CH_3CN)_2Cl_2$; however, this condition resulted in incomplete conversion of the ligand and a low isolated yield. Consequently, the metal-to-ligand ratio was increased to 1:2. Single crystals suitable for X-ray diffraction analysis were obtained by slow vapour diffusion of methanol into a DMSO solution of the complex at low temperature (in a refrigerator). ^{1}H NMR (400 MHz, DMSO-D_6) δ 8.79 – 8.05 (m, 1H), 7.98 – 7.64 (m, 2H), 7.51 – 7.11 (m, 13H), 6.62 – 6.35 (m, 1H), 6.21 – 5.35 (m, 4H), 4.42 – 3.86 (m, 2H). ^{13}C NMR (101 MHz, DMSO-D_6) δ 153.6, 147.9, 139.2, 135.5, 134.1, 129.4, 129.1, 128.9, 128.9, 128.8, 128.6, 128.5, 128.4, 128.0, 127.2, 126.6, 126.2, 125.0, 106.9, 55.4, 44.4, 42.5, 31.0, 30.7. IR υ_{max}.(cm^{-1}): 1547 (m, N=N stretch), 3094 (w, triazole C_{sp2}–H stretch). HRMS (ESI^+) *m/z* calculated for $C_{26}H_{23}ClN_5Pd^+$ $[L1PdCl]^+$ = 546.0671; found 546.0676. m.p: 220-225 °C.

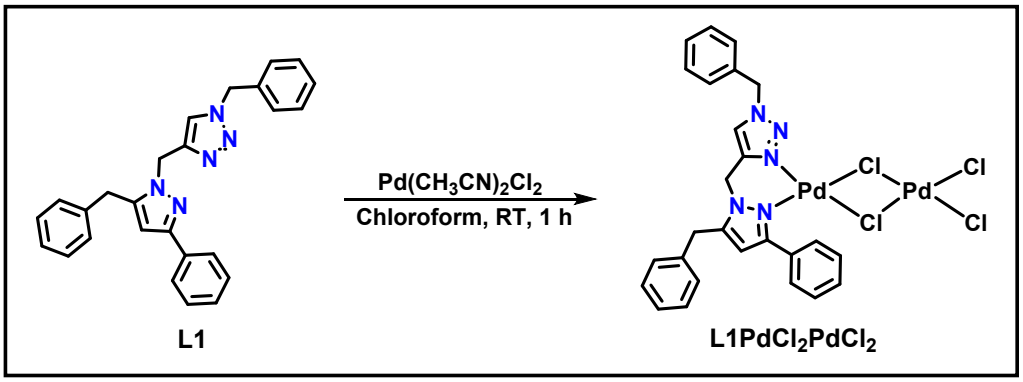

Scheme S2: Synthesis of $L1PdCl_2PdCl_2$ complex

Characterization of alkyne, ligand and Pd-complex

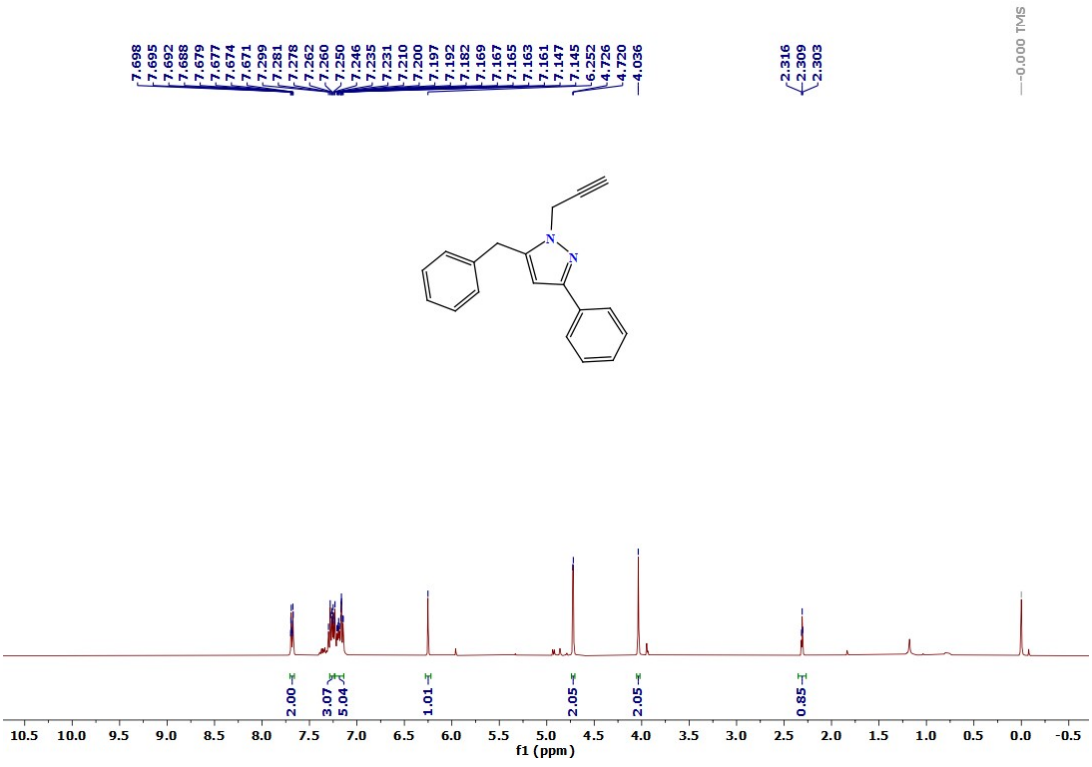

Fig S3: ^{1}H-NMR Spectrum of **bppp** in $CDCl_3$ (400 MHz)

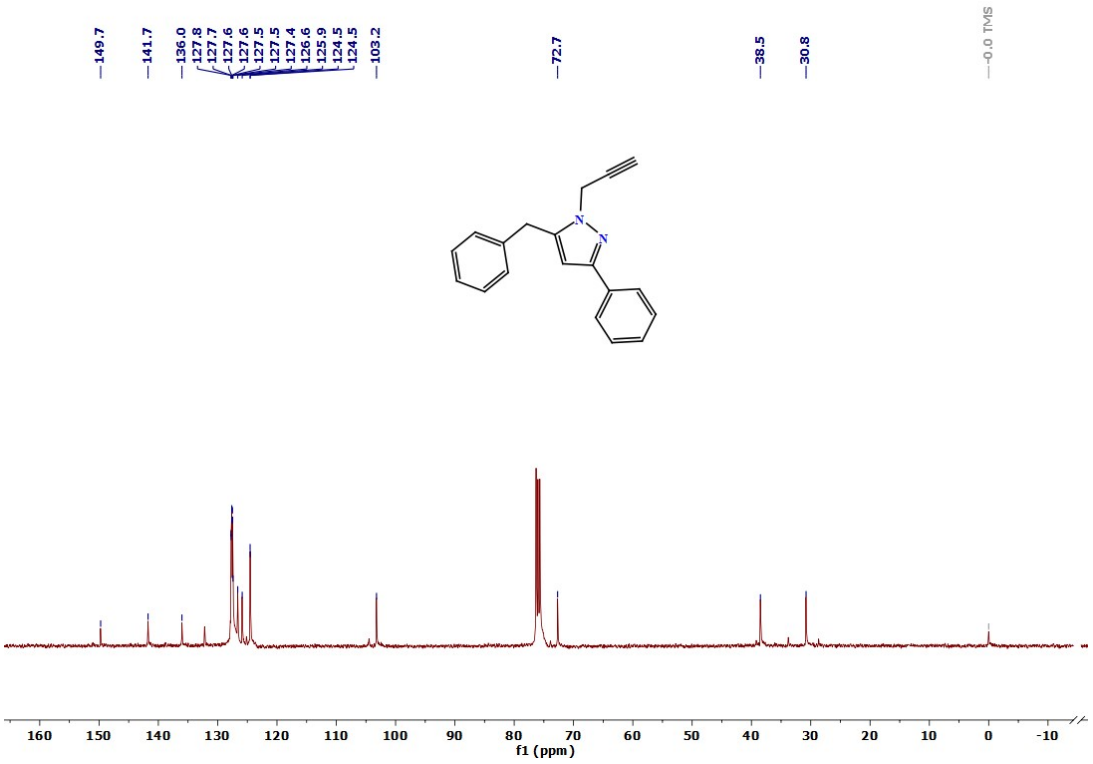

Fig S4: $^{13}C\{^{1}H\}$ NMR Spectrum of **bppp** in $CDCl_3$(101MHz)

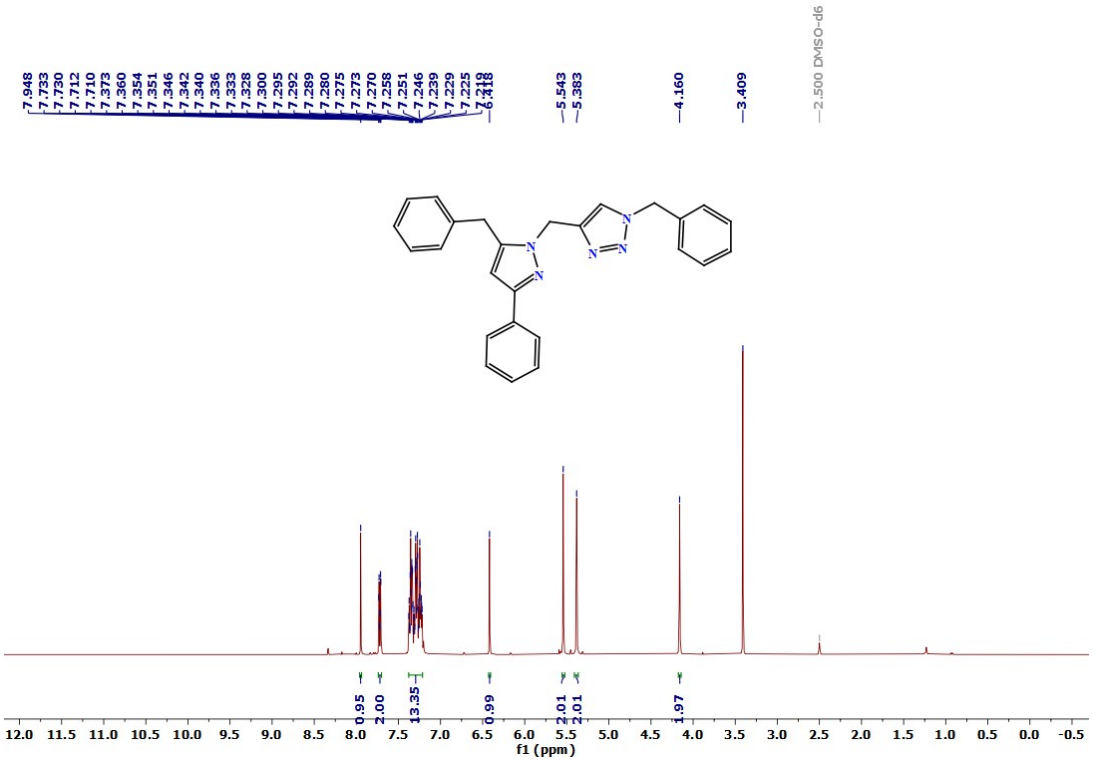

Fig S5: ^{1}H-NMR Spectrum of **L1** in DMSO-D_6 (400 MHz)

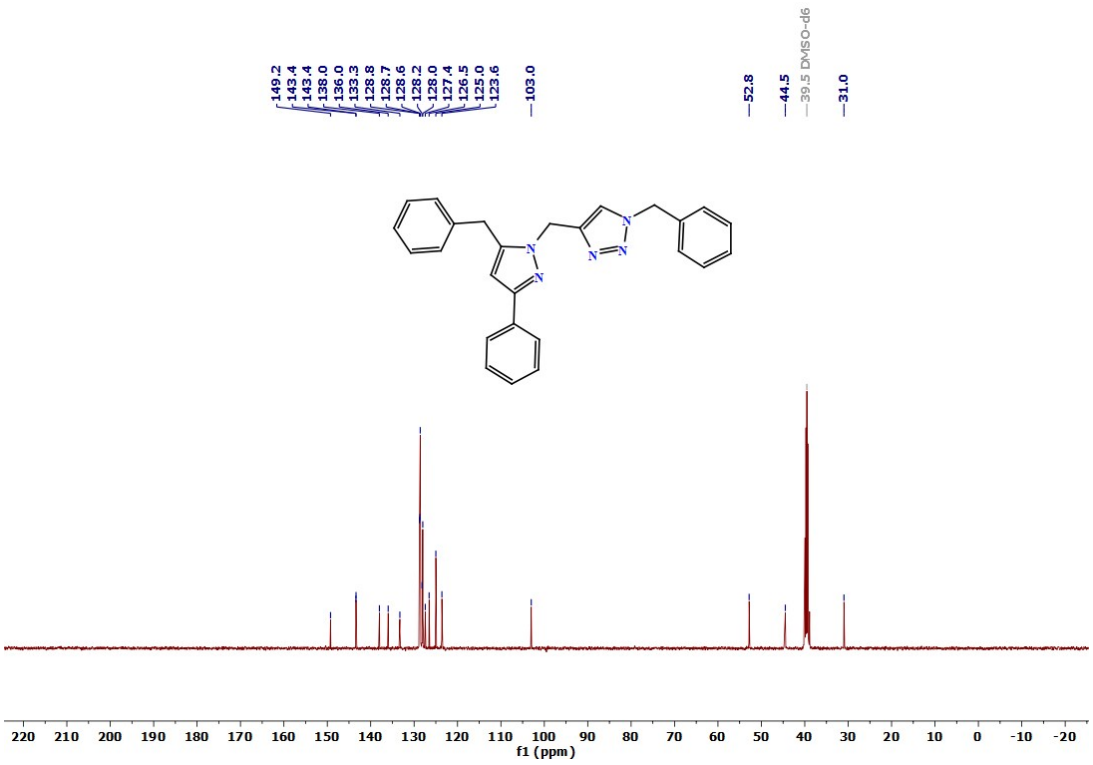

Fig S6: $^{13}C\{^{1}H\}$ NMR Spectrum of **L1** in DMSO-D_6 (101 MHz)

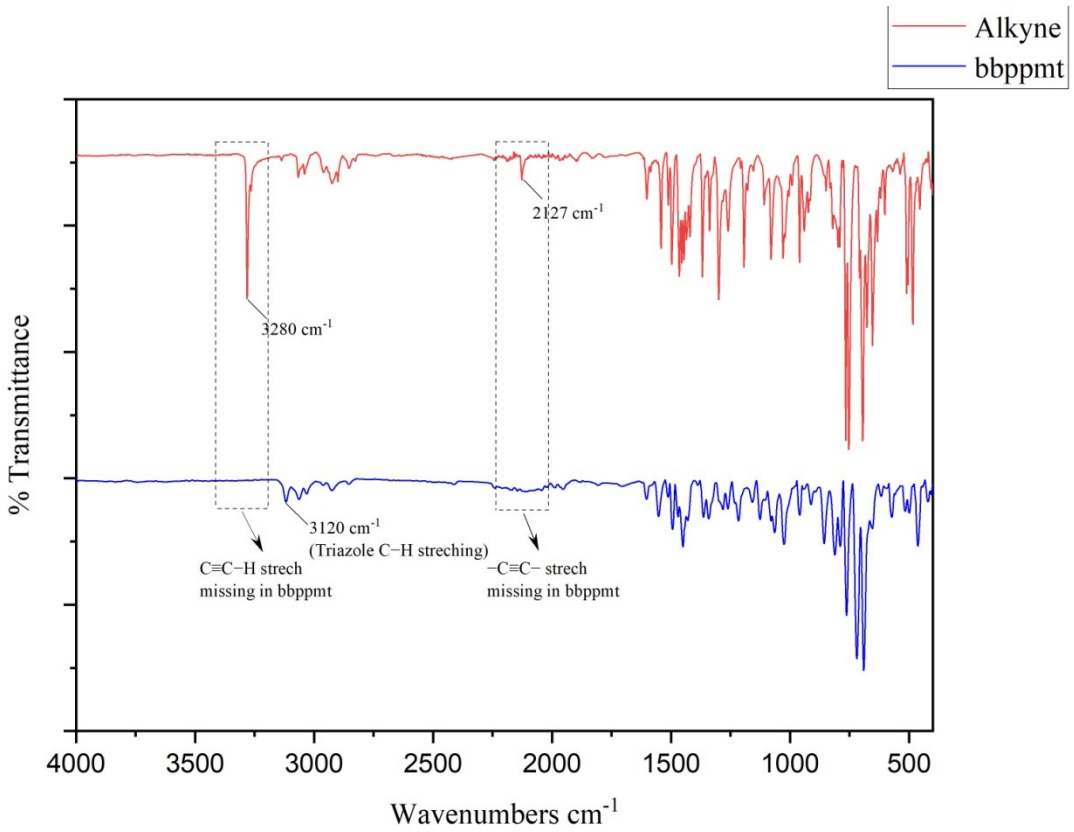

Fig S7: FT-IR data comparison between alkyne **bppp** and Ligand **L1**

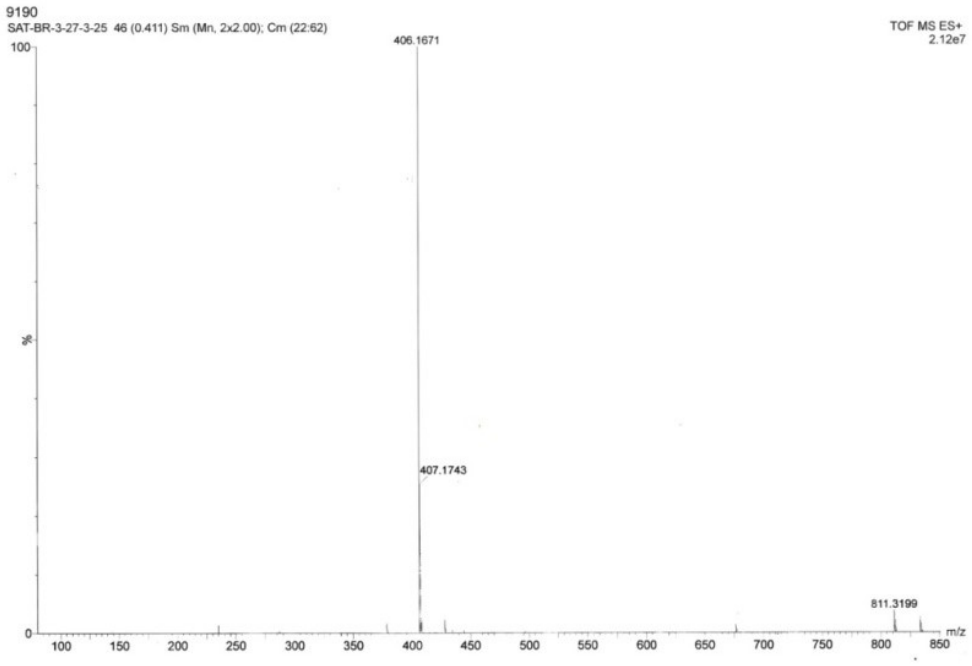

Fig S8: HRMS (ESI$^+$) of ligand **L1** showing $[M+H]^+$ molecular ion peak.

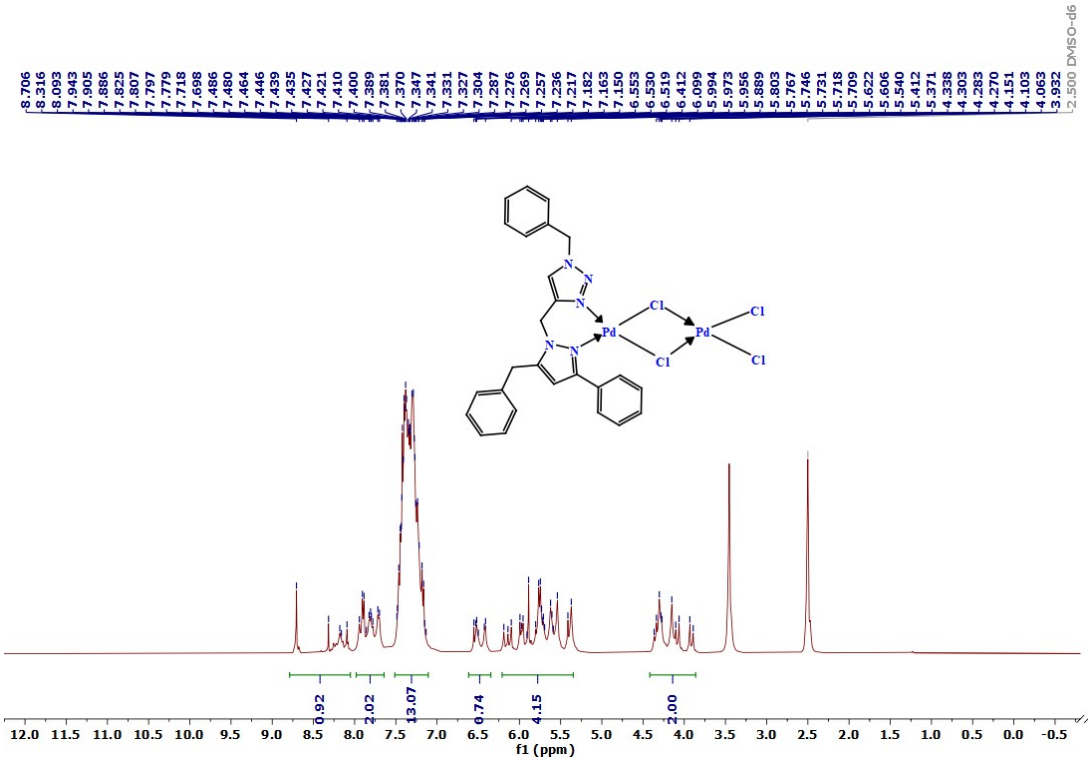

Fig S9: ^{1}H-NMR Spectrum of **L1PdCl$_2$PdCl$_2$** in DMSO-D_6 (400 MHz)

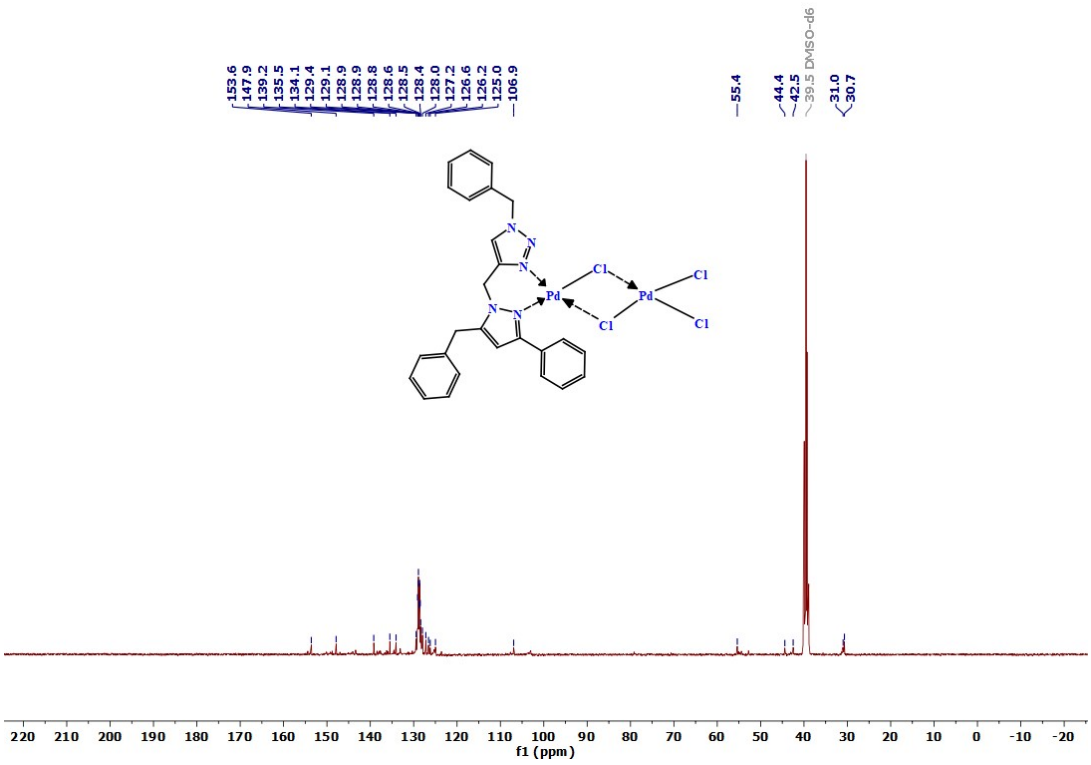

Fig S10: $^{13}C\{^{1}H\}$ NMR Spectrum of **L1PdCl$_2$PdCl$_2$** in DMSO-D_6 (101 MHz)

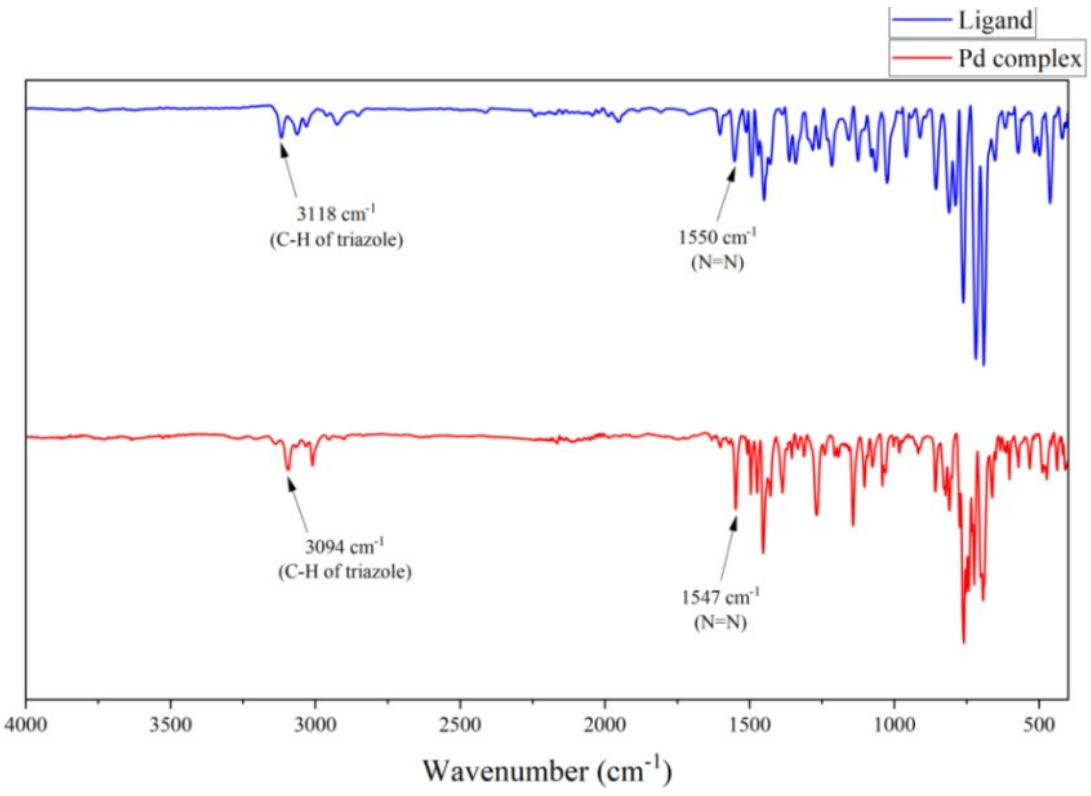

Fig S11: FT-IR data comparison between ligand **L1** and **L1PdCl$_2$PdCl$_2$** complex

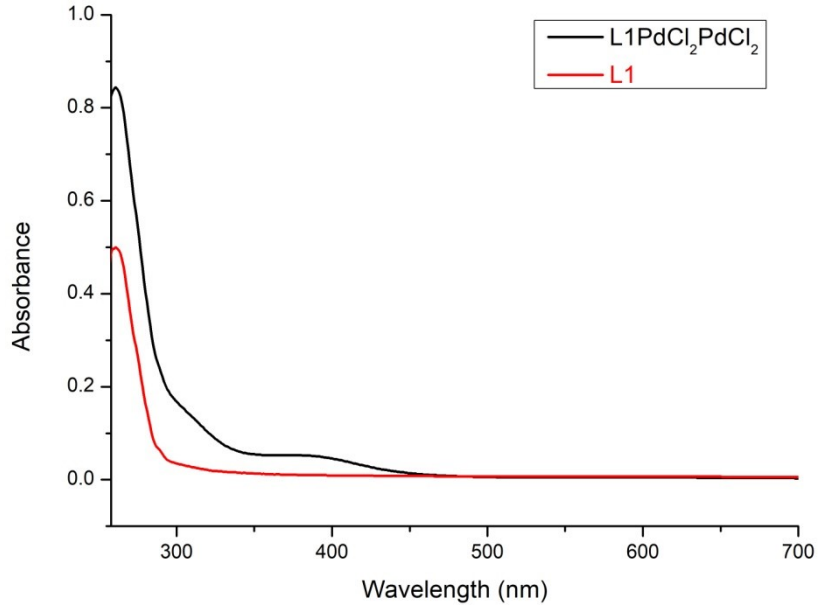

Fig S12: UV-vis data comparison between ligand **L1** and **L1PdCl$_2$PdCl$_2$** complex

In UV-visible absorption spectra, the Pd complex exhibits a higher absorption intensity at 262 nm with molar absorptivity (ε) of 3.38×10^4 L·mol^{-1}·cm^{-1}, compared to the free ligand with ε value of 2.00×10^4 L·mol^{-1}·cm^{-1} at the same concentration (2.5×10^{-5} M). The enhanced molar absorptivity, together with the appearance of a new broad absorption band at longer wavelengths, is consistent with coordination of the ligand to the Pd center and the associated modification of its electronic structure.

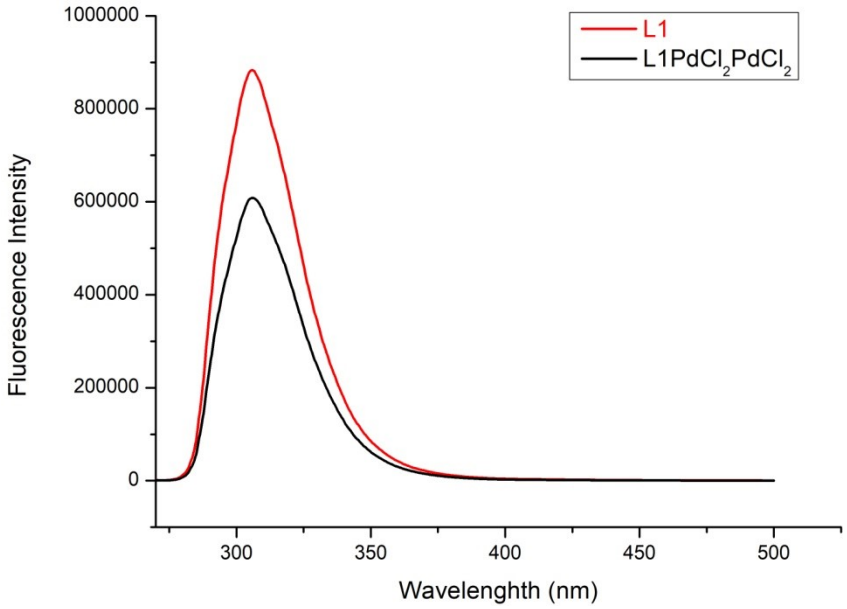

Fig S13: Fluorescence data comparison between ligand **L1** and **L1PdCl$_2$PdCl$_2$** complex with excitation at 262 nm

The fluorescence emission properties of the free ligand and its Pd complex were investigated under identical experimental conditions at a concentration of 2.5 × 10^{-5} M. Upon excitation at 262 nm, the free ligand exhibited a strong emission band centered at 305.76 nm. In contrast, the corresponding Pd complex displayed a markedly reduced emission intensity under the same conditions. Quantitatively, the emission intensity decreased from 8.84 × 10^5 for the ligand to 6.07 × 10^5 for the Pd complex, corresponding to approximately 31% fluorescence quenching. This emission suppression is attributed to enhanced non-radiative decay pathways induced by coordination to the Pd(II) center, likely arising from heavy-atom effects and metal-ligand electronic interactions.

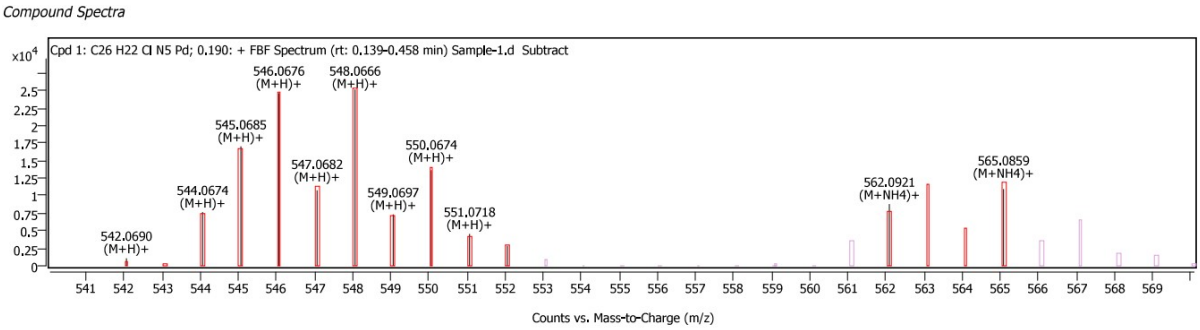

Fig S14: HRMS (ESI⁺) of **L1PdCl$_2$PdCl$_2$** complex showing [L1PdCl]⁺ molecular ion peak

3. Crystallographic information of catalyst

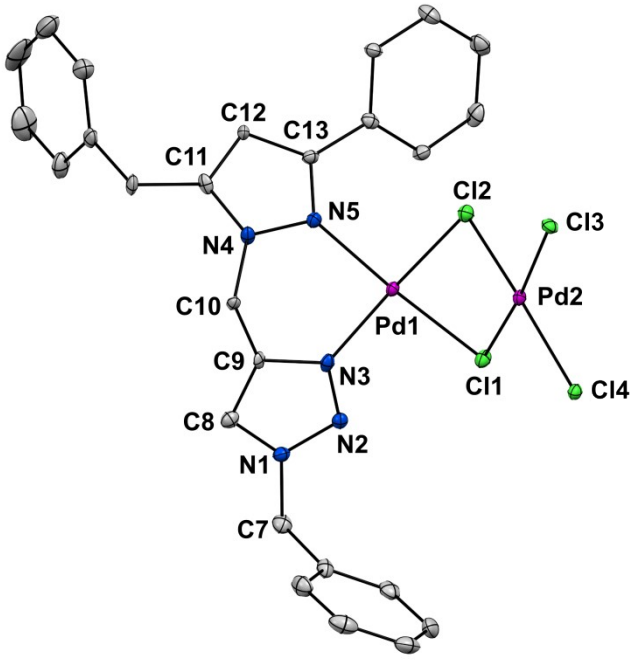

Fig S15: Solid-state molecular structure of **Pd-complex**. Thermal ellipsoids were drawn with 30% probability. All the hydrogen atoms are omitted for the clarity in the molecular structure.

Table 1: Crystal data and structure refinement for **Pd-complex**

Identification code	17julc_0m_a
Empirical formula	$C_{26}H_{23}Cl_4N_5Pd_2$
Formula weight	760.147
Temperature/K	273.15
Crystal system	orthorhombic
Space group	$P2_12_12_1$
a/Å	10.8998(6)
b/Å	12.2746(7)
c/Å	22.4806(13)
α/°	90
β/°	90
γ/°	90
Volume/Å^3	3007.7(3)
Z	4
ρ_{calc}g/cm^3	1.679
μ/mm^{-1}	1.576
F(000)	1491.1
Crystal size/mm^3	0.2 × 0.2 × 0.1
Radiation	Mo Kα (λ = 0.71073)
2Θ range for data collection/°	6.18 to 56.66
Index ranges	-14 ≤ h ≤ 14, -16 ≤ k ≤ 16, -29 ≤ l ≤ 30
Reflections collected	49407
Independent reflections	7470 [R_{int} = 0.0479, R_{sigma} = 0.0300]
Data/restraints/parameters	7470/0/335

Goodness-of-fit on F^2	1.012
Final R indexes [I>=2σ (I)]	R_1 = 0.0341, wR_2 = 0.0931
Final R indexes [all data]	R_1 = 0.0352, wR_2 = 0.0937
Largest diff. peak/hole / e $Å^{-3}$	2.20/-0.61
Flack parameter	-0.031(11)
CCDC number	2524634

Table 2: Selected bond lengths (Å) and bond angles (˚) in the molecular structure of **Pd-complex**

Bond lengths (Å)		**Bond angles (˚)**	
Pd1-Cl8	2.2865(11)	Cl6-Pd1-Cl8	173.50(4)
Pd1-Cl6	2.3656(10)	Cl1-Pd1-Cl8	94.36(4)
Pd1-Cl1	2.3577(10)	Cl1-Pd1-Cl6	91.89(4)
Pd1-Cl7	2.2791(11)	Cl7-Pd1-Cl8	80.35(4)
Pd2-Cl8	2.2889(11)	Cl7-Pd1-Cl6	93.46(4)
Pd2-Cl7	2.2733(10)	Cl7-Pd1-Cl1	174.50(4)
Pd2-N5	2.026(4)	Cl7-Pd2-Cl8	80.42(4)
Pd2-N10	2.088(4)	N5-Pd2-Cl8	171.11(10)
		N5-Pd2-Cl7	96.13(10)
		N10-Pd2-Cl8	96.86(11)
		N10-Pd2-Cl7	176.33(10)
		N10-Pd2-N5	86.91(14)

4. General procedure for the assembly of N-substituted carbazoles

Table 3: Optimization of reaction conditions

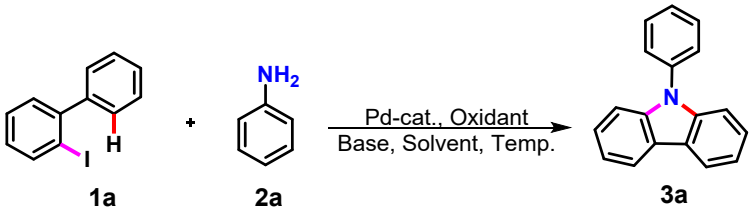

1a **2a** **3a**

Entry [a]	Catalyst (mol %)	Oxidant (equiv.)	Base	Solvent	Temperature (°C)	% Yield [b]
1	Pd-cat. (10)	$Cu(OAc)_2$ (1)	K_2CO_3	DMF	120	85
2	Pd-cat.(5)	$Cu(OAc)_2$ (1)	K_2CO_3	DMF	120	85
3	Pd-cat. (2.5)	$Cu(OAc)_2$ (1)	K_2CO_3	DMF	120	43
4	-	$Cu(OAc)_2$ (1)	K_2CO_3	DMF	120	N.R.
5	$PdCl_2$ (5)	$Cu(OAc)_2$ (1)	K_2CO_3	DMF	120	Trace
6	$Pd(OAc)_2$ (5)	$Cu(OAc)_2$ (1)	K_2CO_3	DMF	120	33
7	$Pd(CH_3CN)_2Cl_2$ (5)	$Cu(OAc)_2$ (1)	K_2CO_3	DMF	120	37
8	Pd-cat.(5)	Ag_2O (1)	K_2CO_3	DMF	120	N.R.
9	Pd-cat. (5)	AgOAc (1)	K_2CO_3	DMF	120	N.R.
10	Pd-cat. (5)	$CuSO_4$(1)	K_2CO_3	DMF	120	Trace
11	Pd-cat. (5)	$Cu(OAc)_2$(0.5)	K_2CO_3	DMF	120	34
12	Pd-cat. (5)	$Cu(OAc)_2$ (1)	$NaHCO_3$	DMF	120	25
13	Pd-cat. (5)	$Cu(OAc)_2$ (1)	K_3PO_4	DMF	120	39
14	Pd-cat. (5)	$Cu(OAc)_2$ (1)	Cs_2CO_3	DMF	120	93
15	Pd-cat. (5)	$Cu(OAc)_2$ (1)	-	DMF	120	N.R.
16	Pd-cat. (5)	$Cu(OAc)_2$ (1)	Cs_2CO_3	1,4-Dioxane	120	N.R.
17	Pd-cat. (5)	$Cu(OAc)_2$ (1)	Cs_2CO_3	CH_3CN	120	N.R.
18	Pd-cat. (5)	$Cu(OAc)_2$ (1)	Cs_2CO_3	DMSO	120	N.R.
19	Pd-cat. (5)	$Cu(OAc)_2$ (1)	Cs_2CO_3	Toluene	120	N.R.
20	Pd-cat. (5)	$Cu(OAc)_2$ (1)	Cs_2CO_3	DMF	R.T.	N.R.
21	Pd-cat. (5)	$Cu(OAc)_2$ (1)	Cs_2CO_3	DMF	110	59
22	Pd-cat. (5)	$Cu(OAc)_2$ (1)	Cs_2CO_3	DMF	130	93

[a] Reaction conditions **1a** (0.35 mmol), **2a** (1.2 equiv., 0.42 mmol), 5 mol % Pd-cat., 1.0 equiv. oxidant, 1.0 equiv. base, 2 mL solvent, 120 °C, air, 12 h. [b] The isolated yield of **3a**.

General procedure for the assembly of N-substituted carbazoles using 2-iodobiphenyls and amine/benzenesulfonamide derivatives

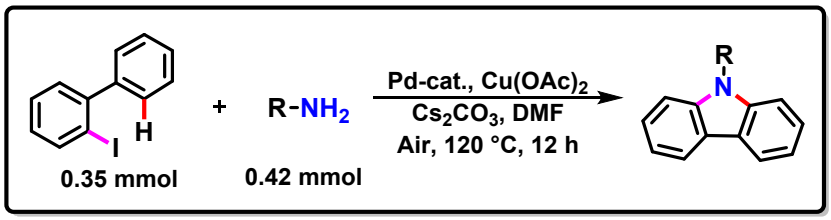

A dry sealed tube equipped with magnetic stirrer was charged with 2-iodobiphenyls/3-iodo-2-phenylimidazo[1,2-a]pyridine (0.35 mmol), aromatic amine/aliphatic amine/benzenesulfonamide derivative (0.42 mmol), $Cu(OAc)_2$ (1 eqv.), Cs_2CO_3 (1 eqv.), Pd-catalyst(5 mol%) and DMF (2 mL). The reaction mixture was sealed and stirred at 120 °C for 12 hours and then cooled at room temperature. Water (10 mL) was added to the resultant mixture. The product was extracted with ethyl acetate (10 mL × 3), and the combined organic layers were washed with brine (10 mL × 2) and dried over Na_2SO_4. The solvent was removed under reduced pressure, and the residue obtained was purified *via* silica gel chromatography (230-400 mesh particle size) in hexane to afford the desired N-substituted carbazoles.

5. Mechanistic analysis

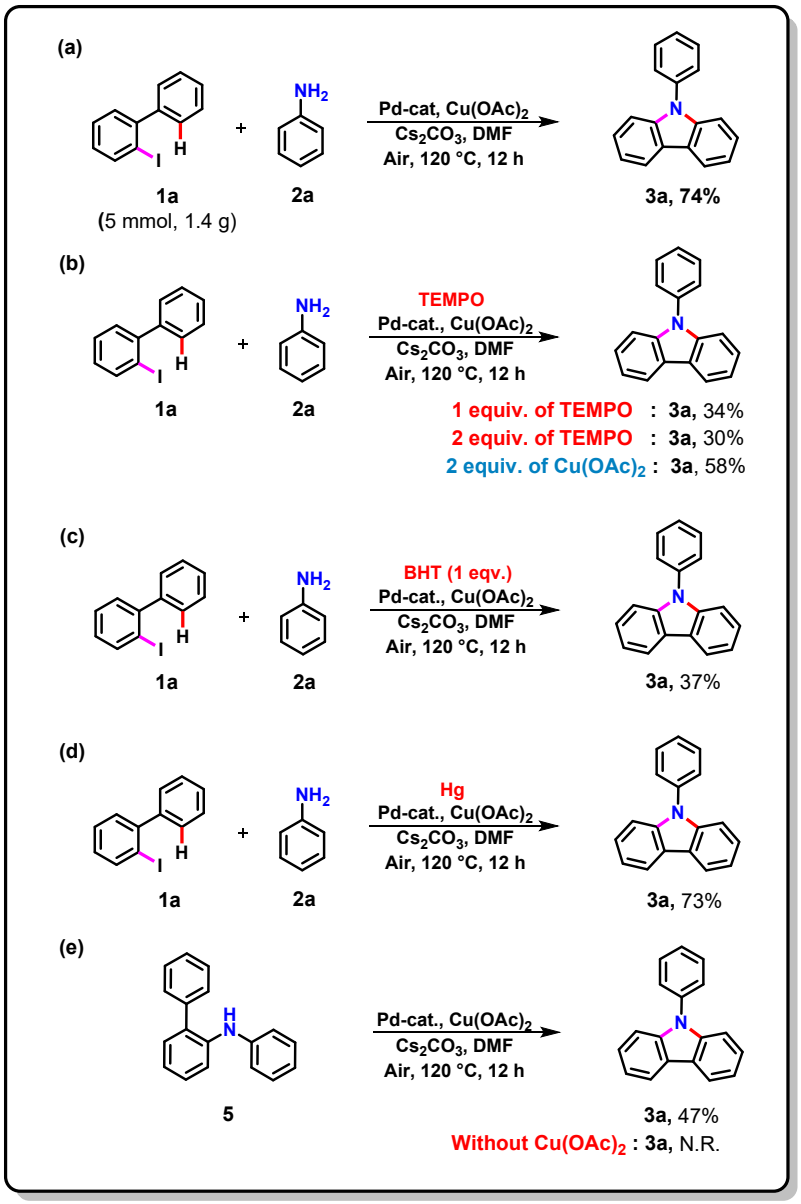

Scheme S3: (a) Scale-up to 5 mmol reaction. (b) to (e) Control experiments for mechanistic studies.

Gram-scale synthesis

A dry sealed tube equipped with a magnetic stir bar was charged with 2-iodobiphenyl (5.0 mmol, 1.4 g), aniline (6.0 mmol, 0.57 mL), $Cu(OAc)_2$ (5.0 mmol, 0.91 g), Cs_2CO_3 (5.0 mmol, 1.0 equiv 1.63 g), Pd-catalyst (5 mol%, 190 mg), and DMF (20 mL).The reaction mixture was sealed and stirred at 120 °C for 12 h. After completion (monitored by TLC), the reaction mixture was cooled to room temperature and diluted with water (50 mL). The resulting mixture was extracted with ethyl acetate (3 × 30 mL). The combined organic layers were washed with brine (2 × 30 mL) and dried over anhydrous Na_2SO_4. The solvent was removed under reduced pressure, and the crude residue was purified by silica gel column chromatography (230–400 mesh) using hexane/ethyl acetate as the eluent to afford the desired N-substituted carbazole in 74% (0.9 g) isolated yield.

Reaction with radical scavenger

A 15 mL oven-dried screw-cap reaction tube was charged with 2-iodobiphenyl 1a (0.35 mmol), aniline 2a (0.42 mmol), TEMPO (0.35 mmol), Pd-catalyst (5 mol %), $Cu(OAc)_2$ (1.0 equiv), Cs_2CO_3 (1.0 equiv) and DMF (2 mL). The reaction mixture was heated at 120 °C with stirring for 12 h. Water (10 mL) was added to the resultant mixture. The product was extracted with ethyl acetate (10 mL × 3), and the combined organic layers were washed with brine (10 mL × 2) and dried over Na_2SO_4. The solvent was removed under reduced pressure, and the residue obtained was purified *via* silica gel chromatographyto afford the desired product 3a in 34% yield. When 2 equivalents of TEMPO were introduced as a radical scavenger, only a marginal decrease in yield was observed (30%), which may be attributed to the poisoning of $Cu(OAc)_2$ rather than effective radical trapping. Furthermore, increasing the loading of $Cu(OAc)_2$to 2.0 equivalents under otherwise identical conditions led to an improved yield of 58%. Apart from TEMPO,BHT (1 eqv.) was also employed as a radical scavenger under the standard reaction conditions. In the presence of BHT, the reaction afforded the desired product in 37% yield, indicating that the reaction is not significantly inhibited. These observations suggest that free radical intermediates are unlikely to play a significant role in the catalytic cycle, and the reaction most likely proceeds *via* a conventional Pd-mediated pathway.

Mercury poisoning experiment

We have conducted a mercury drop experiment to determine the heterogeneity or homogeneity of Pd-catalyst in C-H bond activation process. A standard mercury drop test involved charging the reaction tube with 0.35 mmol of 2-iodobiphenyl, 0.42 mmol of aniline, 5 mol % of Pd-catalyst, 0.35 mmol of $Cu(OAc)_2$, 0.35 mmol of Cs_2CO_3 and 2 mL of DMF solvent. After adding a drop of mercury to this reaction mixture, the mixture was agitated for 12 hours at 120 °C. Under these conditions, no significant suppression of the reaction was observed, and the desired product was obtained in 73% yield. This result suggests that the catalytically active species are predominantly homogeneous in nature under the applied reaction conditions.

Reaction with N-phenyl-[1,1'-biphenyl]-2-amine

N-phenyl-[1,1'-biphenyl]-2-amine was independently synthesized according to a reported literature procedure[3, 4] and further confirmed by ^{1}H-NMR spectroscopy (Fig S14). A reaction flask equipped with magnetic stirrer was charged with 0.40 mmol N-phenyl-[1,1'-biphenyl]-2-amine, 5 mol % of Pd-catalyst, 0.40 mmol of $Cu(OAc)_2$, 0.40 mmol of Cs_2CO_3 and 2 mL of DMF solvent. The reaction mixture was heated at 120 °C with stirring for 12 h. After cooling to room temperature, water (10 mL) was added and the mixture was extracted with ethyl acetate (3 × 10 mL) and dried over Na_2SO_4. The solvent was removed under reduced pressure, and the residue obtained was purified *via* silica gel chromatography to afford the desired product 3a in 47% yield. Notably, no product formation was observed when the reaction was conducted in the absence of $Cu(OAc)_2$.

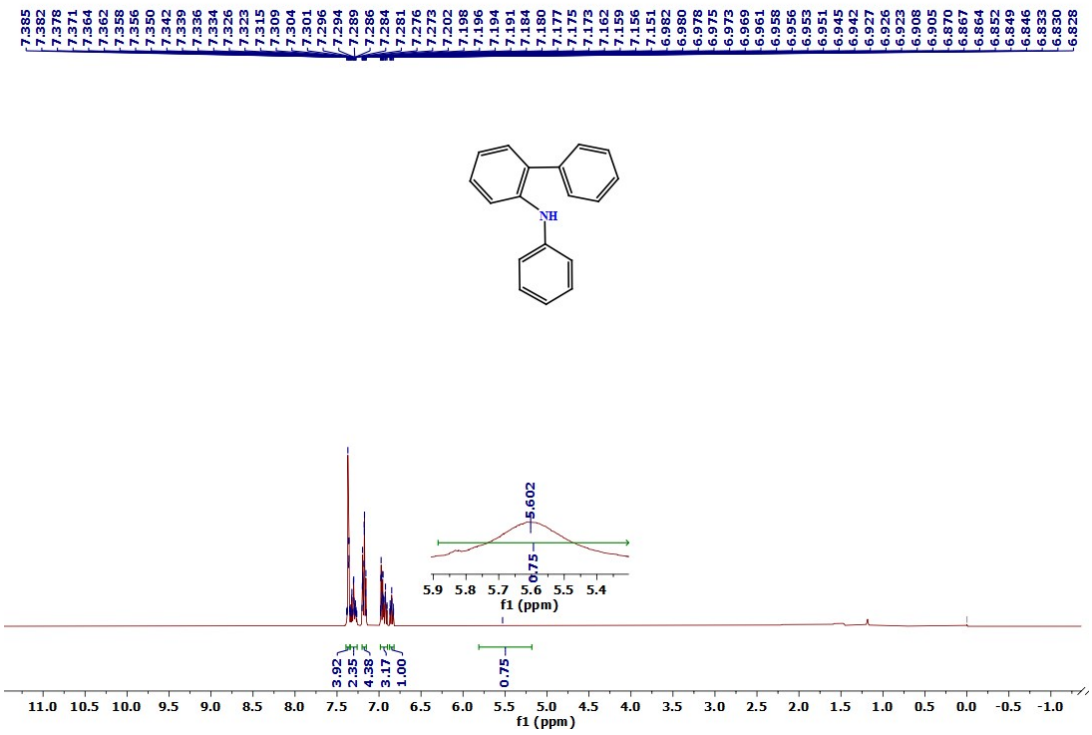

Fig. S16: ^{1}H-NMR Spectrum of N-phenyl-[1,1′-biphenyl]-2-aminein $CDCl_3$ (400 MHz)

^{1}H NMR (400 MHz, CHLOROFORM-*D*) δ 7.39 – 7.35 (m, 4H), 7.34 – 7.26 (m, 2H), 7.20 – 7.15 (m, 4H), 6.98 – 6.90 (m, 3H), 6.87 – 6.82 (m, 1H), 5.53 (s, 1H).

Scheme S4: Substrate scope with respect to benzamides

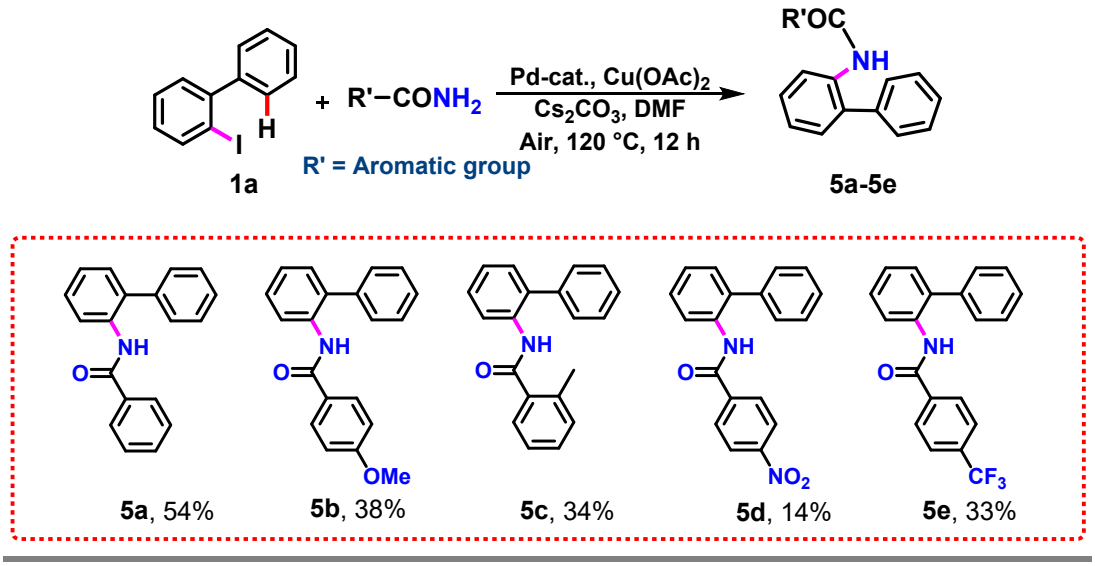

Reaction conditions **1a** (0.35 mmol), **2a"- 2e"** (1.2 equiv., 0.42 mmol), 5 mol % Pd-cat., 1.0 equiv. $Cu(OAc)_2$, 1.0 equiv. Cs_2CO_3, 2 mL DMF, 120 °C, air, 12 h.

6. Characterization data of N-substituted carbazoles

9-phenyl-9H-carbazole (3a)

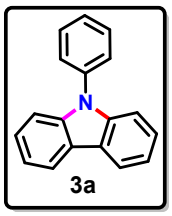

White solid. Yield – 93%. ^{1}H NMR (400 MHz, CHLOROFORM-*D*) δ 7.41 – 7.36 (m, 2H), 6.83 – 6.77 (m, 4H), 6.69 – 6.61 (m, 5H), 6.55 – 6.50 (m, 2H). ^{13}C NMR (101 MHz, CHLOROFORM-*D*) δ 141.1, 137.9, 130.0, 127.6, 127.3, 126.1, 123.5, 120.5, 120.1, 110.0. All data matches with the already existing data.[5]

9-(p-tolyl)-9H-carbazole (3b)

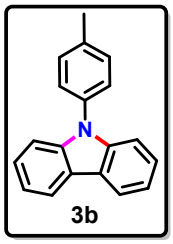

White solid. Yield – 59%. ^{1}H NMR (400 MHz, CHLOROFORM-*D*) δ 8.22 – 8.19 (m, 2H), 7.50 – 7.42 (m, 8H), 7.36 – 7.31 (m, 2H), 2.53 (s, 3H). ^{13}C NMR (101 MHz, CHLOROFORM-*D*) δ 141.2, 137.5, 135.1, 130.6, 127.1, 126.0, 123.3, 120.4, 119.8, 109.9, 21.37. All data matches with the already existing data.[5]

9-(4-chlorophenyl)-9H-carbazole (3c)

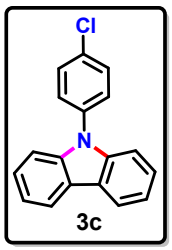

White solid. Yield – 84%. ^{1}H NMR (400 MHz, CHLOROFORM-*D*) δ 8.20 (d, *J* = 7.6 Hz, 2H), 7.63 – 7.57 (m, 2H), 7.56 – 7.51 (m, 2H), 7.49 – 7.41 (m, 4H), 7.39 – 7.33 (m, 2H). ^{13}C NMR (101 MHz, CHLOROFORM-*D*) δ 140.8, 136.4, 133.1, 130.2, 128.5, 126.2, 123.6, 120.5, 120.3, 109.7. All data matches with the already existing data.[5]

9-(4-(trifluoromethyl)phenyl)-9H-carbazole (3d)

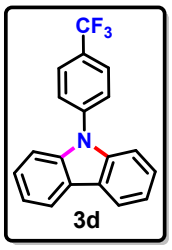

White solid. Yield – 80%. ^{1}H NMR (400 MHz, CHLOROFORM-*D*) δ 8.07 – 8.01 (m, 2H), 7.76 (d, *J* = 8.0 Hz, 2H), 7.60 (d, *J* = 8.4 Hz, 2H), 7.34 – 7.29 (m, 4H), 7.24 – 7.19 (m, 2H). ^{13}C NMR (101 MHz, CHLOROFORM-*D*) δ 141.2, 140.4, 129.3 (q, $J_{C\text{-}F}$ = 32.9 Hz), 127.3 (q, $J_{C\text{-}F}$ = 3.8 Hz), 127.2, 124.1 (q, $J_{C\text{-}F}$ = 273.7 Hz), 126.4, 123.9, 120.7, 120.6, 109.7. All data matches with the already existing data.[6]

9-(4-nitrophenyl)-9H-carbazole (3e)

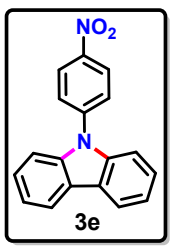

Yellow solid. Yield – 29%. ^{1}H NMR (400 MHz, CHLOROFORM-*D*) δ 8.59 – 8.52 (m, 2H), 8.49 – 8.45 (m, 1H), 7.65 (dd, *J* = 8.4, 1.2 Hz, 1H), 7.62 – 7.56 (m, 2H), 7.47 – 7.43 (m, 1H), 7.41 – 7.37 (m, 1H), 7.37 – 7.34 (m, 3H), 7.01 – 6.95 (m, 1H). ^{13}C NMR (101 MHz, CHLOROFORM-*D*) δ 145.44, 140.83, 131.52, 130.17, 129.24, 129.10, 127.45, 127.01, 126.70, 126.45, 125.09, 123.75, 123.24, 123.20, 122.37. All data matches with the already existing data.[7]

9-(4-iodophenyl)-9H-carbazole (3f)

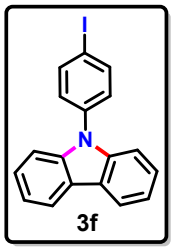

Yellow solid. Yield – 33%. ^{1}H NMR (400 MHz, CHLOROFORM-*D*) δ 8.09 – 8.04 (m, 2H), 7.88 – 7.81 (m, 2H), 7.36 – 7.29 (m, 4H), 7.27 – 7.19 (m, 4H). ^{13}C NMR (101 MHz, CHLOROFORM-*D*) δ 139.5, 138.1, 136.5, 127.9, 125.1, 122.5, 119.4, 119.2, 108.5, 91.0. All data matches with the already existing data.[8]

9-(4-isopropylphenyl)-9H-carbazole (3g)

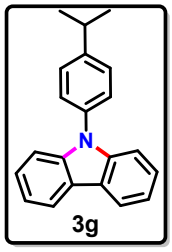

White solid. Yield – 66%. ^{1}H NMR (400 MHz, CHLOROFORM-*D*) δ 8.06 – 8.02 (m, 2H), 7.38 – 7.29 (m, 8H), 7.17 (ddd, *J* = 7.9, 6.0, 2.0 Hz, 2H), 2.93 (hept, *J* = 6.9 Hz, 1H), 1.25 (d, *J* = 6.9 Hz, 6H). ^{13}C NMR (101 MHz, CHLOROFORM-*D*) δ 148.3, 141.2, 135.4, 127.9, 127.1, 126.0, 123.4, 120.4, 119.8, 110.0, 34.1, 24.2. All data matches with the already existing data.[5]

4-(9H-carbazol-9-yl)benzoic acid (3h)

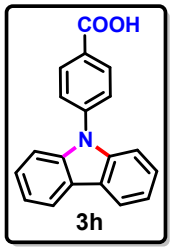

Light yellow solid. Yield – 54%. ^{1}H NMR (400 MHz, CHLOROFORM-*D*) δ 8.33 – 8.28 (m, 2H), 8.10 – 8.06 (m, 2H), 7.69 – 7.64 (m, 2H), 7.46 – 7.42 (m, 2H), 7.37 (ddd, *J* = 8.3, 7.1, 1.2 Hz, 2H), 7.28 – 7.23 (m, 2H). ^{13}C NMR (101 MHz, CHLOROFORM-*D*) δ 171.2, 143.1, 140.3, 132.2, 127.7, 126.6, 126.4, 124.0, 120.8, 120.6, 109.9. All data matches with the already existing data.[9]

4-(9H-carbazol-9-yl)benzamide (3i)

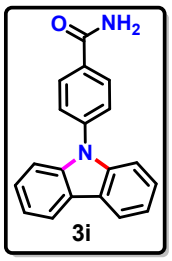

White solid. Yield – 97%. ^{1}H NMR (400 MHz, CHLOROFORM-*D*) δ 8.08 (d, *J* = 8.0 Hz, 2H), 8.00 (d, *J* = 8.0 Hz, 2H), 7.63 (d, *J* = 8.4 Hz, 2H), 7.40 – 7.33 (m, 4H), 7.28 – 7.22 (m, 2H), 6.08 (s, 1H), 5.73 (s, 1H). ^{13}C NMR (101 MHz, $CDCl_3$) δ 167.3, 140.3, 139.3, 130.8, 128.1, 125.8, 125.2, 122.7, 119.5, 119.4, 108.6. HRMS (ESI^{+}) *m/z* calculated for $C_{19}H_{15}N_2O^{+}$ $[M+H]^{+}$ = 287.1179; found 287.1178.

9-(o-tolyl)-9H-carbazole (3j)

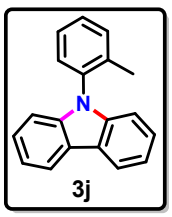

Pale yellow solid. Yield – 54%. ^{1}H NMR (400 MHz, CHLOROFORM-*D*) δ 8.23 – 8.20 (m, 2H), 7.51 – 7.41 (m, 6H), 7.35 – 7.30 (m, 2H), 7.12 – 7.08 (m, 2H), 2.02 (s, 3H). ^{13}C NMR (101 MHz, CHLOROFORM-*D*) δ 141.3, 137.5, 136.1, 131.6, 129.4, 128.9, 127.4, 126.0, 123.1, 120.5, 119.6, 109.9, 17.7. All data matches with the already existing data.[5]

9-(2-fluorophenyl)-9H-carbazole (3k)

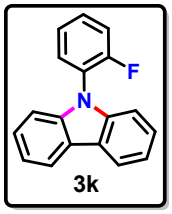

Pale yellow solid. Yield – 89%. ^{1}H NMR (400 MHz, CHLOROFORM-*D*) δ 8.06 – 8.01 (m, 2H), 7.44 (td, *J* = 7.6, 2.0 Hz, 1H), 7.34 – 7.16 (m, 7H), 7.15 – 7.11 (m, 2H). ^{13}C NMR (101 MHz, CHLOROFORM-*D*) δ 158.5 (d, $J_{C\text{-}F}$ = 253.0 Hz), 141.0, 130.0, 129.7 (d, $J_{C\text{-}F}$ = 7.7 Hz), 126.2, 125.3, 125.2 (d, $J_{C\text{-}F}$ = 4.2 Hz), 123.7, 120.4, 120.3, 117.5 (d, $J_{C\text{-}F}$ = 19.7 Hz), 110.0. All data matches with the already existing data.[10]

9-(2-iodophenyl)-9H-carbazole (3l)

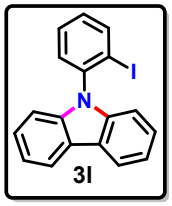

Pale yellow solid. Yield – 39%. ^{1}H NMR (400 MHz, CHLOROFORM-*D*) δ 8.08 – 8.05 (m, 2H), 7.97 (d, *J* = 7.2 Hz, 2H), 7.85 – 7.82 (m, 2H), 7.55 – 7.45 (m, 4H), 7.28 (td, *J* = 7.6, 0.8 Hz, 2H). ^{13}C NMR (101 MHz, CHLOROFORM-*D*) δ 139.7, 139.5, 139.3, 129.6, 129.3, 128.7, 124.9, 122.2, 119.4, 118.9, 109.1, 98.2. All data matches with the already existing data.[11]

9-(2-chlorophenyl)-9H-carbazole (3m)

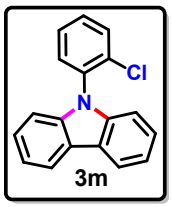

Pale yellow solid. Yield – 81%. ^{1}H NMR (400 MHz, CHLOROFORM-*D*) δ 8.04 – 7.99 (m, 2H), 7.55 – 7.48 (m, 1H), 7.36 – 7.24 (m, 5H), 7.18 – 7.13 (m, 2H), 7.00 – 6.93 (m, 2H). ^{13}C NMR (101 MHz, CHLOROFORM-*D*) δ 141.0, 135.2, 133.8, 131.2, 131.0, 129.9, 128.2, 126.1, 123.4, 120.5, 120.1, 110.1. All data matches with the already existing data.[5]

9-(3,4-dimethylphenyl)-9H-carbazole (3n)

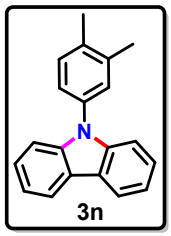

Yellow solid. Yield – 61%. ^{1}H NMR (400 MHz, CHLOROFORM-*D*) δ 8.02 – 7.97 (m, 2H), 7.69 (dt, *J* = 8.4, 0.8 Hz, 2H), 7.34 – 7.29 (m, 2H), 7.21 – 7.16 (m, 2H), 7.11 – 7.09 (m, 1H), 6.87 – 6.81 (m, 1H), 2.51 (s, 3H), 2.27 (s, 3H). ^{13}C NMR (101 MHz, CHLOROFORM-*D*) δ 141.2, 138.4, 136.2, 135.4, 131.0, 128.2, 125.9, 124.6, 123.3, 120.4, 119.8, 110.0, 20.1, 19.7. All data matches with the already existing data.[5]

9-(2,5-dibromophenyl)-9H-carbazole (3o)

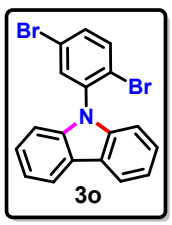

White solid. Yield – 31%. ^{1}H NMR (400 MHz, CHLOROFORM-*D*) δ 8.07 – 8.04 (m, 2H), 7.96 (d, *J* = 7.2 Hz, 2H), 7.84 – 7.80 (m, 2H), 7.50 – 7.45 (m, 3H), 7.30 – 7.25 (m, 2H). ^{13}C NMR (101 MHz, CHLOROFORM-*D*) δ 143.9, 138.9, 130.2, 130.0, 126.9, 123.3, 123.0, 121.8, 119.5, 118.6, 112.3, 109.9. All data matches with the already existing data.[12]

9-(pyridin-2-yl)-9H-carbazole (3p)

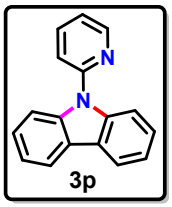

Pale yellow solid. Yield – 34%. ^{1}H NMR (400 MHz, CHLOROFORM-*D*) δ 8.64 (ddd, *J* = 4.8, 2.0, 0.8 Hz, 1H), 8.06 – 8.01 (m, 2H), 7.82 (ddd, *J* = 8.2, 7.2, 2.0 Hz, 1H), 7.77 – 7.74 (m, 2H), 7.56 – 7.53 (m, 1H), 7.36 (ddd, *J* = 8.4, 7.2, 1.2 Hz, 2H), 7.26 – 7.19 (m, 3H). ^{13}C NMR (101 MHz, CHLOROFORM-*D*) δ 152.0, 149.8, 139.7, 138.6, 126.4, 124.5, 121.4, 121.1, 120.3, 119.2, 111.3. All data matches with the already existing data.[5]

9-(4-chloropyridin-2-yl)-9H-carbazole (3q)

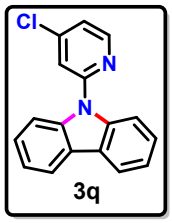

White solid. Yield – 41%. ^{1}H NMR (400 MHz, CHLOROFORM-*D*) δ 8.54 (d, *J* = 5.2 Hz, 1H), 8.03 (dt, *J* = 7.6, 0.8 Hz, 2H), 7.79 (dd, *J* = 8.4, 0.8 Hz, 2H), 7.59 (d, *J* = 1.6 Hz, 1H), 7.38 (ddd, *J* = 8.4, 7.2, 1.2 Hz, 2H), 7.28 – 7.21 (m, 3H). ^{13}C NMR (101 MHz, CHLOROFORM-*D*) δ 153.0, 150.4, 146.0, 139.3, 128.9, 126.6, 124.7, 121.5, 120.4, 119.0, 111.4. HRMS (ESI^{+}) *m/z* calculated for $C_{17}H_{12}ClN_2^{+}$ [M+H]$^{+}$ = 279.0684; found 279.0683.

9-(4,6-dimethylpyridin-2-yl)-9H-carbazole (3r)

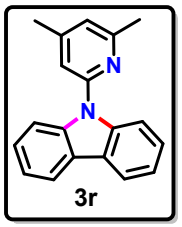

Yellow solid. Yield – 74%. ^{1}H NMR (400 MHz, CHLOROFORM-*D*) δ 8.02 – 7.97 (m, 2H), 7.69 (dt, *J* = 8.4, 0.8 Hz, 2H), 7.31 (td, *J* = 8.4, 1.2 Hz, 2H), 7.21 – 7.16 (m, 2H), 7.11 – 7.09 (m, 1H), 6.87 – 6.81 (m, 1H), 2.51 (s, 3H), 2.27 (s, 3H). ^{13}C NMR (101 MHz, CHLOROFORM-*D*) δ 157.4, 150.1, 149.0, 138.7, 125.0, 123.1, 120.9, 119.5, 119.1, 115.7, 110.2, 23.2, 20.1. HRMS (ESI^{+}) *m/z* calculated for $C_{19}H_{17}N_2^{+}$ [M+H]$^{+}$ = 273.1386; found 273.1386.

9-(pyrimidin-2-yl)-9H-carbazole (3s)

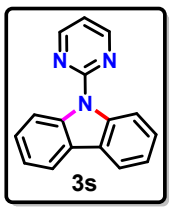

Pale yellow solid. Yield – 37%. ^{1}H NMR (400 MHz, CHLOROFORM-*D*) δ 8.76 (dt, *J* = 8.4, 0.8 Hz, 2H), 8.70 (d, *J* = 4.8 Hz, 2H), 8.00 – 7.96 (m, 2H), 7.41 (ddd, *J* = 8.6, 7.2, 1.6 Hz, 2H), 7.28 (td, *J* = 7.6, 0.8 Hz, 2H), 6.96 (t, *J* = 4.8 Hz, 1H). ^{13}C NMR (101 MHz, CHLOROFORM-*D*) δ 158.07, 156.78, 138.09, 125.55, 124.71, 121.22, 118.46, 115.20, 114.90. All data matches with the already existing data.[13]

2-(9H-carbazol-9-yl)benzo[d]thiazole (3t)

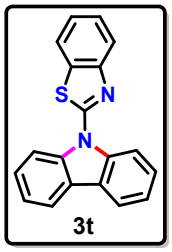

Pale yellow solid. Yield – 30%. ^{1}H NMR (400 MHz, CHLOROFORM-*D*) δ 7.44 – 7.32 (m, 6H), 7.23 – 7.11 (m, 4H), 6.99 (td, *J* = 7.6, 1.2 Hz, 1H), 6.88 – 6.81 (m, 1H). ^{13}C NMR data matches with the already existing data.[14]

9-(phenylsulfonyl)-9H-carbazole (4a)

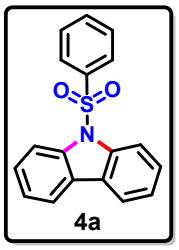

White solid. Yield – 83%. ^{1}H NMR (400 MHz, CHLOROFORM-*D*) δ 8.25 (dd, *J* = 8.4, 2.0 Hz, 2H), 7.83 – 7.70 (m, 4H), 7.44 – 7.37 (m, 2H), 7.36 – 7.30 (m, 1H), 7.30 – 7.24 (m, 2H), 7.23 – 7.17 (m, 2H). ^{13}C NMR (101 MHz, CHLOROFORM-*D*) δ 138.4, 138.0, 133.9, 129.2, 127.6, 126.6, 126.5, 124.1, 120.2, 115.2. All data matches with the already existing data.[15]

9-((4-chlorophenyl)sulfonyl)-9H-carbazole (4b)

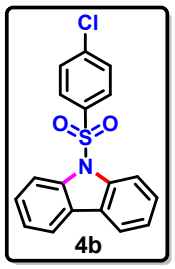

White solid. Yield – 53%.^{1}H NMR (400 MHz, CHLOROFORM-*D*) δ 8.22 (dt, *J* = 8.4, 0.8 Hz, 2H), 7.83 – 7.80 (m, 2H), 7.65 – 7.62 (m, 2H), 7.41 (ddd, *J* = 8.4, 7.2, 1.2 Hz, 2H), 7.32 – 7.27 (m, 2H), 7.19 – 7.15 (m, 2H). ^{13}C NMR (101 MHz, CHLOROFORM-*D*) δ 140.6, 138.3, 136.2, 129.5, 128.0, 127.7, 126.7, 124.4, 120.3, 115.3. All data matches with the already existing data.[16]

9-((4-(trifluoromethyl)phenyl)sulfonyl)-9H-carbazole (4c)

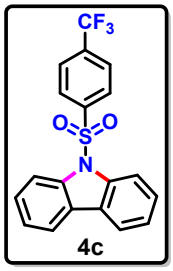

White solid. Yield – 48%. ^{1}H NMR (400 MHz, CHLOROFORM-*D*) δ 8.25 (dq, *J* = 8.4, 0.8 Hz, 2H), 7.87 – 7.81 (m, 4H), 7.51 – 7.48 (m, 2H), 7.44 (ddt, *J* = 8.4, 7.2, 1.2 Hz, 2H), 7.35 – 7.30 (m, 2H). ^{13}C NMR (101 MHz, CHLOROFORM-*D*) δ 139.9, 137.1, 134.3 (q, $J_{C\text{-}F}$ = 33.2 Hz), 126.7, 125.9, 125.6, 125.2 (q, $J_{C\text{-}F}$ = 3.7 Hz), 123.5, 121.8 (q, $J_{C\text{-}F}$ = 273 Hz), 119.2, 114.1. ^{19}F NMR (376 MHz, CHLOROFORM-*D*) δ -106.04. HRMS (ESI^{+}) *m/z* calculated for $C_{19}H_{13}F_3NO_2S^{+}$ $[M+H]^{+}$ = 376.0614; found 376.0615.

9-((4-methoxyphenyl)sulfonyl)-9H-carbazole (4d)

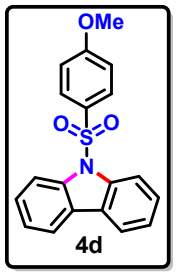

White solid. Yield – 26%. ^{1}H NMR (400 MHz, CHLOROFORM-*D*) δ 8.25 (dt, *J* = 8.4, 0.8 Hz, 2H), 7.81 (ddd, *J* = 7.8, 1.4, 0.7 Hz, 2H), 7.70 – 7.60 (m, 2H), 7.40 (ddd, *J* = 8.4, 7.2, 1.2 Hz, 2H), 7.27 (td, *J* = 7.6, 0.8 Hz, 2H), 6.68 – 6.59 (m, 2H), 3.59 (s, 3H). ^{13}C NMR (101 MHz, CHLOROFORM-*D*) δ 163.8, 138.5, 129.6, 128.8, 127.5, 126.5, 124.0, 120.1, 115.3, 114.3, 55.6. All data matches with the already existing data.[16]

9-tosyl-9H-carbazole (4e)

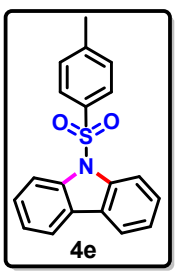

White solid. Yield – 47%. ^{1}H NMR (400 MHz, CHLOROFORM-*D*) δ 8.25 (dt, *J* = 8.4, 0.8 Hz, 2H), 7.82 – 7.77 (m, 2H), 7.63 – 7.58 (m, 2H), 7.43 – 7.37 (m, 2H), 7.29 – 7.23 (m, 2H), 7.00 – 6.95 (m, 2H), 2.13 (s, 3H). ^{13}C NMR (101 MHz, CHLOROFORM-*D*) δ 145.0, 138.5, 135.1, 129.8, 127.5, 126.6, 126.5, 124.0, 120.1, 115.3, 21.6. All data matches with the already existing data.[17]

9-((4-(tert-butyl)phenyl)sulfonyl)-9H-carbazole (4f)

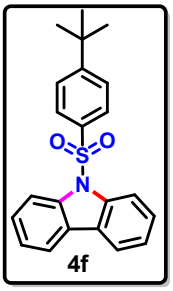

White solid. Yield – 55%. ^{1}H NMR (400 MHz, CHLOROFORM-*D*) δ 8.37 – 8.33 (m, 2H), 7.94 – 7.91 (m, 2H), 7.78 – 7.75 (m, 2H), 7.53 – 7.47 (m, 2H), 7.39 – 7.31 (m, 4H), 1.19 (s, 9H). ^{13}C NMR (101 MHz, CHLOROFORM-*D*) δ 156.6, 137.3, 134.1, 126.4, 125.3, 125.2, 125.1, 122.7, 118.9, 114.0, 34.1, 29.8. All data matches with the already existing data.[18]

9-(o-tolylsulfonyl)-9H-carbazole (4g)

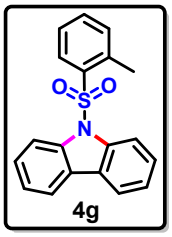

White solid. Yield – 26%. ^{1}H NMR (400 MHz, CHLOROFORM-*D*) δ 8.02 – 7.98 (m, 2H), 7.93 – 7.88 (m, 2H), 7.72 (dd, *J* = 8.0, 1.2 Hz, 1H), 7.35 (ddd, *J* = 8.4, 7.2, 1.2 Hz, 2H), 7.31 – 7.26 (m, 3H), 7.17 – 7.08 (m, 2H), 2.29 (s, 3H). ^{13}C NMR (101 MHz, CHLOROFORM-*D*) δ 138.77, 138.38, 138.02, 133.62, 133.08, 129.04, 127.38, 126.36, 125.60, 123.68, 120.24, 114.94, 20.66. All data matches with the already existing data.[19]

9-((2-fluorophenyl)sulfonyl)-9H-carbazole (4h)

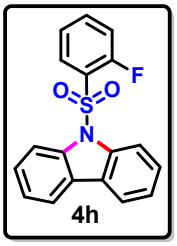

White solid. Yield – 59%. ^{1}H NMR (400 MHz, CHLOROFORM-*D*) δ 8.12 – 8.07 (m, 2H), 8.00 – 7.95 (m, 1H), 7.86 – 7.82 (m, 2H), 7.39 – 7.33 (m, 3H), 7.29 – 7.25 (m, 2H), 7.16 – 7.10 (m, 1H), 6.89 – 6.84 (m, 1H). ^{13}C NMR (101 MHz, CHLOROFORM-*D*) δ 158.4 (d, $J_{C\text{-}F}$ = 259.4 Hz), 137.0, 135.0 (d, *J* = 8.4 Hz), 129.4, 126.2, 125.2 (d, $J_{C\text{-}F}$ = 14.4 Hz), 124.9, 123.3 (d, $J_{C\text{-}F}$ = 3.9 Hz), 122.8, 118.9, 116.4 (d, $J_{C\text{-}F}$ = 20.9 Hz), 114.0. ^{19}F NMR (376 MHz, CHLOROFORM-*D*) δ -106.04. HRMS (ESI^{+}) *m/z* calculated for $C_{18}H_{13}FNO_2S^{+}$ [M+H]$^{+}$ = 326.0646; found 326.0646.

9-(pyridin-2-ylsulfonyl)-9H-carbazole (4i)

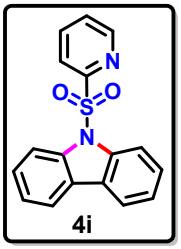

White solid. Yield – 19%. ^{1}H NMR (400 MHz, CHLOROFORM-*D*) δ 8.40 – 8.35 (m, 1H), 8.25 (dt, *J* = 8.4, 0.8 Hz, 2H), 8.00 – 7.96 (m, 1H), 7.87 – 7.83 (m, 2H), 7.73 (td, *J* = 7.6, 1.6 Hz, 1H), 7.42 – 7.37 (m, 2H), 7.31 – 7.27 (m, 3H). ^{13}C NMR (101 MHz, CHLOROFORM-*D*) δ 155.6, 150.5, 138.8, 138.1, 127.7, 127.5, 126.3, 124.0, 122.3, 120.0, 115.4. All data matches with the already existing data.[20]

9-((4-(9H-carbazol-9-yl)phenyl)sulfonyl)-9H-carbazole (4j)

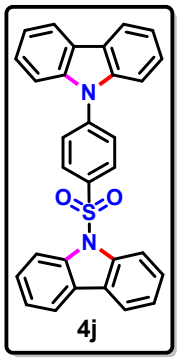

White solid. ^{1}H NMR (400 MHz, CHLOROFORM-*D*) δ 8.34 (dt, *J* = 8.4, 0.8 Hz, 2H), 8.02 – 7.98 (m, 4H), 7.91 (ddd, *J* = 7.7, 1.3, 0.7 Hz, 2H), 7.53 – 7.46 (m, 4H), 7.40 – 7.31 (m, 2H), 7.29 – 7.19 (m, 6H). Yield – 43%. ^{13}C NMR (101 MHz, CHLOROFORM-*D*) δ 143.18, 139.86, 138.45, 136.00, 128.58, 127.78, 126.81, 126.66, 126.41, 124.33, 124.07, 121.11, 120.61, 120.35, 115.24, 109.69. HRMS (ESI^{+}) *m/z* calculated for $C_{30}H_{21}N_2O_2S^{+}$ [M+H]$^{+}$ = 473.1318; found 473.1317.

5-phenyl-5H-pyrido[2',1':2,3]imidazo[4,5-b]indole (4k)

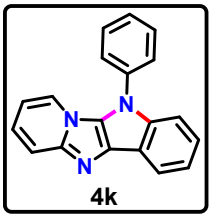

Yellow solid. Yield – 54%. ^{1}H NMR (400 MHz, CHLOROFORM-*D*) δ 8.02 – 8.00 (m, 1H), 7.92 – 7.84 (m, 3H), 7.77 – 7.75 (m, 1H), 7.57 – 7.53 (m, 1H), 7.38 – 7.33 (m, 2H), 7.27 – 7.20 (m, 2H), 7.12 – 6.96 (m, 2H), 6.68 (td, *J* = 6.8, 1.2 Hz, 1H). ^{13}C NMR (101 MHz, CHLOROFORM-*D*) δ 144.5, 132.5, 129.0, 128.7, 128.0, 127.7, 127.5, 127.0, 125.1, 124.6, 123.9, 118.8, 117.9, 116.4, 111.5, 107.1. All data matches with the already existing data.

5-(phenylsulfonyl)-5H-pyrido[2',1':2,3]imidazo[4,5-b]indole (4l)

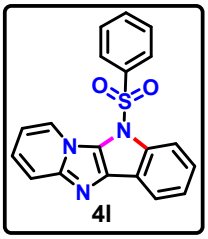

Yellow solid. Yield – 28%.^{1}H NMR (400 MHz, CHLOROFORM-*D*) δ 8.31 (dt, *J* = 6.8, 1.2 Hz, 1H), 8.14 – 8.11 (m, 2H), 7.73 – 7.69 (m, 1H), 7.48 – 7.21 (m, 8H), 7.06 – 7.01 (m, 1H). ^{13}C NMR (101 MHz, CHLOROFORM-*D*) δ 147.0, 139.6, 131.4, 130.9, 130.3, 129.4, 129.2, 128.9, 128.4, 128.2, 128.1, 127.8, 127.5, 125.8, 118.3, 114.9, 113.0. HRMS (ESI^{+}) *m/z* calculated for $C_{19}H_{13}N_3O_2S^{+}$ $[M]^{+}$ = 347.0728; found 347.0727.

9-cyclohexyl-9H-carbazole (4m)

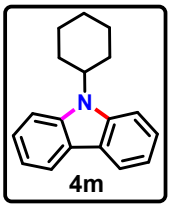

Pale yellow solid. Yield – 23%. ^{1}H NMR (400 MHz, CHLOROFORM-*D*) δ 8.10 – 8.00 (m, 2H), 7.54 – 7.46 (m, 2H), 7.38 – 7.33 (m, 2H), 7.18 – 7.11 (m, 2H), 4.47 – 4.37 (m, 1H), 2.39 – 2.27 (m, 2H), 1.99 – 1.85 (m, 4H), 1.81 – 1.74 (m, 1H), 1.49 – 1.39 (m, 2H), 1.33 (tt, *J* = 13.2, 3.2 Hz, 1H). ^{13}C NMR (101 MHz, CHLOROFORM-*D*) δ 139.82, 125.38, 123.38, 120.40, 118.60, 110.36, 55.50, 30.86, 26.66, 25.82. All data matches with the already existing data.[21]

N-([1,1'-biphenyl]-2-yl)-N-propyl-[1,1'-biphenyl]-2-amine (4n)

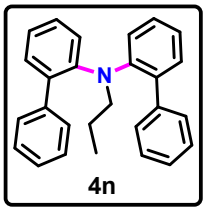

Yellow solid. Yield – 31%. ^{1}H NMR (400 MHz, CHLOROFORM-*D*) δ 8.59 – 8.52 (m, 2H), 8.49 – 8.44 (m, 1H), 8.04 – 8.01 (m, 1H), 7.67 – 7.62 (m, 1H), 7.61 – 7.55 (m, 2H), 7.46 – 7.30 (m, 8H), 7.15 (ddd, *J* = 7.8, 6.8, 1.2 Hz, 2H), 7.01 – 6.95 (m, 1H), 4.21 (t, *J* = 7.6 Hz, 2H), 1.85 (h, *J* = 7.6 Hz, 2H), 0.91 (t, *J* = 7.6 Hz, 3H). ^{13}C NMR (101 MHz, CHLOROFORM-*D*) δ 145.5, 140.9, 140.6, 131.7, 131.6, 131.1, 130.4, 130.2, 129.8, 129.3, 129.2, 127.5, 127.1, 126.8, 126.5, 125.7, 125.1, 123.8, 123.3, 122.9, 122.4, 120.5, 118.8, 108.8, 44.8, 22.4, 12.0. HRMS (ESI^{+}) *m/z* calculated for $C_{27}H_{25}N^{+}$ $[M]^{+}$ = 363.1987; found 363.1967.

N-([1,1'-biphenyl]-2-yl)benzamide (5a)

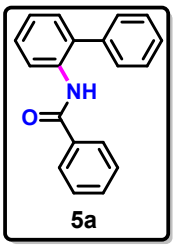

White solid. Yield – 54%. ^{1}H NMR (400 MHz, CHLOROFORM-*D*) δ 8.46 (dd, *J* = 8.4, 1.2 Hz, 1H), 7.93 (s, 1H), 7.55 – 7.50 (m, 2H), 7.46 – 7.42 (m, 2H), 7.41 – 7.34 (m, 5H), 7.33 – 7.29 (m, 2H), 7.23 (dd, *J* = 7.6, 1.6 Hz, 1H), 7.14 (td, *J* = 7.6, 1.2 Hz, 1H). ^{13}C NMR (101 MHz, CHLOROFORM-*D*) δ 165.1, 138.2, 135.1, 134.9, 132.5, 131.9, 130.1, 129.5, 129.4, 128.9, 128.8, 128.3, 127.0, 124.5, 121.3. All data matches with the already existing data.[22]

N-([1,1'-biphenyl]-2-yl)-4-methoxybenzamide (5b)

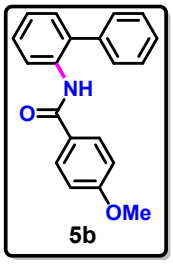

Yellow solid. Yield – 38%. ^{1}H NMR (400 MHz, CHLOROFORM-*D*) δ 8.45 (d, *J* = 8.2 Hz, 1H), 7.85 (s, 1H), 7.51 – 7.42 (m, 4H), 7.40 – 7.32 (m, 4H), 7.24 – 7.20 (m, 1H), 7.13 (t, *J* = 7.6 Hz, 1H), 6.80 (d, *J* = 8.4 Hz, 2H), 3.76 (s, 3H). ^{13}C NMR (101 MHz, $CDCl_3$) δ 163.5, 161.4, 137.1, 134.1, 131.1, 128.9, 128.4, 128.2, 127.7, 127.6, 127.1, 126.0, 123.1, 120.0, 112.9, 54.4. HRMS (ESI$^+$) *m/z* calculated for $C_{20}H_{17}NO_2^+$ $[M]^+$ = 303.1259; found 303.1245.

N-([1,1'-biphenyl]-2-yl)-2-methylbenzamide (5c)

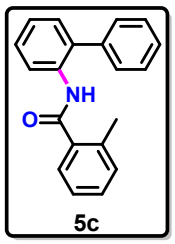

White solid. Yield – 34%. ^{1}H NMR (400 MHz, CHLOROFORM-*D*) δ 8.40 (d, 1H), 7.47 – 7.35 (m, 4H), 7.35 – 7.30 (m, 3H), 7.23 – 7.19 (m, 2H), 7.18 – 7.04 (m, 4H), 2.33 (s, 3H). ^{13}C NMR (101 MHz, CHLOROFORM-*D*) δ 167.95, 138.29, 136.66, 136.41, 135.06, 132.92, 131.45, 130.35, 130.32, 129.42, 129.25, 128.67, 128.23, 126.60, 126.01, 124.74, 121.77, 20.02. All data matches with the already existing data.[23]

N-([1,1'-biphenyl]-2-yl)-4-nitrobenzamide (5d)

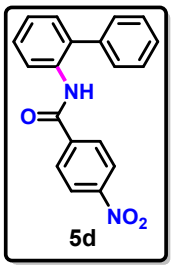

White solid. Yield – 14%.^{1}H NMR (400 MHz, CHLOROFORM-*D*) δ 8.41 (d, *J* = 8.4 Hz, 1H), 8.20 – 8.14 (m, 2H), 7.93 (s, 1H), 7.71 – 7.65 (m, 2H), 7.49 – 7.35 (m, 6H), 7.27 (dd, *J* = 7.6, 1.6 Hz, 1H), 7.23 – 7.19 (m, 1H). ^{13}C NMR (101 MHz, CHLOROFORM-*D*) δ 163.01, 149.79, 140.42, 137.87, 134.37, 132.81, 130.25, 129.52, 129.43, 128.89, 128.62, 128.12, 125.27, 124.15, 121.36. All data matches with the already existing data.[24]

N-([1,1'-biphenyl]-2-yl)-4-(trifluoromethyl)benzamide (5e)

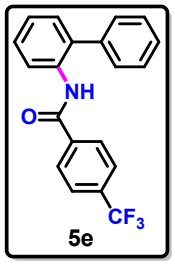

Pale Yellow solid. Yield – 33%. ^{1}H NMR (400 MHz, CHLOROFORM-*D*) δ 8.4 (d, *J* = 8.2 Hz, 1H), 7.9 (s, 1H), 7.6 – 7.6 (m, 2H), 7.6 – 7.6 (m, 2H), 7.5 – 7.4 (m, 2H), 7.4 – 7.4 (m, 4H), 7.3 (dd, *J* = 7.6, 1.6 Hz, 1H), 7.2 – 7.1 (m, 1H). ^{13}C NMR (101 MHz, CHLOROFORM-*D*) δ 163.7, 138.1, 137.9, 134.6, 133.5 (q, $J_{C\text{-}F}$= 32.8 Hz), 132.6, 130.2, 129.4, 128.8, 128.5, 127.4, 125.9 (q, $J_{C\text{-}F}$ = 3.8 Hz), 124.9, 123.7 (q, $J_{C\text{-}F}$ = 272.7 Hz), 121.3. All data matches with the already existing data.[25]

7. NMR spectra of N-substituted carbazoles

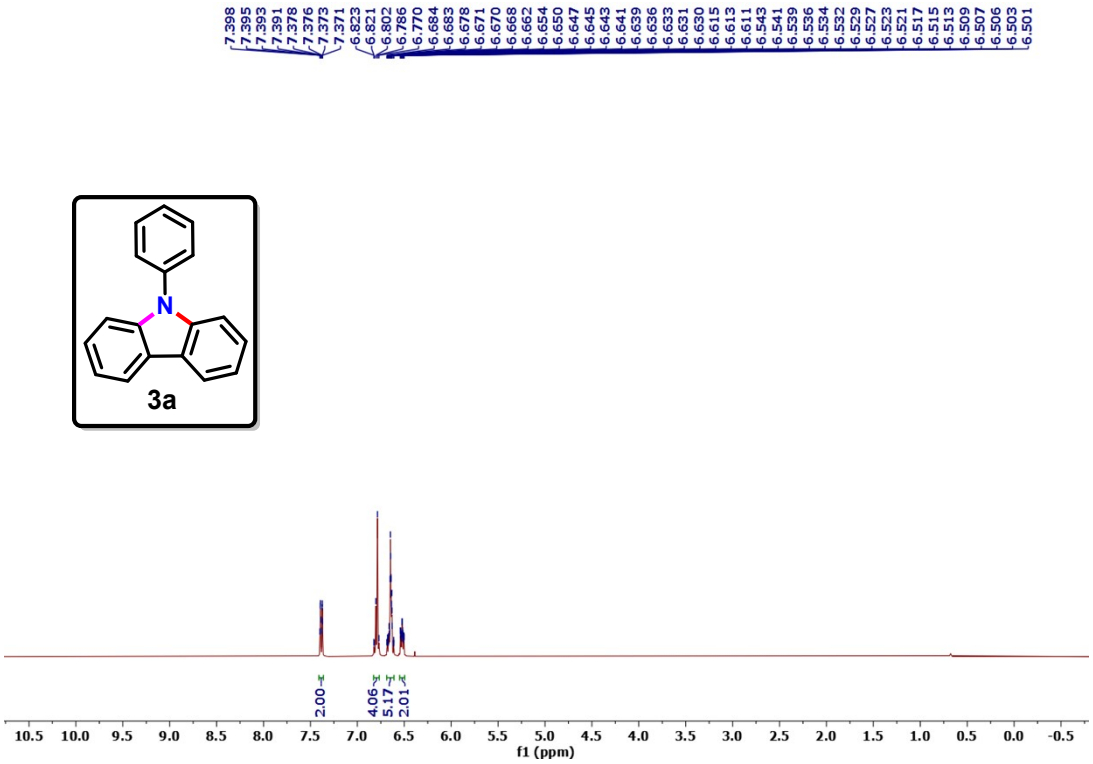

Fig. S17: ^{1}H-NMR Spectrum of **3a** in $CDCl_3$ (400 MHz)

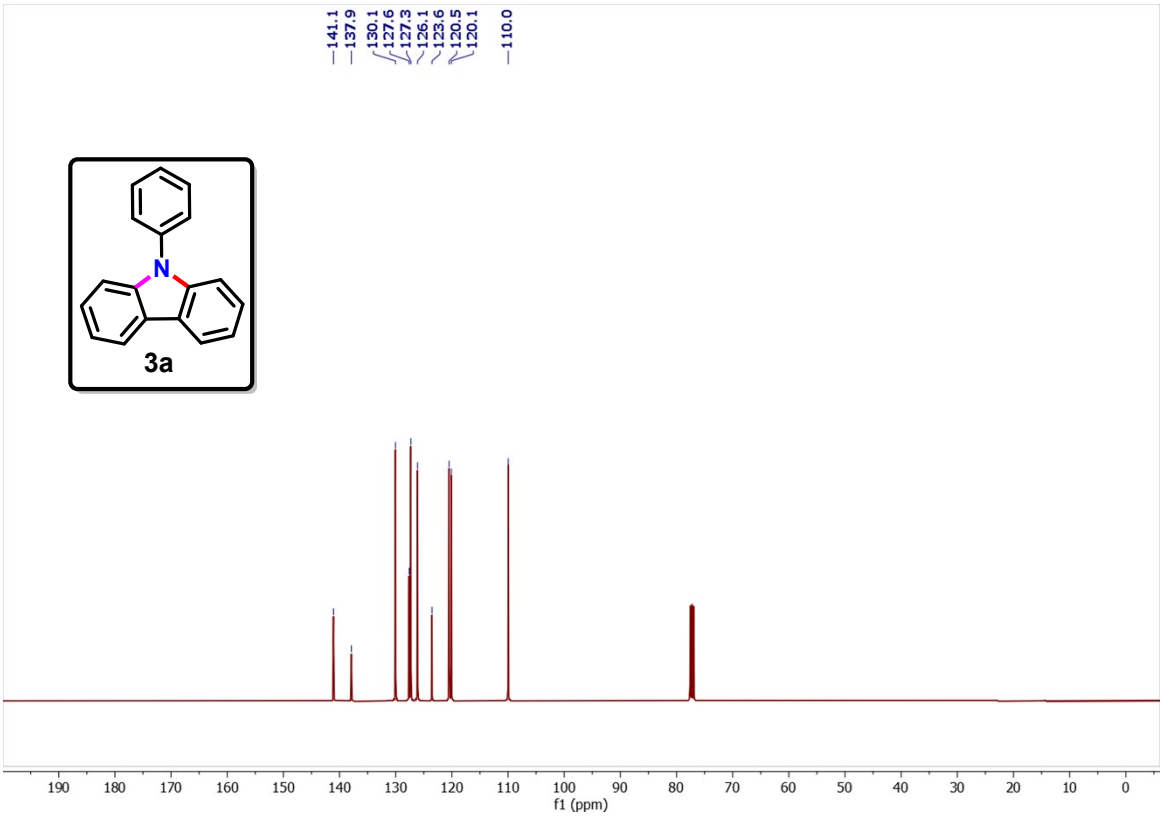

Fig. S18: $^{13}C\{^{1}H\}$-NMR Spectrum of **3a** in $CDCl_3$ (101 MHz)

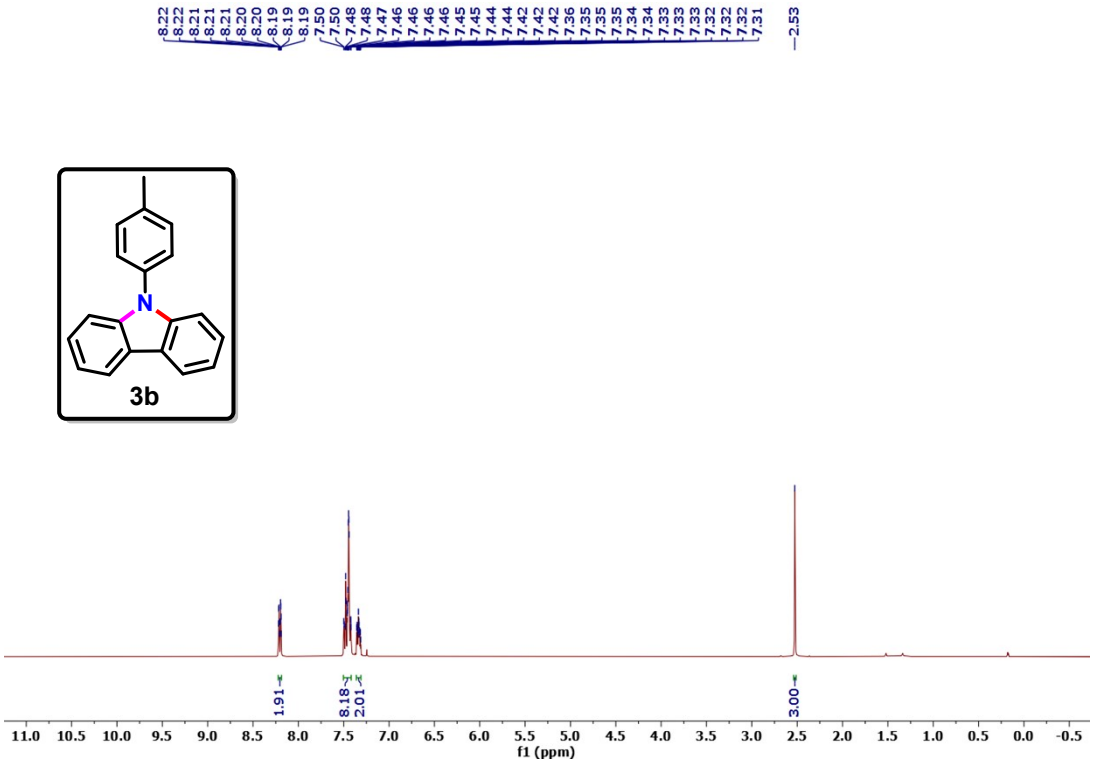

Fig. S19: ^{1}H-NMR Spectrum of **3b** in $CDCl_3$ (400 MHz)

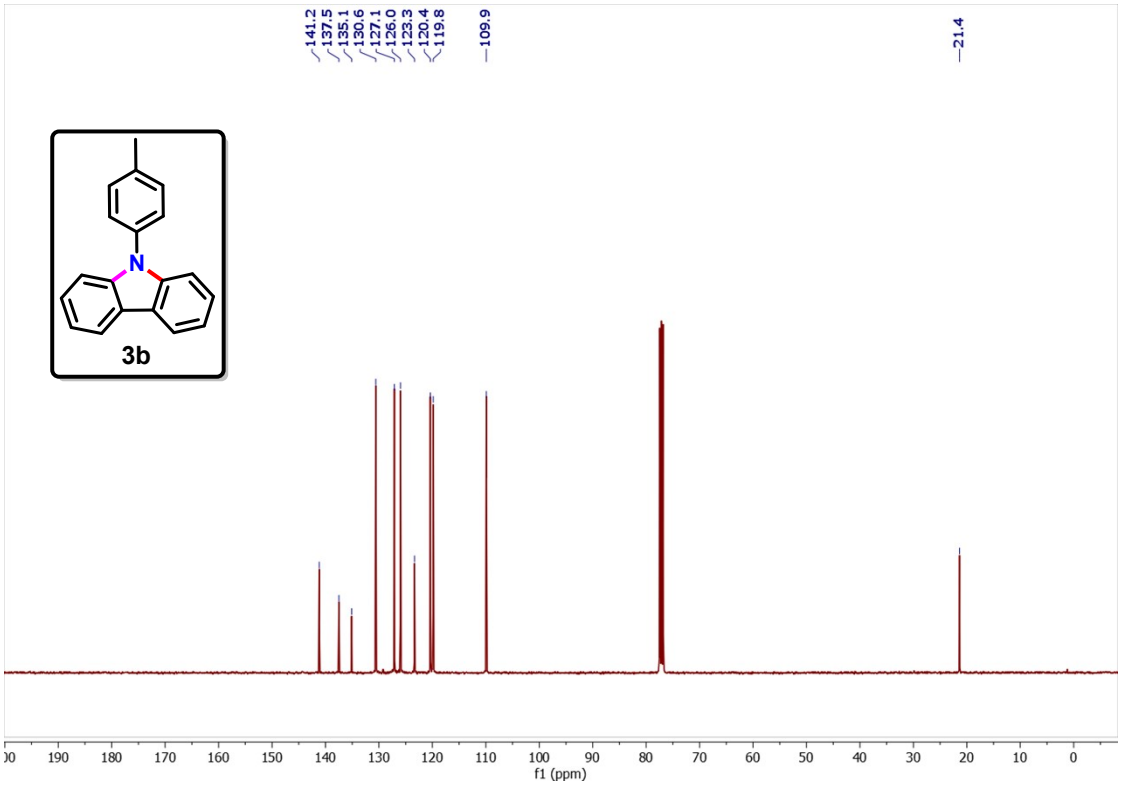

Fig. S20: $^{13}C\{^{1}H\}$-NMR Spectrum of **3b** in $CDCl_3$ (101 MHz)

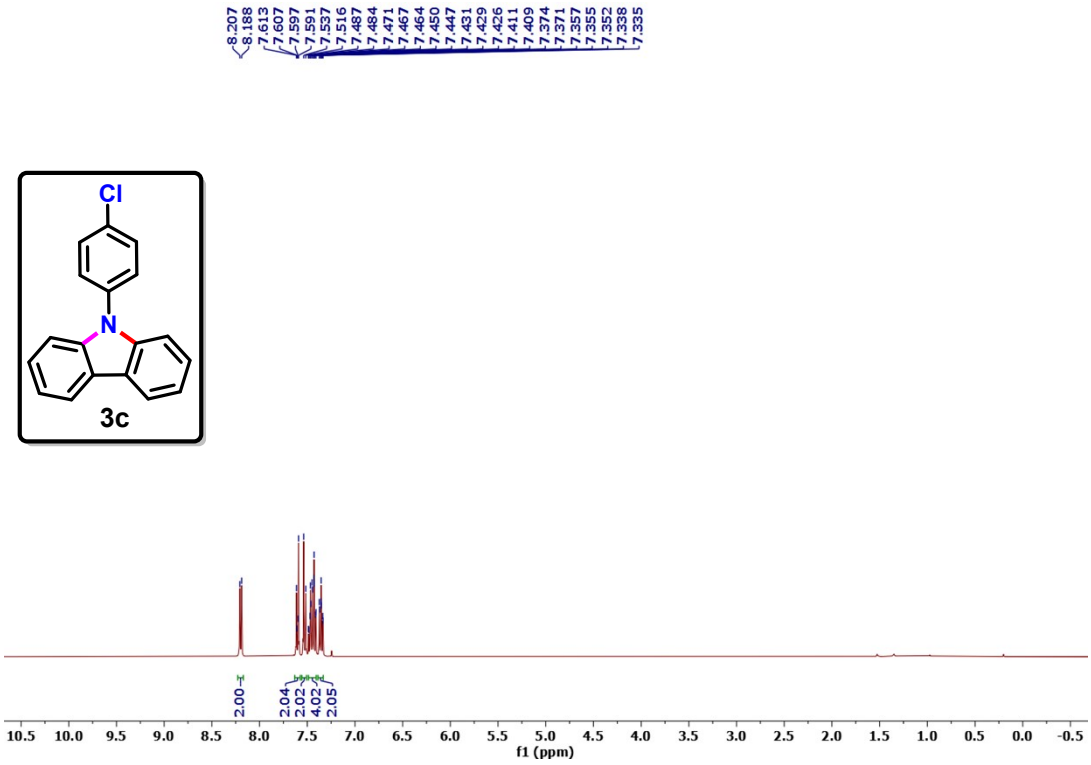

Fig. S21: ^{1}H-NMR Spectrum of **3c** in $CDCl_3$ (400 MHz)

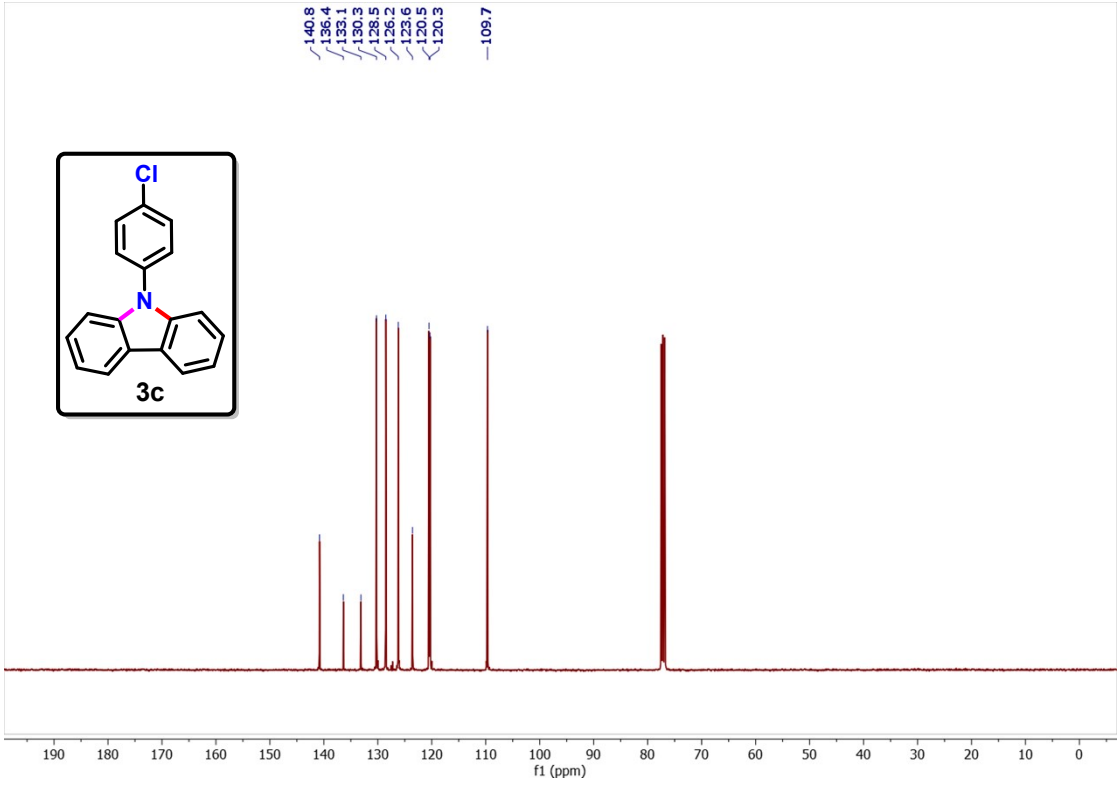

Fig. S22: $^{13}C\{^{1}H\}$-NMR Spectrum of **3c** in $CDCl_3$ (101 MHz)

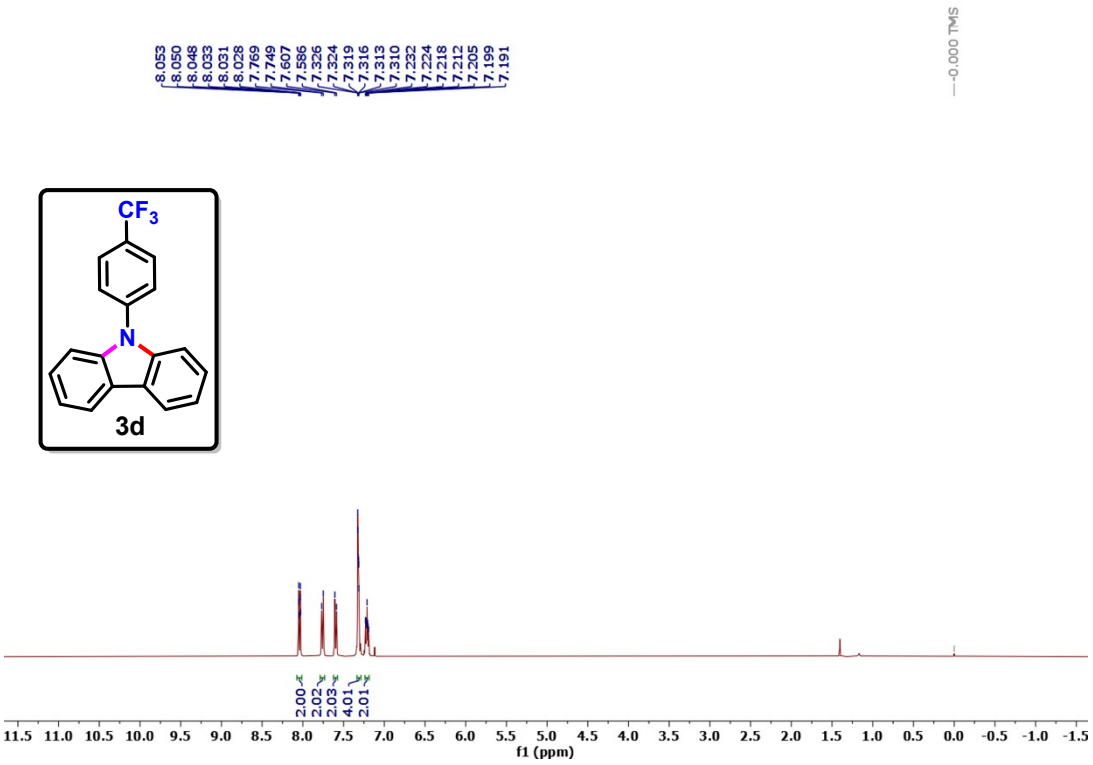

Fig. S23: ^{1}H-NMR Spectrum of **3d** in $CDCl_3$ (400 MHz)

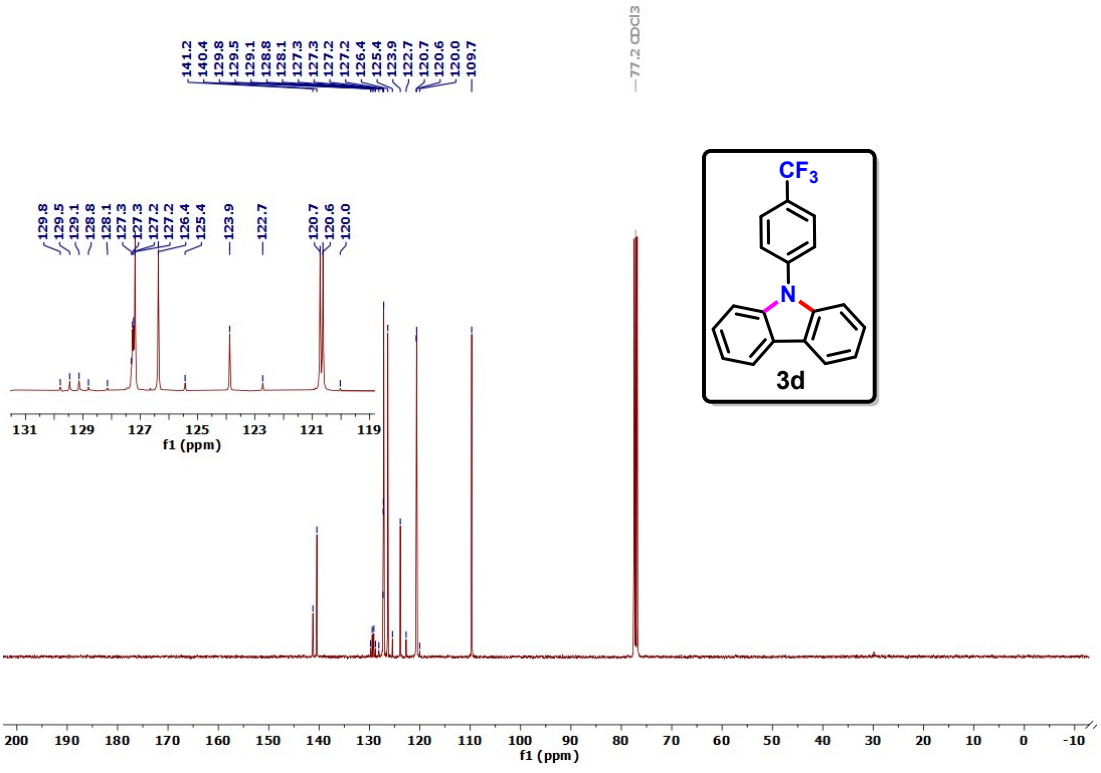

Fig. S24: $^{13}C\{^{1}H\}$-NMR Spectrum of **3d** in $CDCl_3$ (101 MHz)

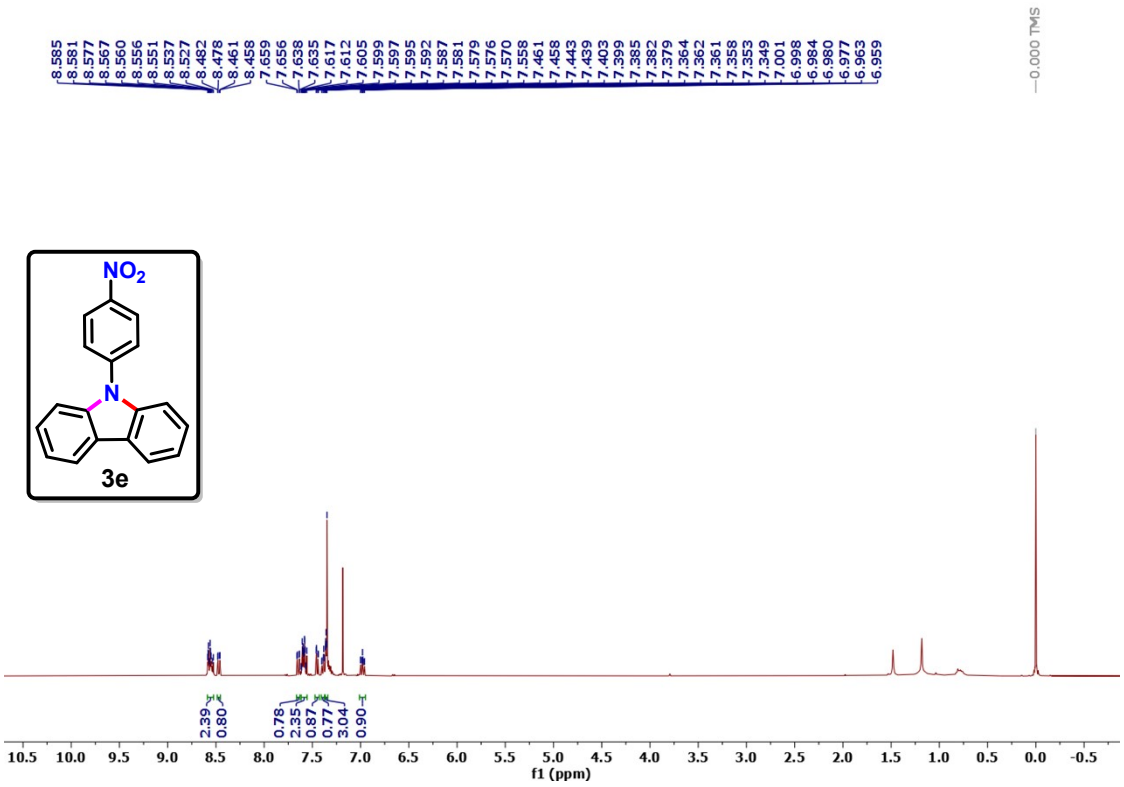

Fig. S25: ^{1}H-NMR Spectrum of **3e** in $CDCl_3$ (400 MHz)

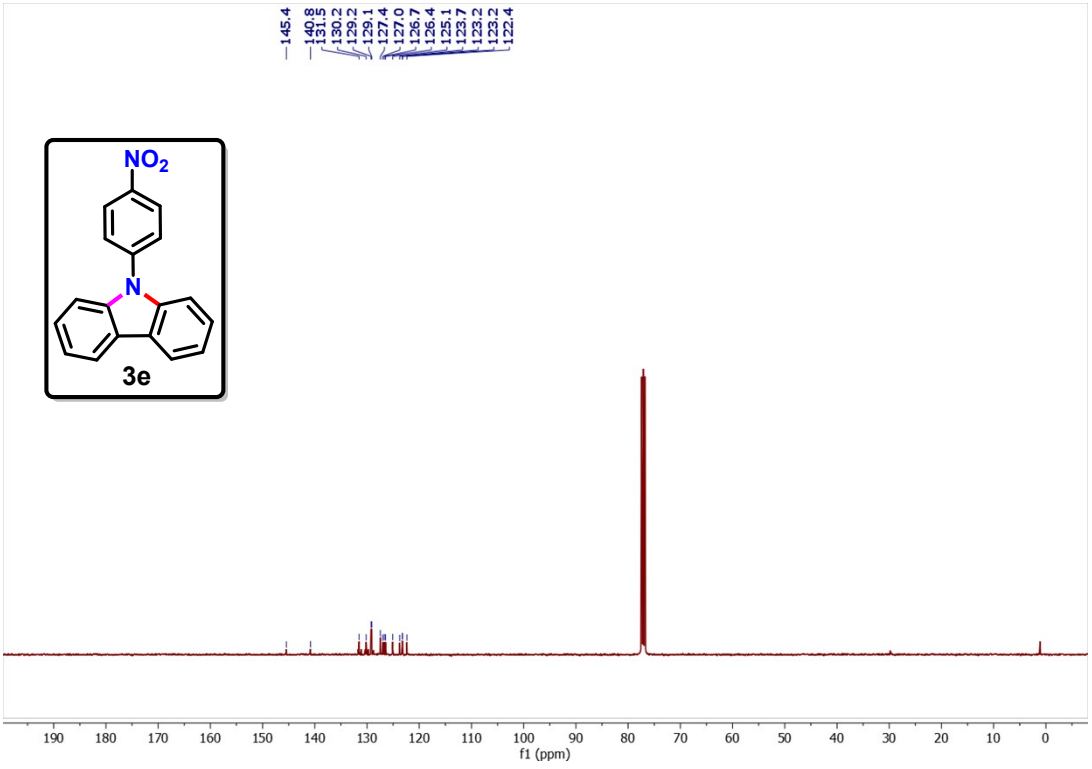

Fig. S26: $^{13}C\{^{1}H\}$-NMR Spectrum of **3e** in $CDCl_3$ (101 MHz)

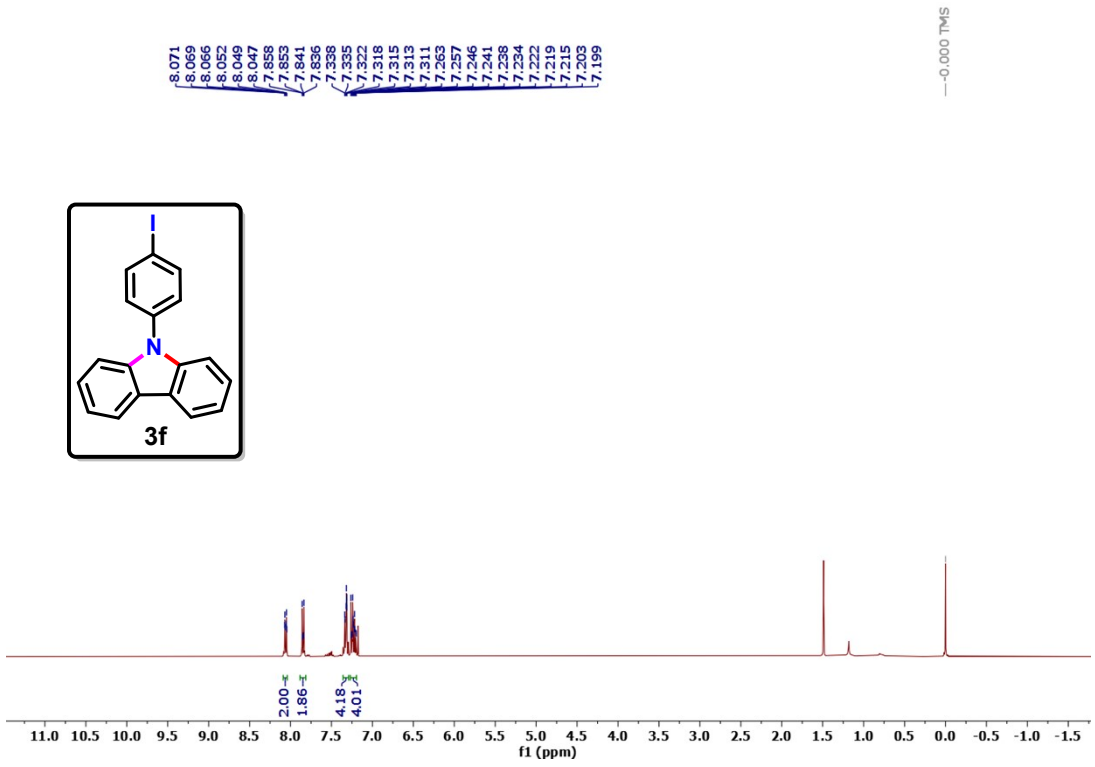

Fig. S27: ^{1}H-NMR Spectrum of **3f** in $CDCl_3$ (400 MHz)

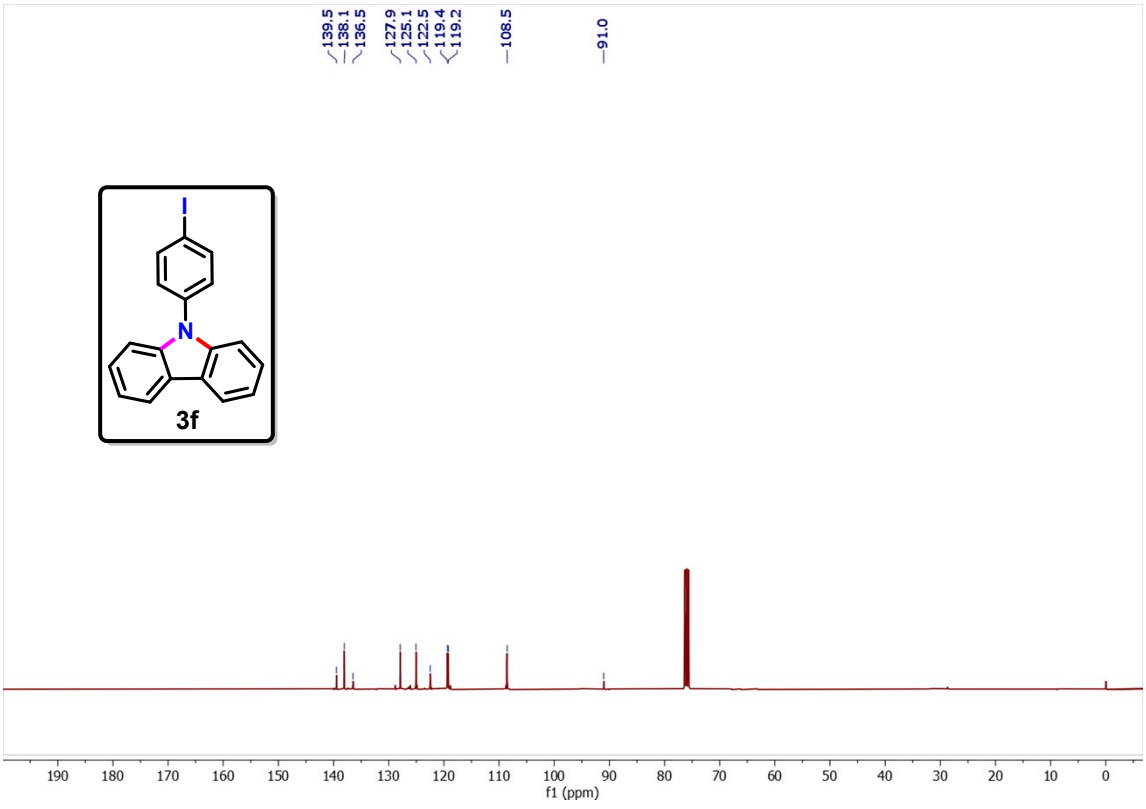

Fig. S28: $^{13}C\{^{1}H\}$-NMR Spectrum of **3f** in $CDCl_3$ (101 MHz)

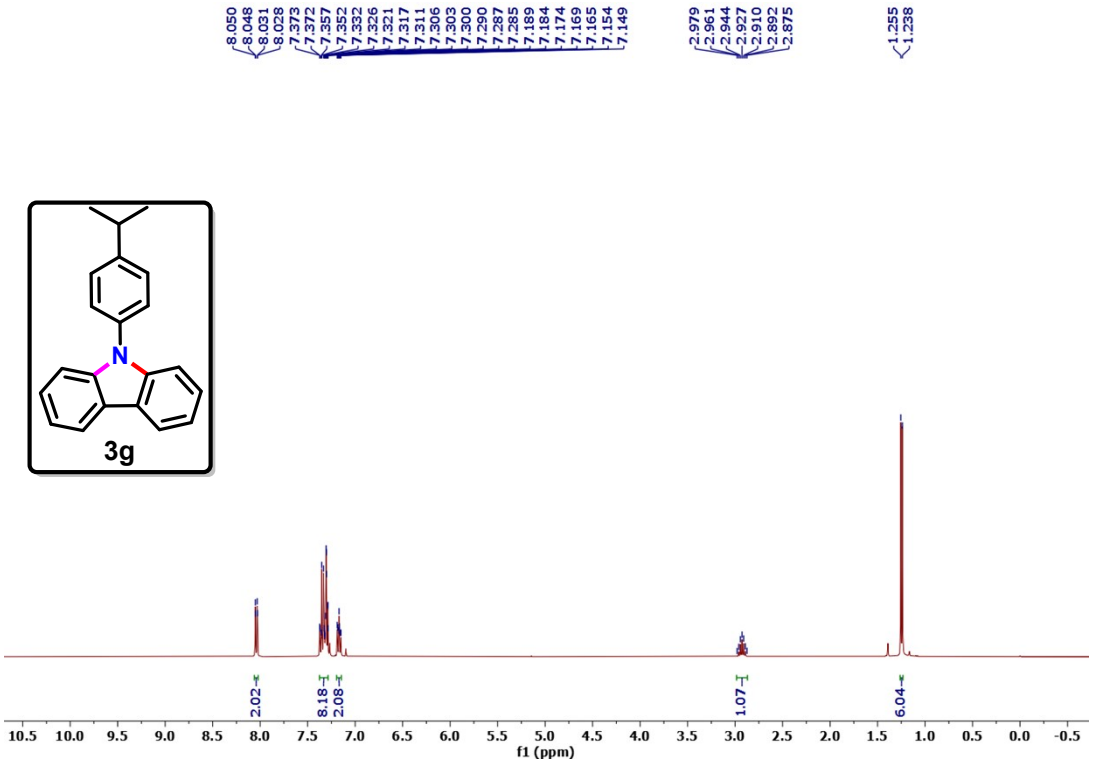

Fig. S29: ^{1}H-NMR Spectrum of **3g** in $CDCl_3$ (400 MHz)

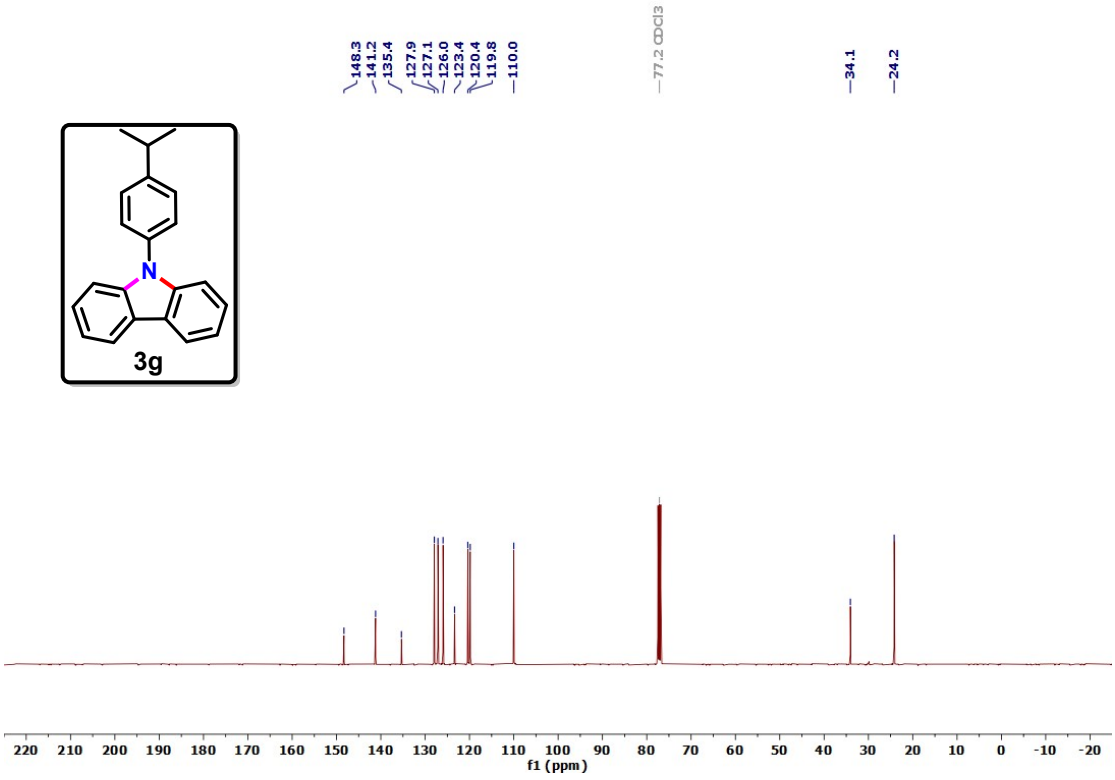

Fig. S30: $^{13}C\{^{1}H\}$-NMR Spectrum of **3g** in $CDCl_3$ (101 MHz)

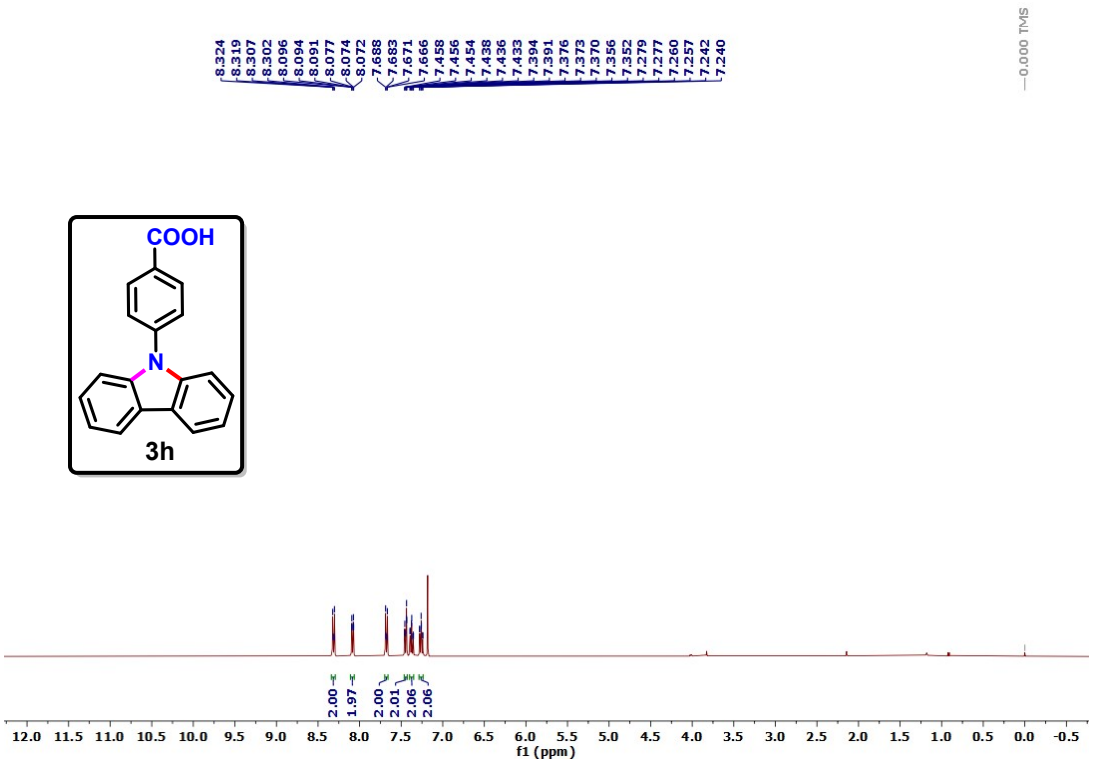

Fig. S31: ^{1}H-NMR Spectrum of **3h** in $CDCl_3$ (400 MHz)

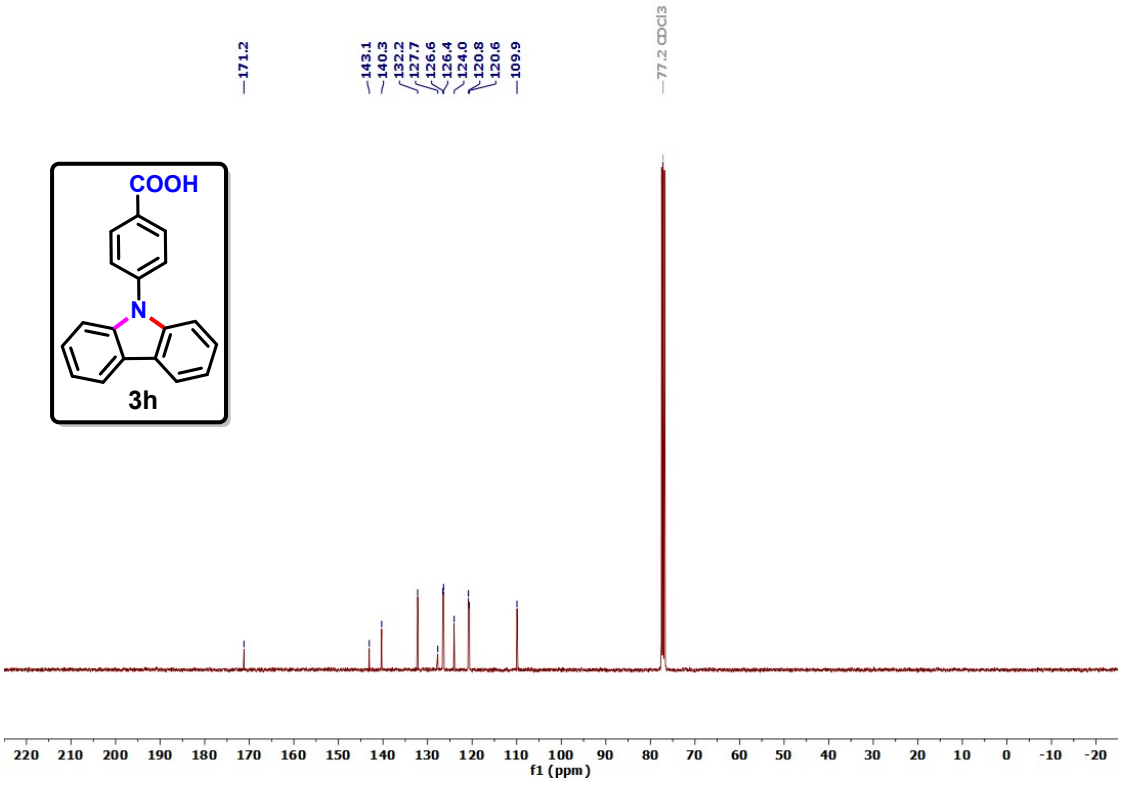

Fig. S32: $^{13}C\{^{1}H\}$-NMR Spectrum of **3h** in $CDCl_3$ (101 MHz)

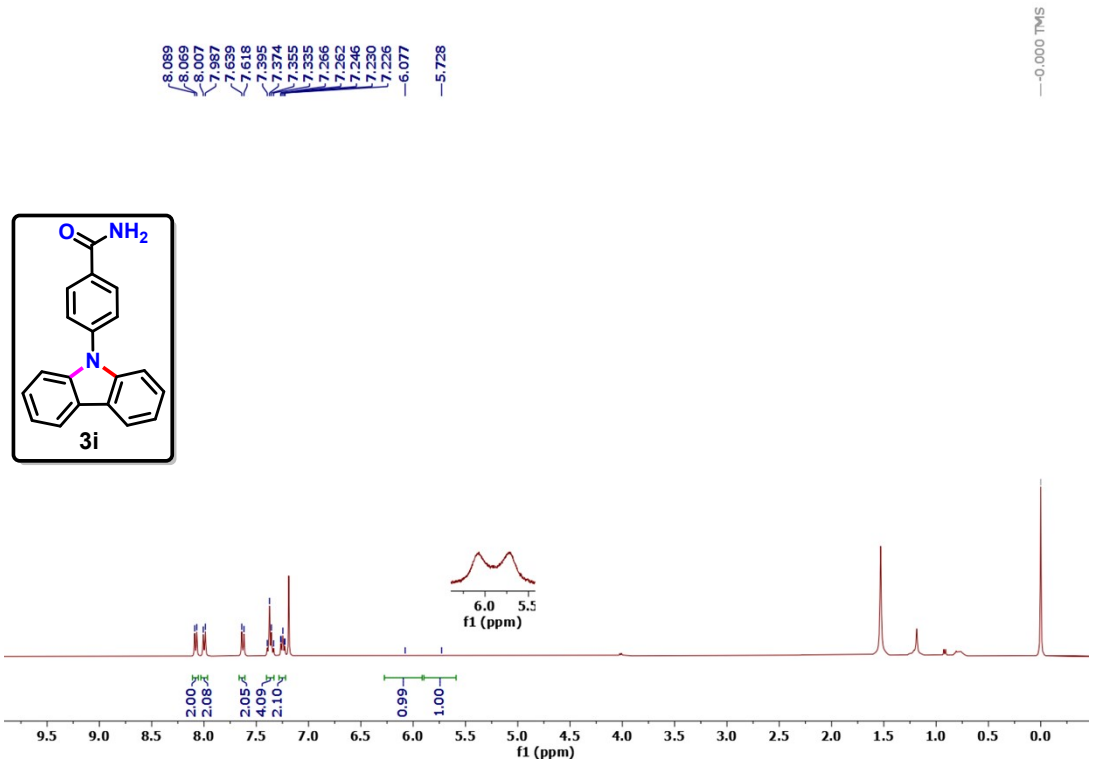

Fig. S33: ^{1}H-NMR Spectrum of **3i** in $CDCl_3$ (400 MHz)

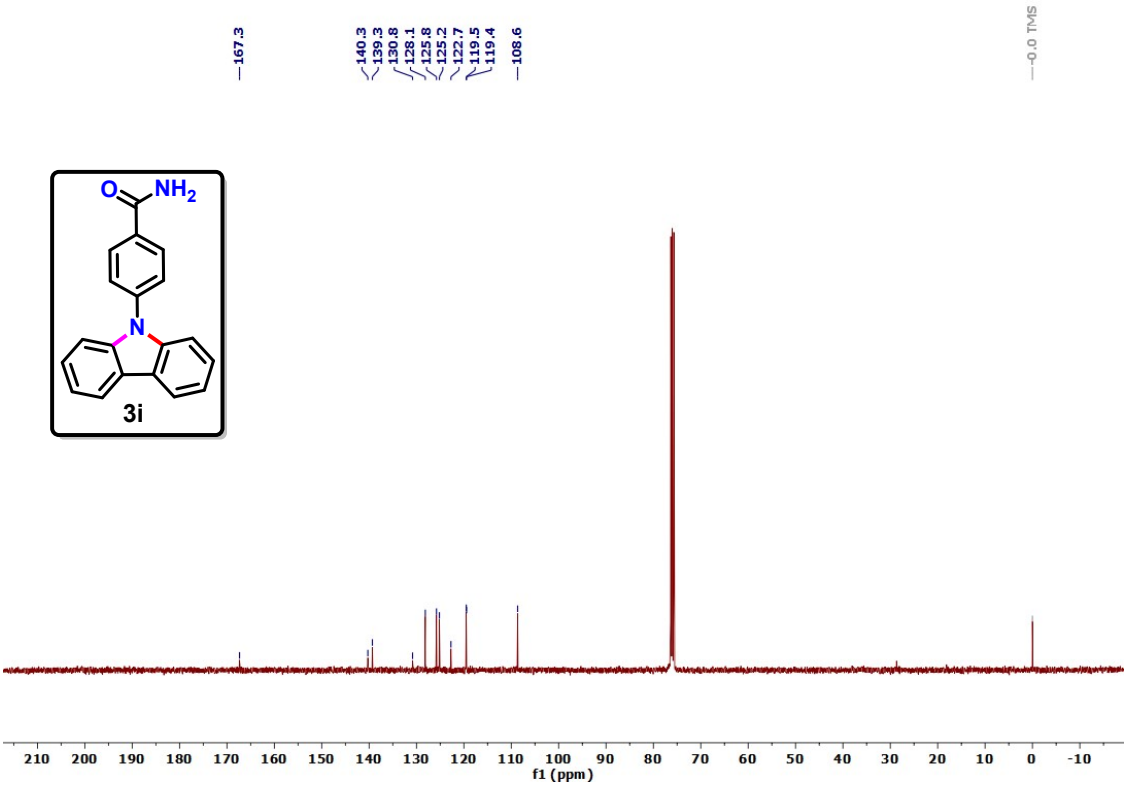

Fig. S34: $^{13}C\{^{1}H\}$-NMR Spectrum of **3i** in $CDCl_3$ (101 MHz)

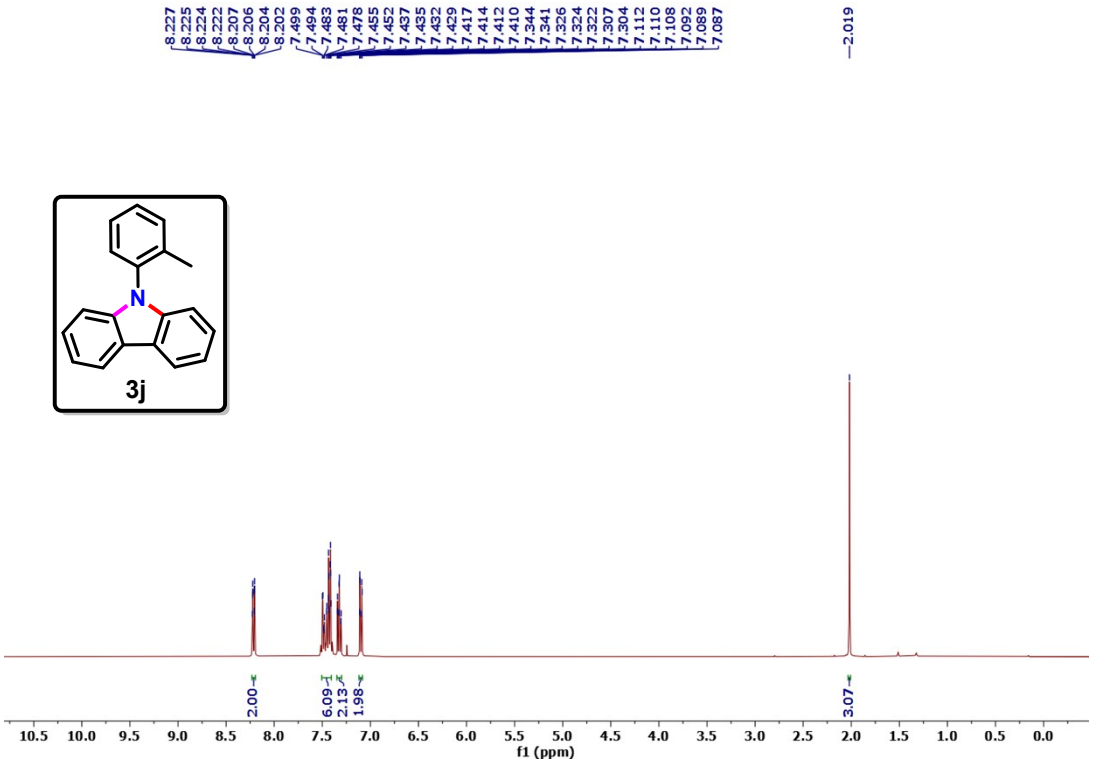

Fig. S35: ^{1}H-NMR Spectrum of **3j** in $CDCl_3$ (400 MHz)

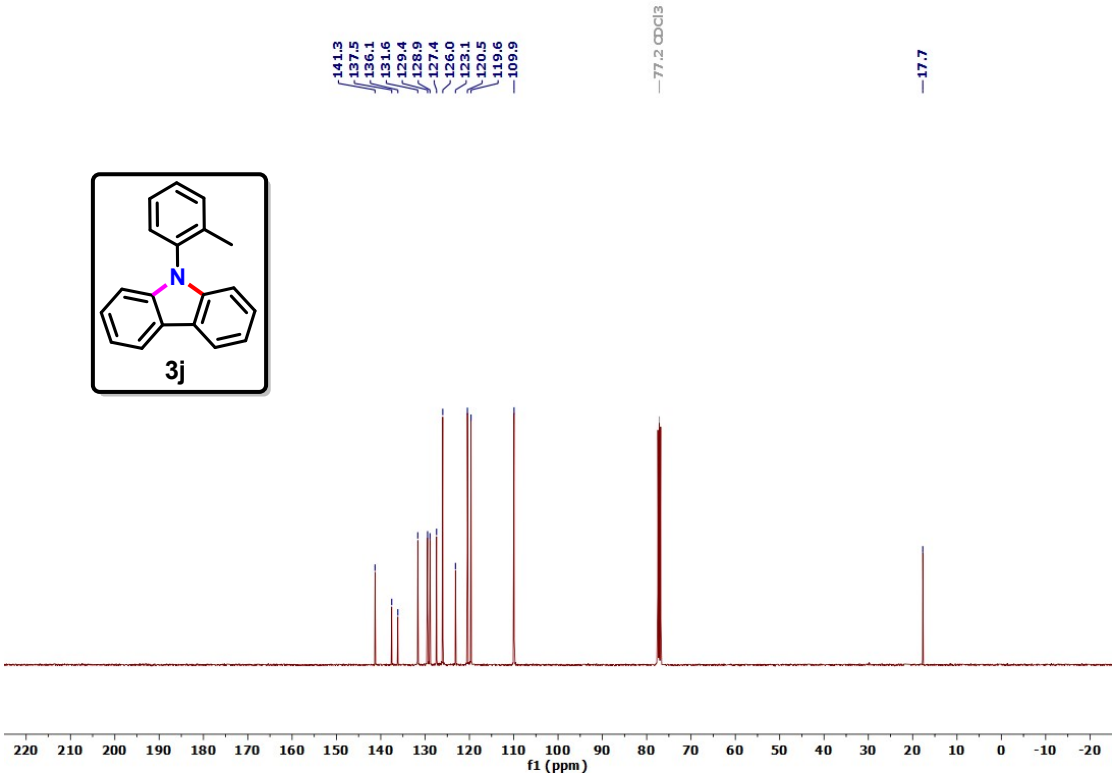

Fig. S36: $^{13}C\{^{1}H\}$-NMR Spectrum of **3j** in $CDCl_3$ (101 MHz)

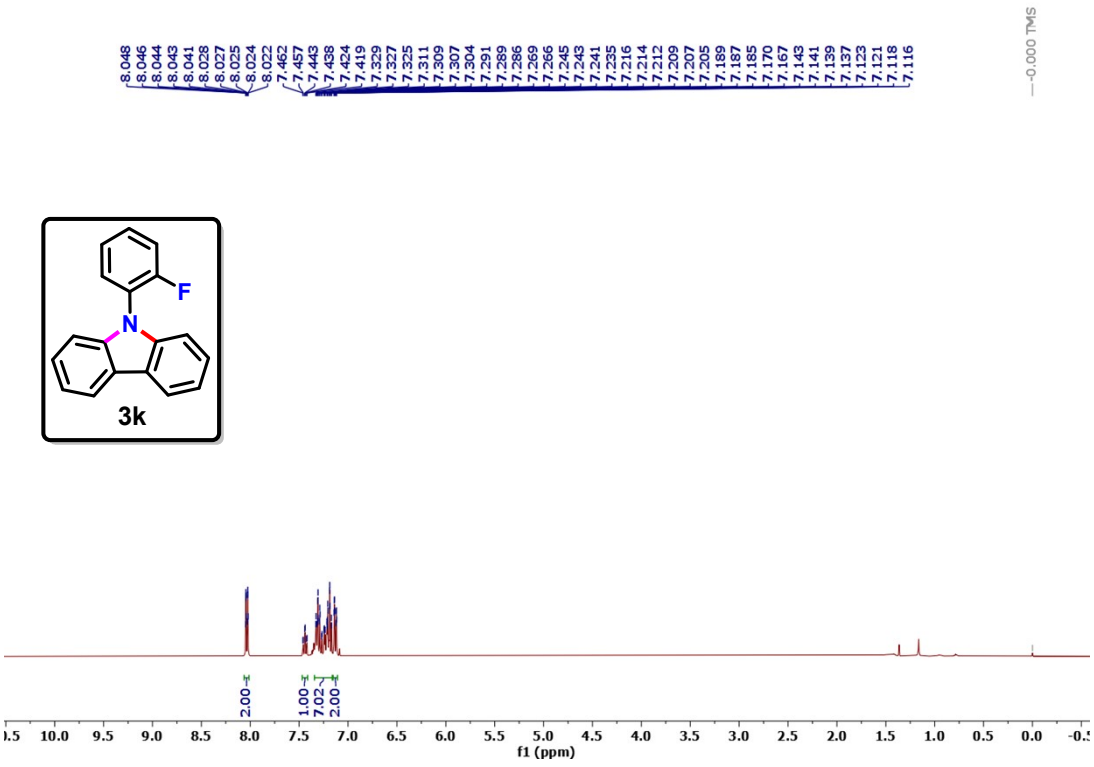

Fig. S37: ^{1}H-NMR Spectrum of **3k** in $CDCl_3$ (400 MHz)

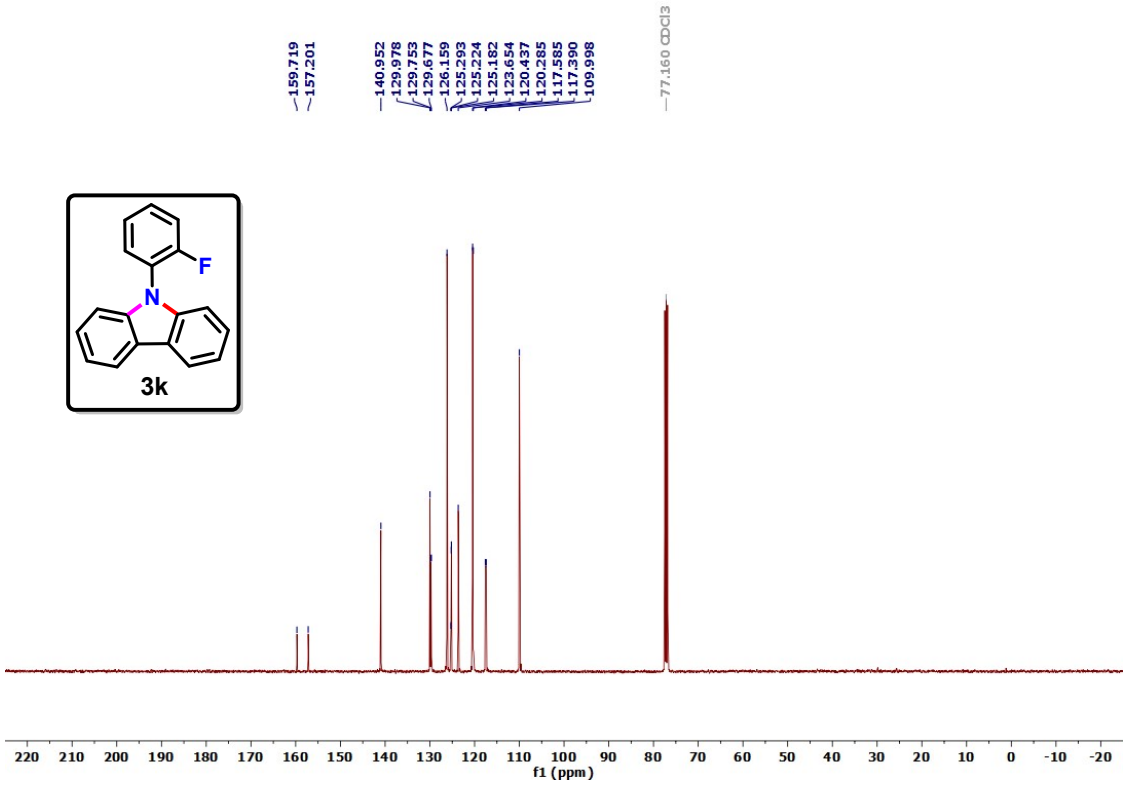

Fig. S38: $^{13}C\{^{1}H\}$-NMR Spectrum of **3k** in $CDCl_3$ (101 MHz)

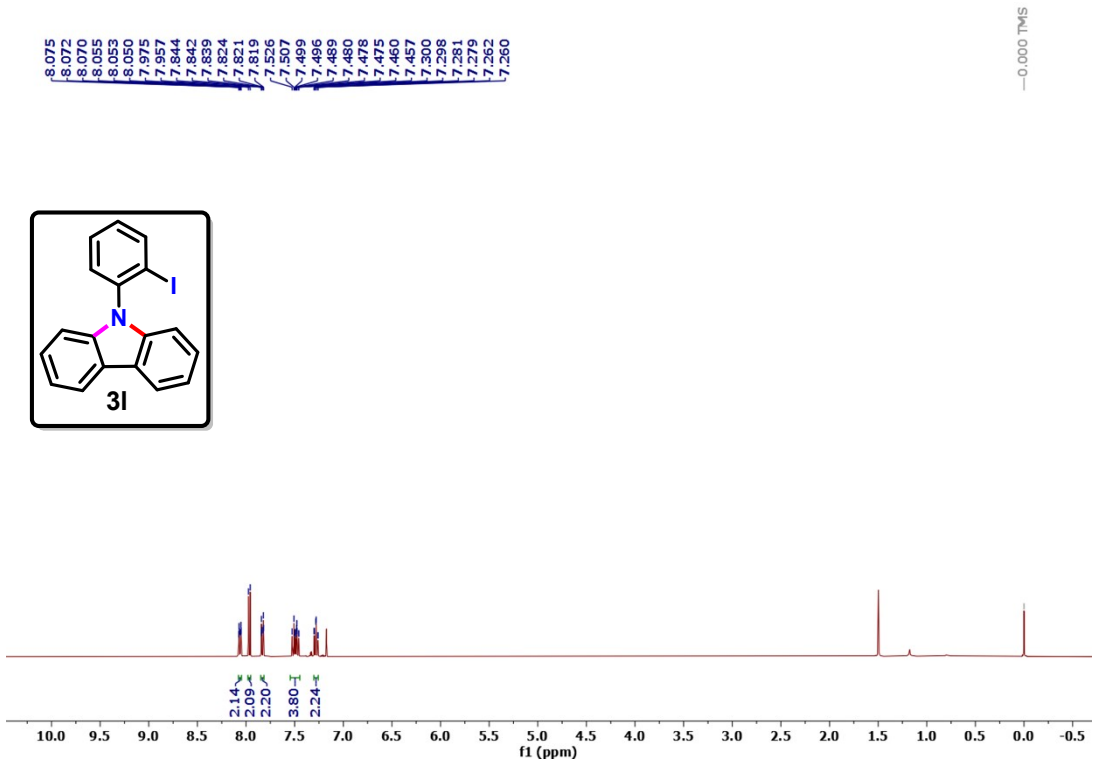

Fig. S39: ^{1}H-NMR Spectrum of **3l** in $CDCl_3$ (400 MHz)

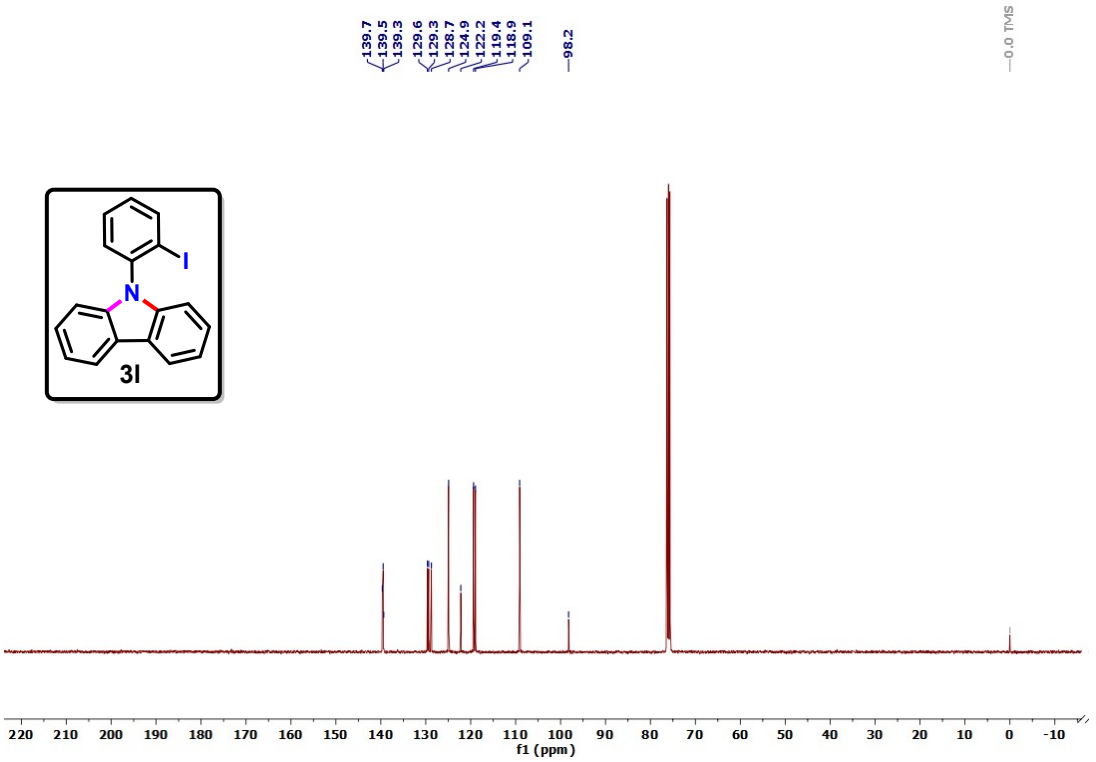

Fig. S40: $^{13}C\{^{1}H\}$-NMR Spectrum of **3l** in $CDCl_3$ (101 MHz)

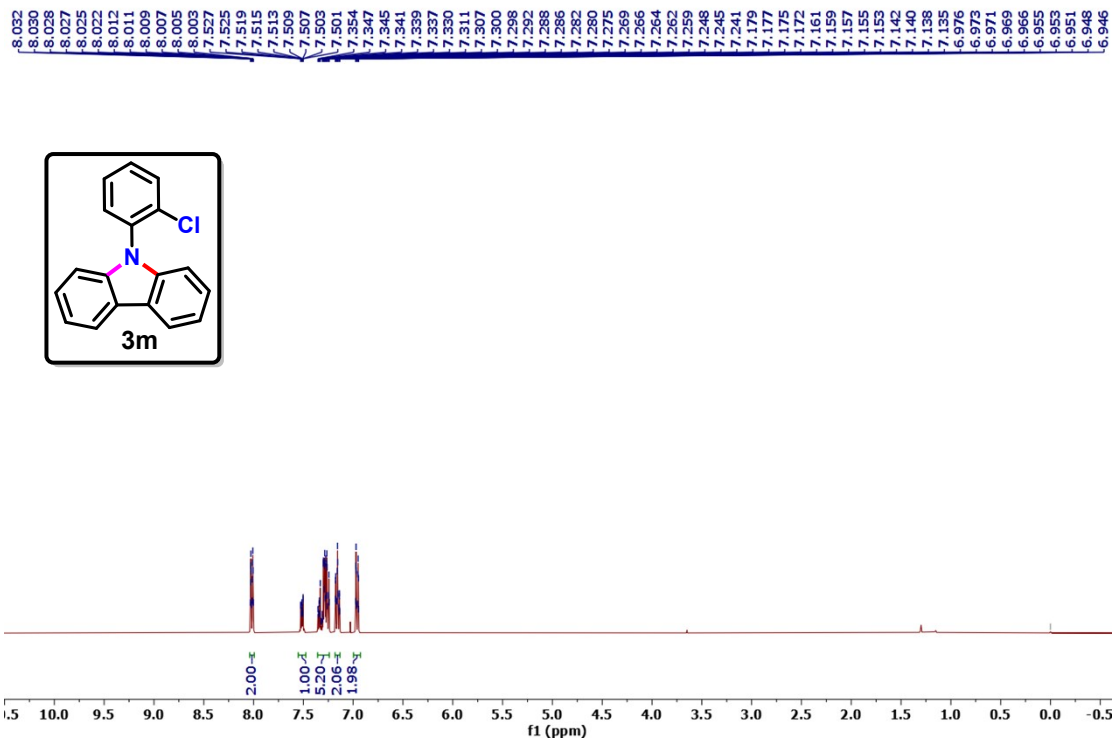

Fig. S41: ^{1}H-NMR Spectrum of **3m** in $CDCl_3$ (400 MHz)

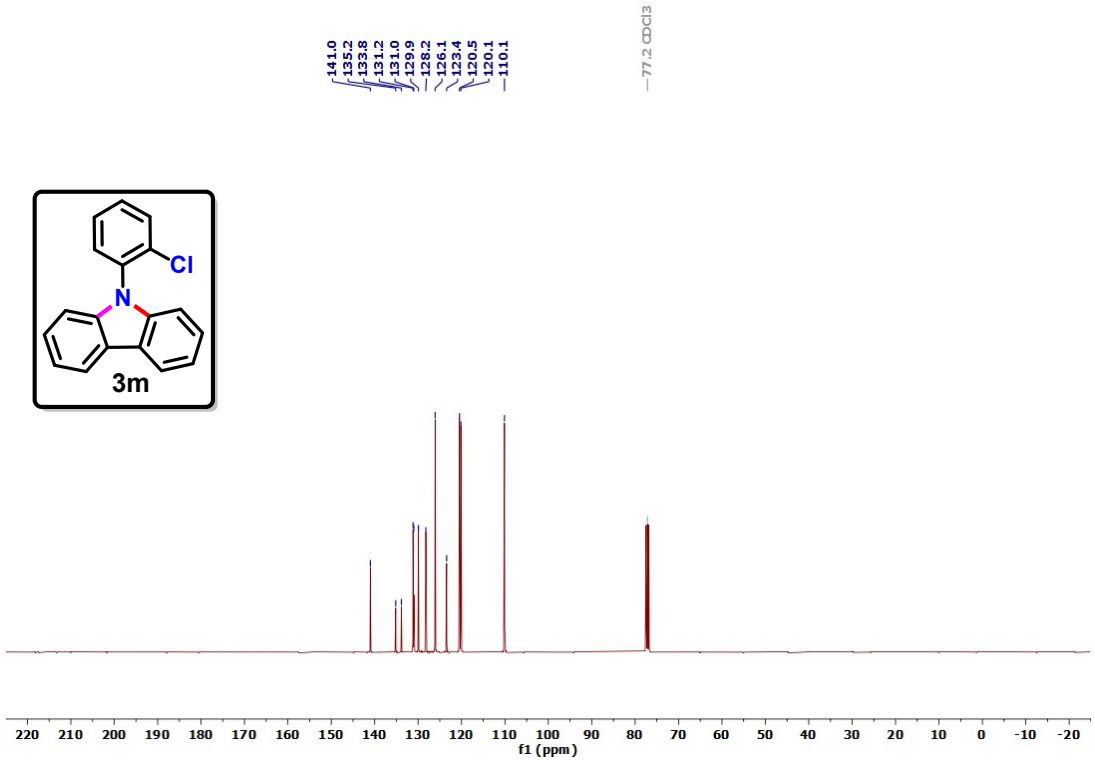

Fig. S42: $^{13}C\{^{1}H\}$-NMR Spectrum of **3m** in $CDCl_3$ (101 MHz)

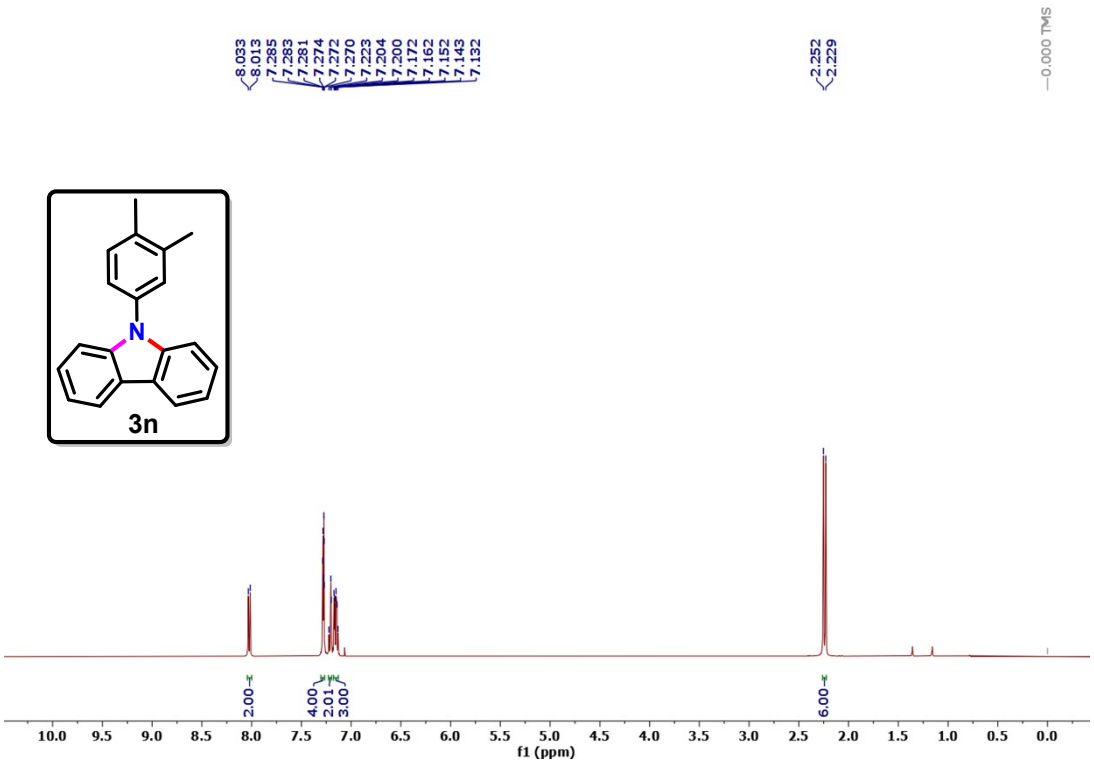

Fig. S43: ^{1}H-NMR Spectrum of **3n** in $CDCl_3$ (400 MHz)

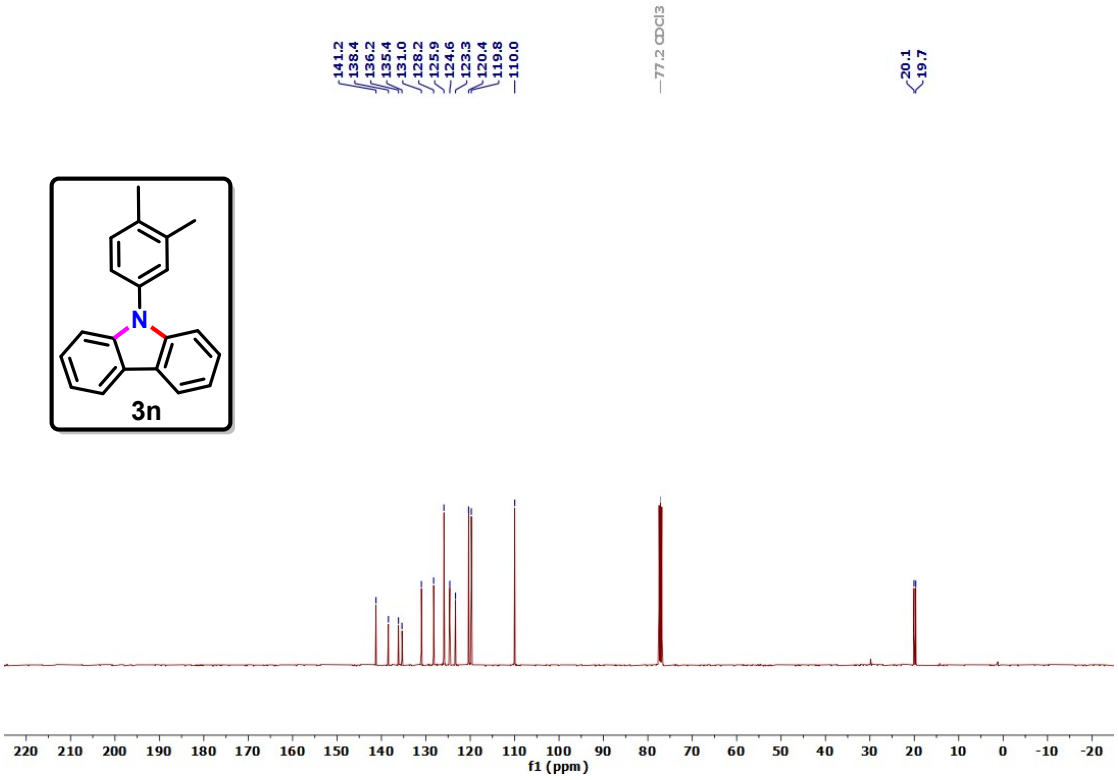

Fig. S44: $^{13}C\{^{1}H\}$-NMR Spectrum of **3n** in $CDCl_3$ (101 MHz)

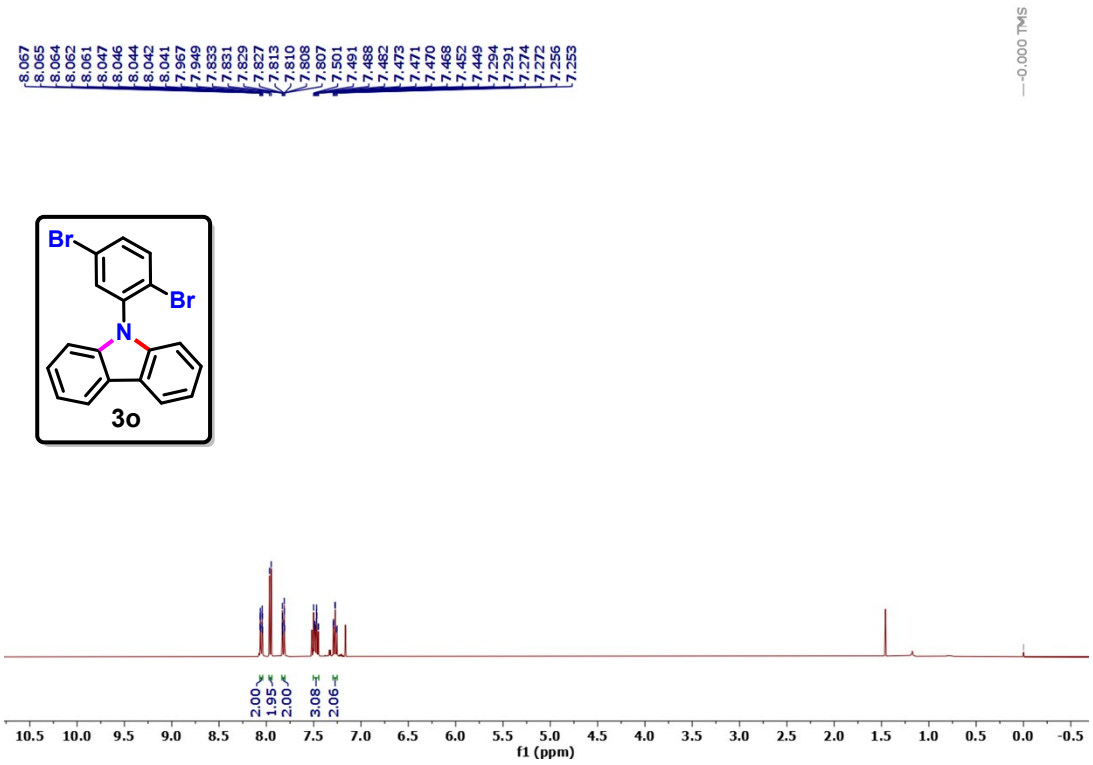

Fig. S45: ^{1}H-NMR Spectrum of **3o** in $CDCl_3$ (400 MHz)

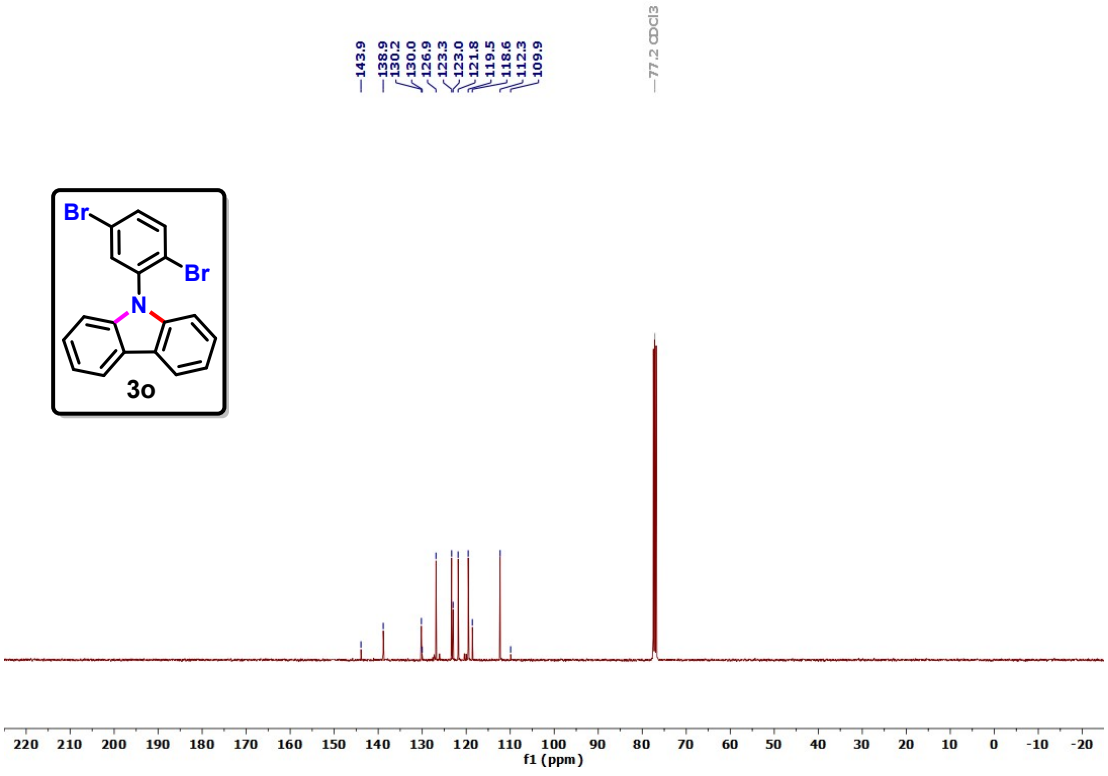

Fig. S46: $^{13}C\{^{1}H\}$-NMR Spectrum of **3o** in $CDCl_3$ (101 MHz)

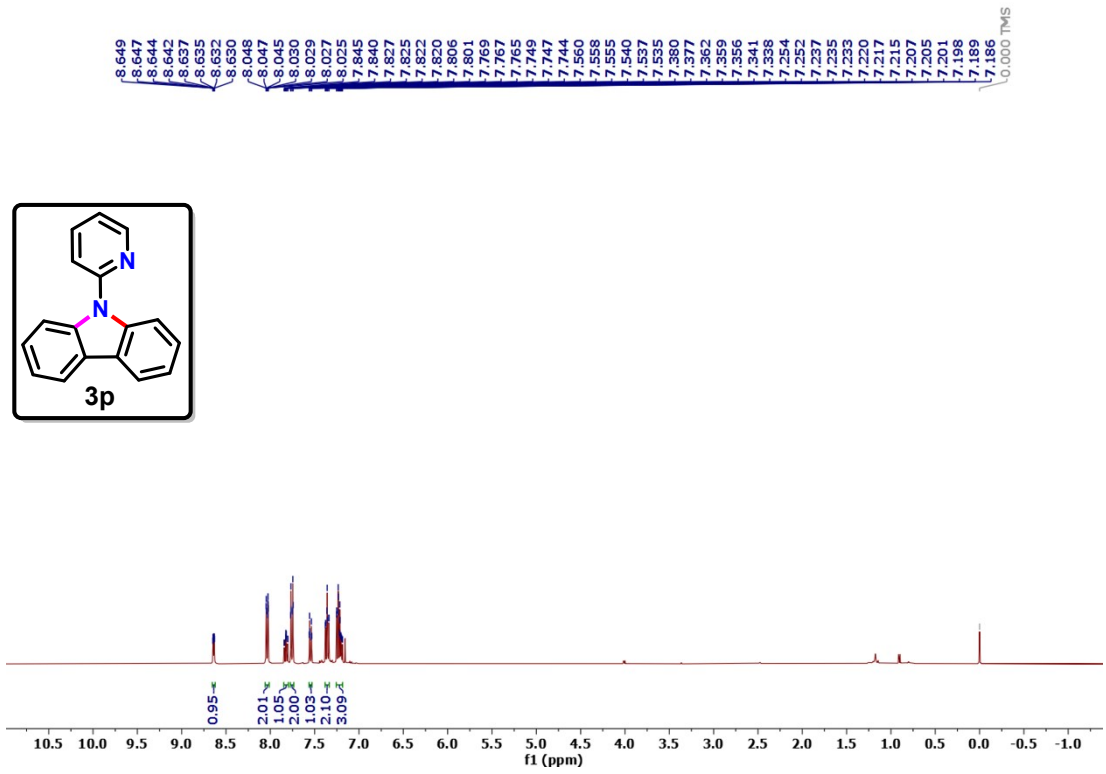

Fig. S47: ^{1}H-NMR Spectrum of **3p** in $CDCl_3$ (400 MHz)

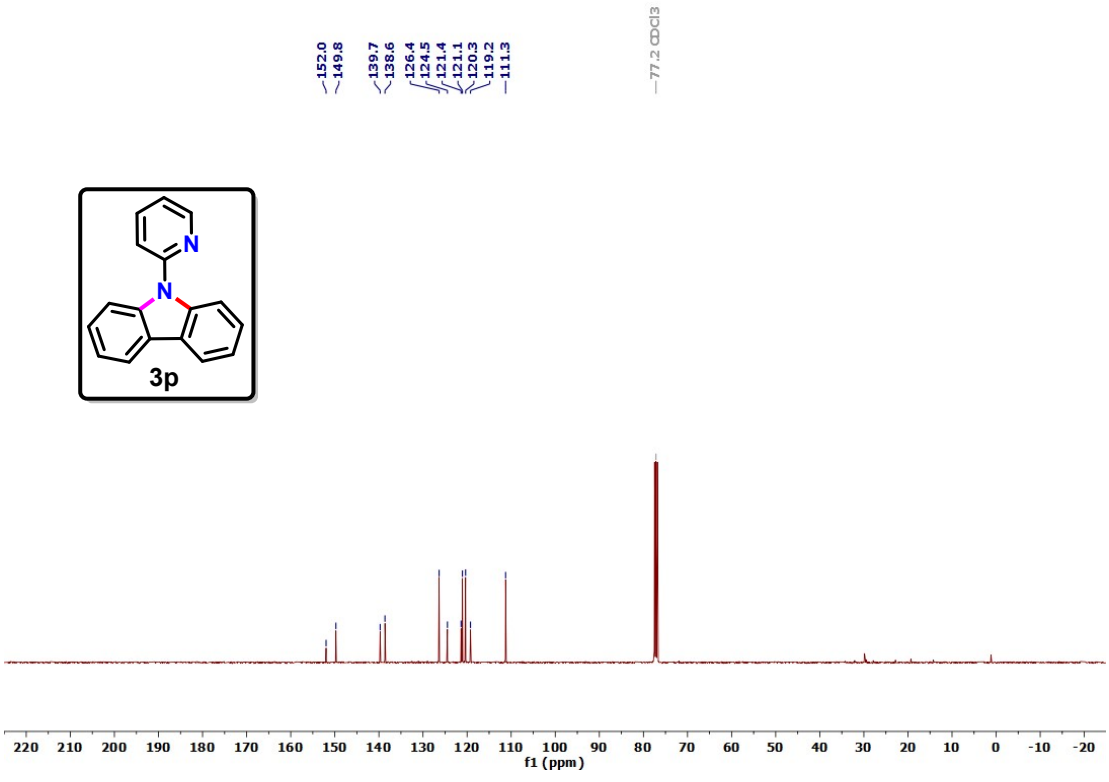

Fig. S48: $^{13}C\{^{1}H\}$-NMR Spectrum of **3p** in $CDCl_3$ (101 MHz)

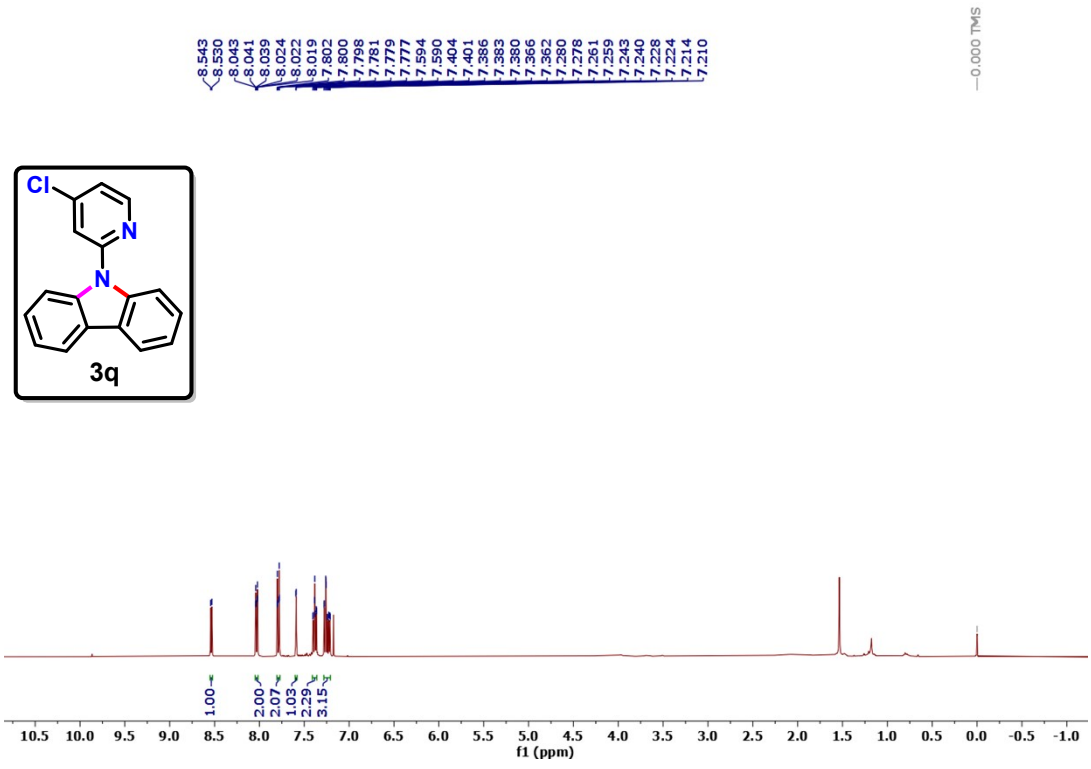

Fig. S49: ^{1}H-NMR Spectrum of **3q** in $CDCl_3$ (400 MHz)

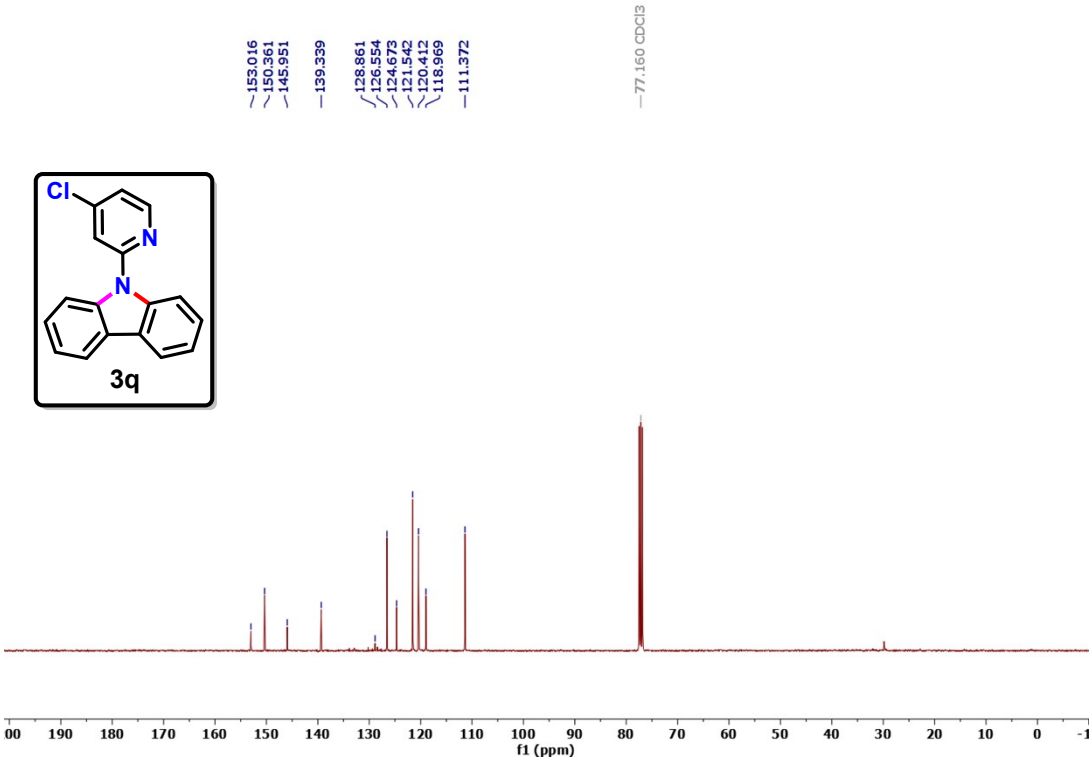

Fig. S50: ^{13}C{1H}-NMR Spectrum of **3q** in $CDCl_3$ (101 MHz)

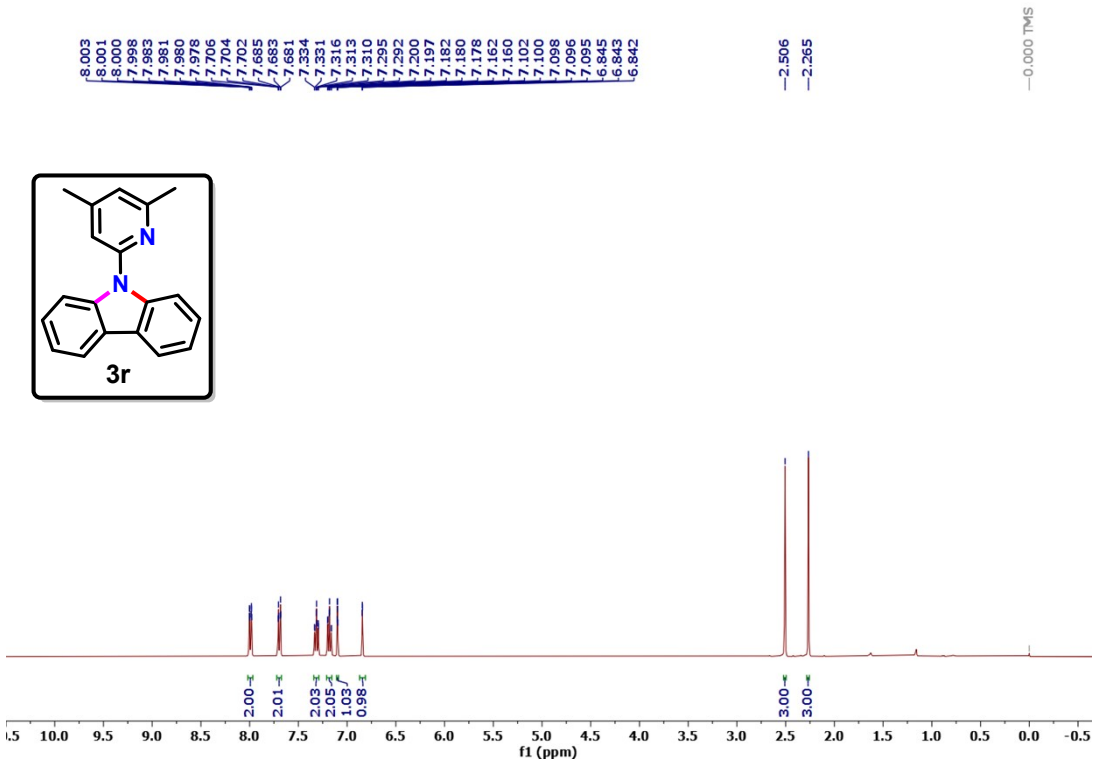

Fig. S51: ^{1}H-NMR Spectrum of **3r** in $CDCl_3$ (400 MHz)

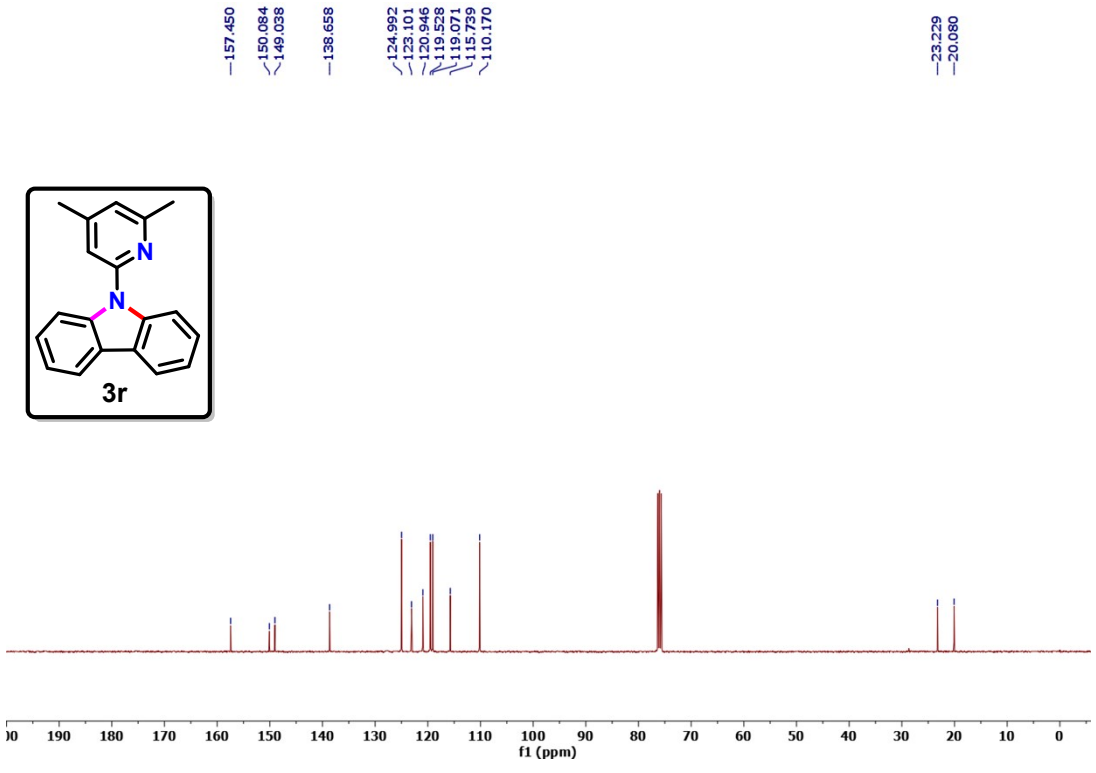

Fig. S52: ^{13}C{1H}-NMR Spectrum of **3r** in $CDCl_3$ (101 MHz)

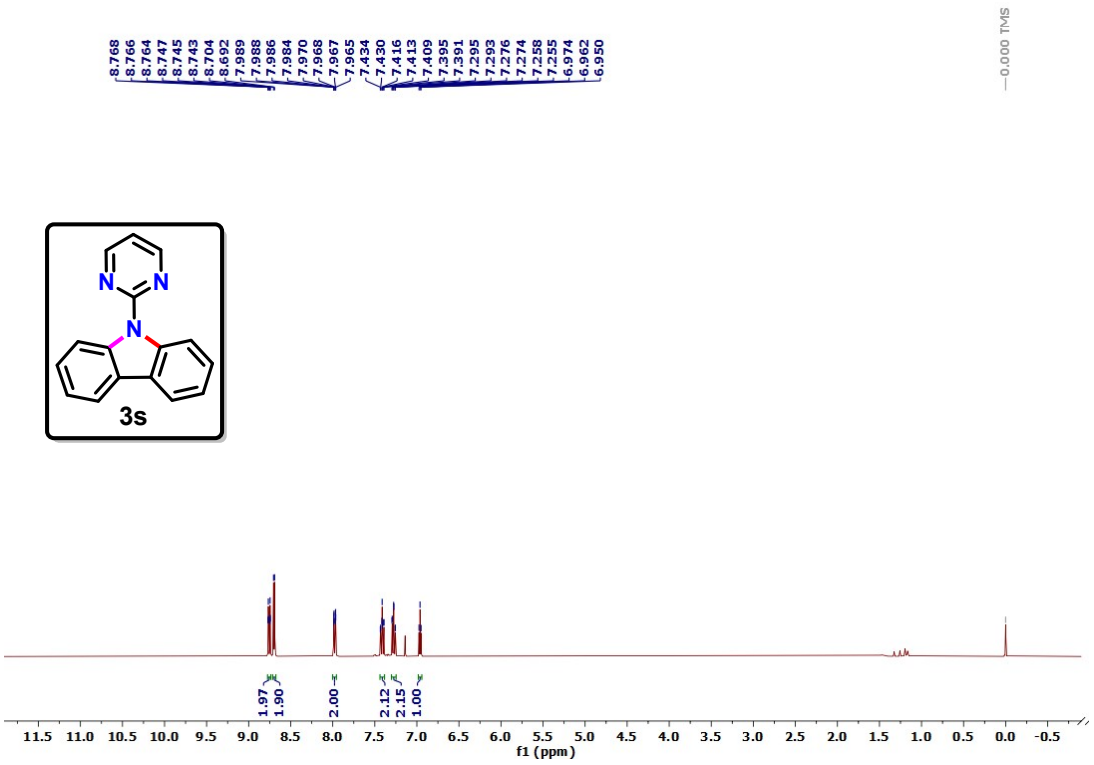

Fig. S53: ^{1}H-NMR Spectrum of **3s** in $CDCl_3$ (400 MHz)

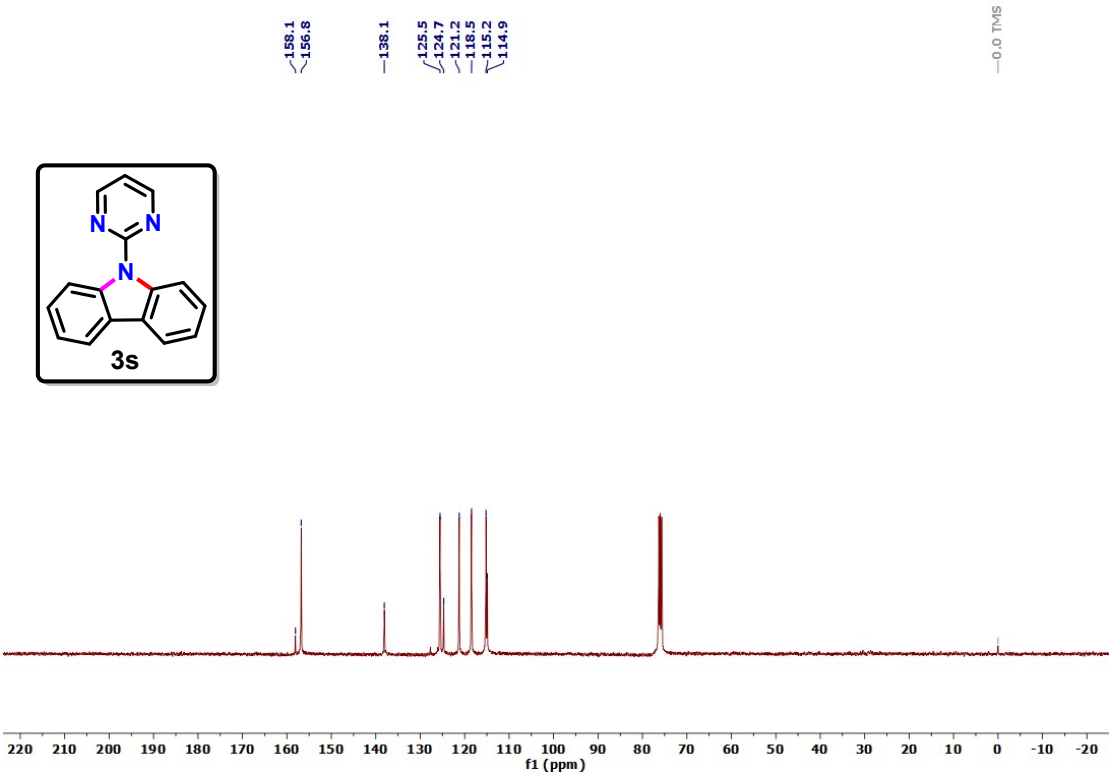

Fig. S54: ^{13}C{1H}-NMR Spectrum of **3s** in $CDCl_3$ (101 MHz)

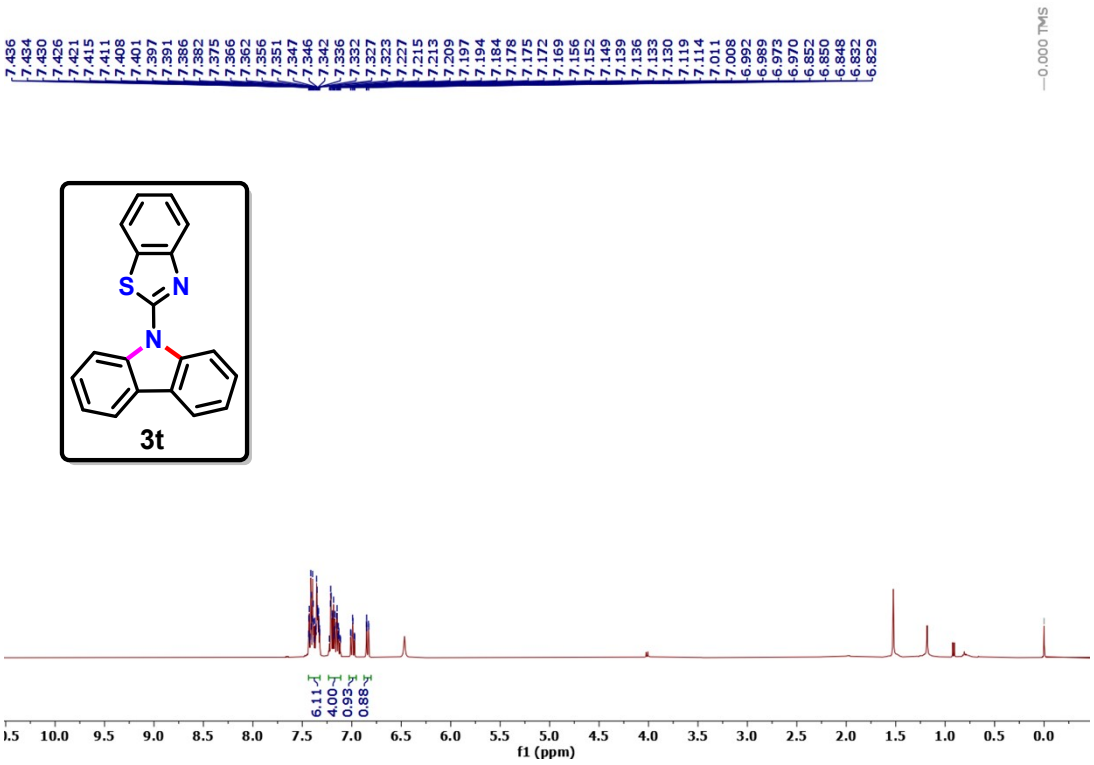

Fig. S55: ^{1}H-NMR Spectrum of **3t** in $CDCl_3$ (400 MHz)

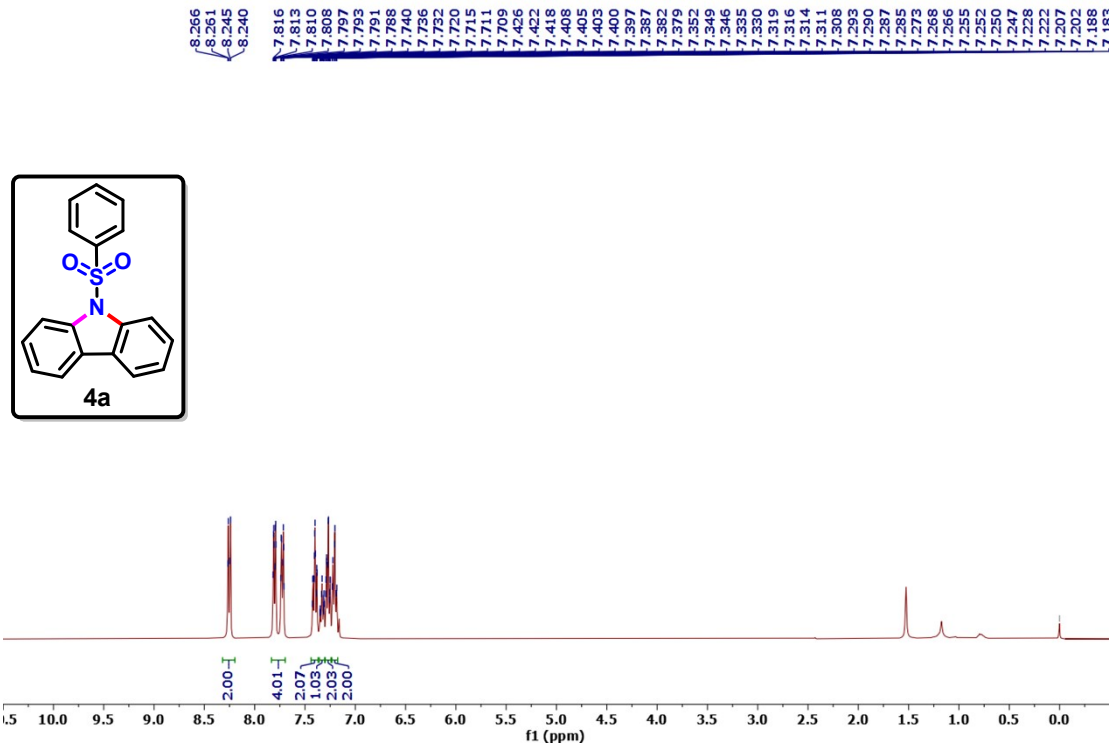

Fig. S56: ^{1}H-NMR Spectrum of **4a** in $CDCl_3$ (400 MHz)

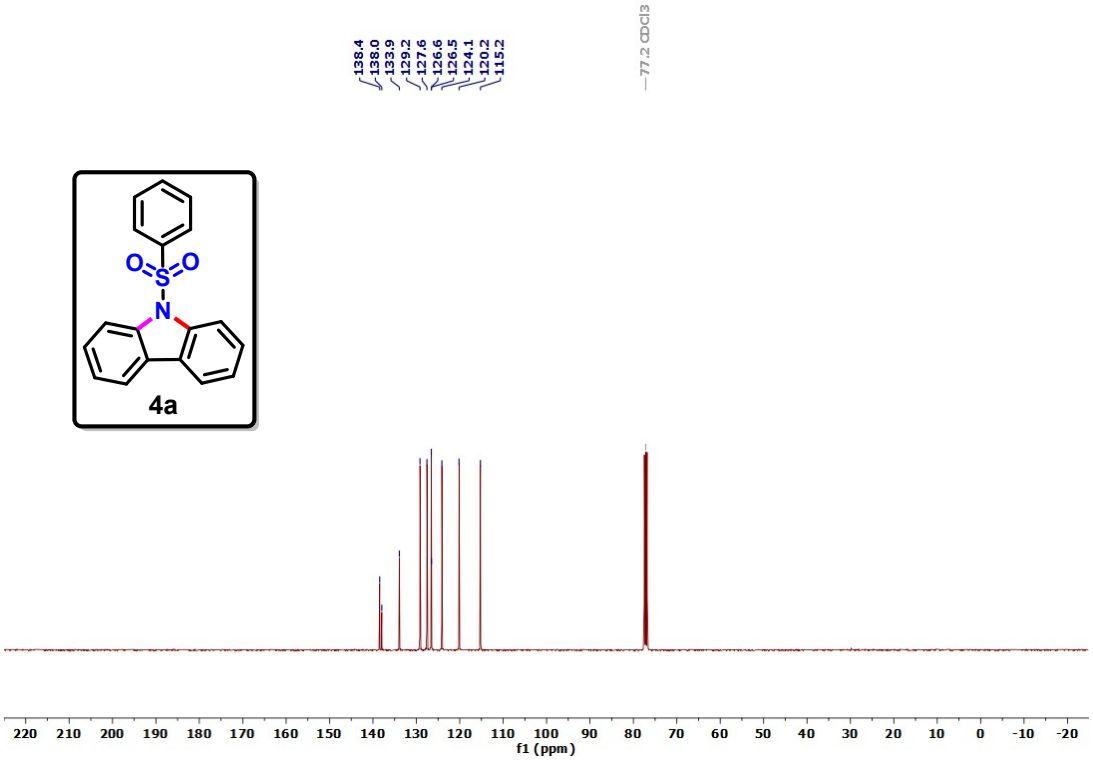

Fig. S57: $^{13}C\{1H\}$-NMR Spectrum of **4a** in $CDCl_3$ (101 MHz)

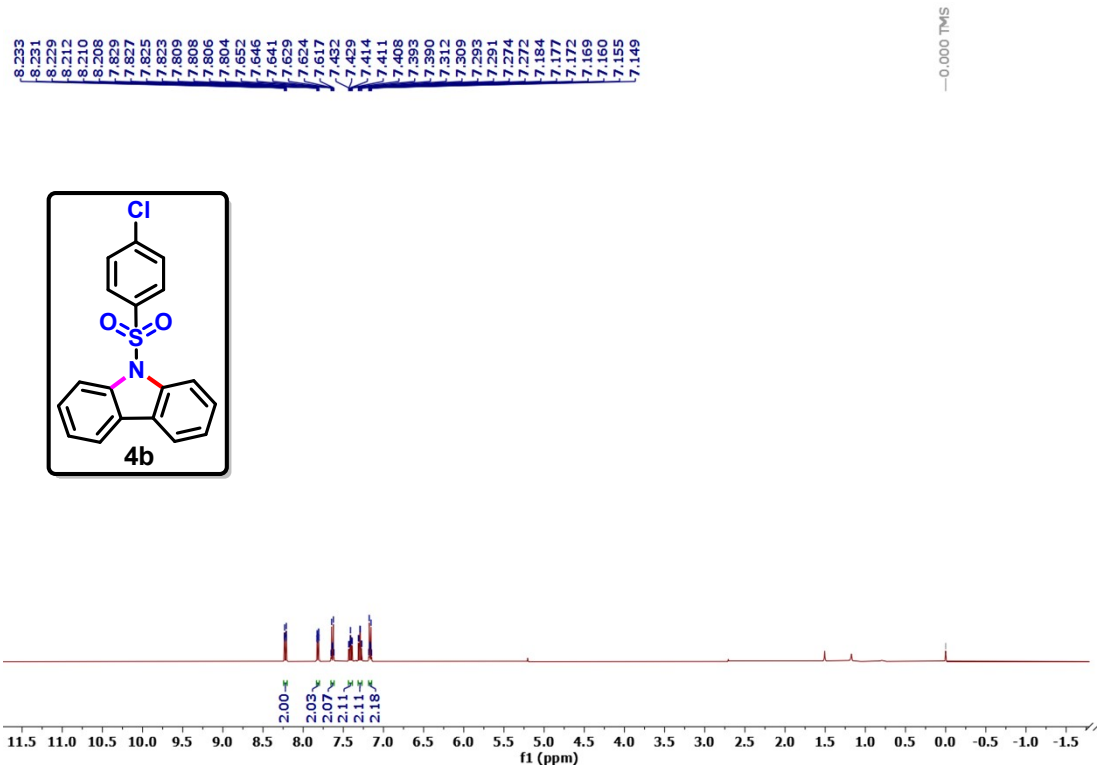

Fig. S58: ^{1}H-NMR Spectrum of **4b** in $CDCl_3$ (400 MHz)

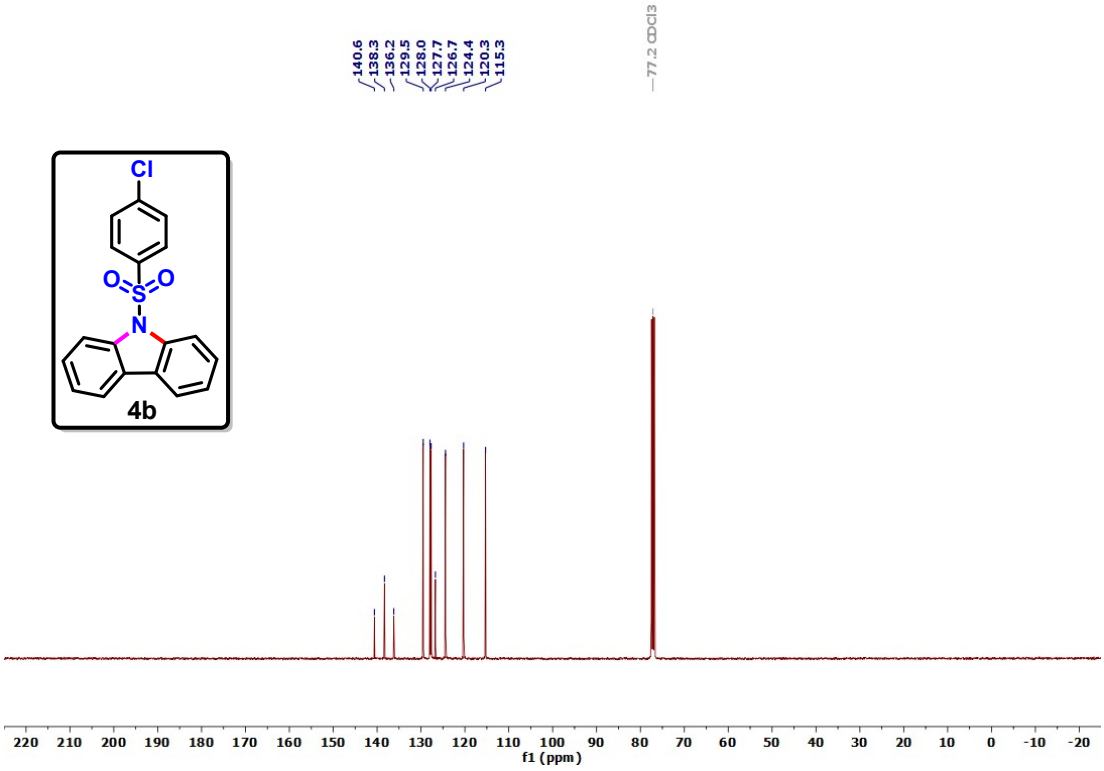

Fig. S59: $^{13}C\{1H\}$-NMR Spectrum of **4b** in $CDCl_3$ (101 MHz)

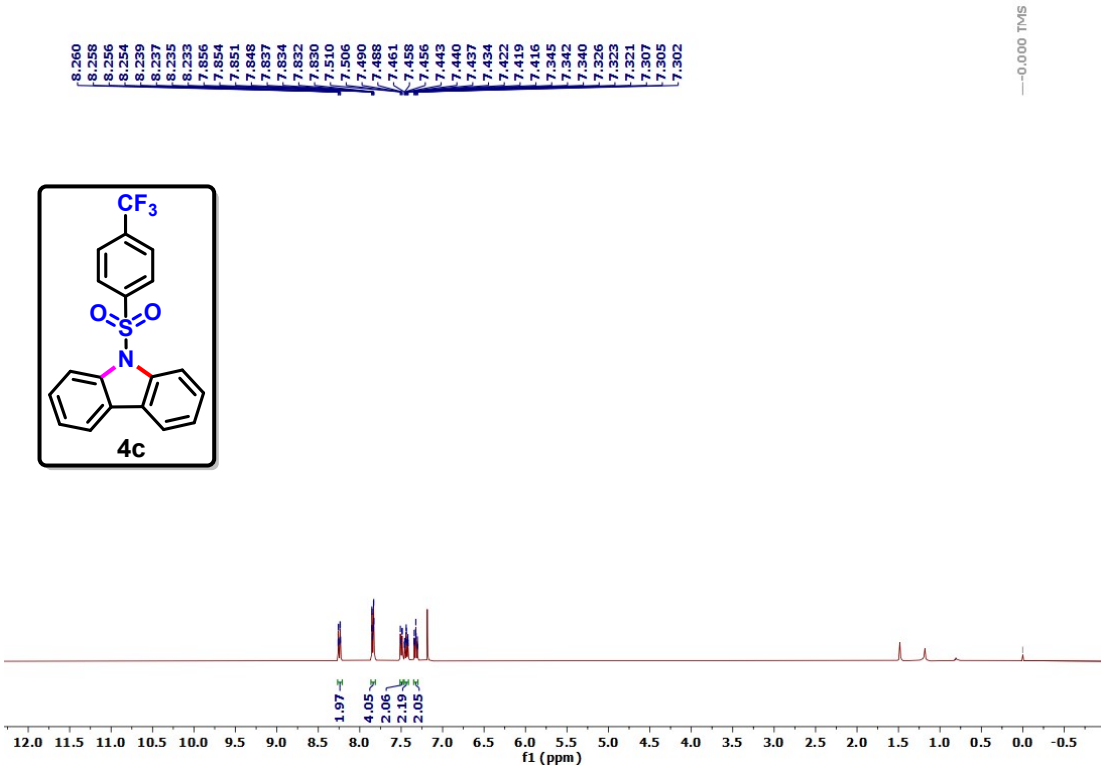

Fig. S60: ^{1}H-NMR Spectrum of **4c** in $CDCl_3$ (400 MHz)

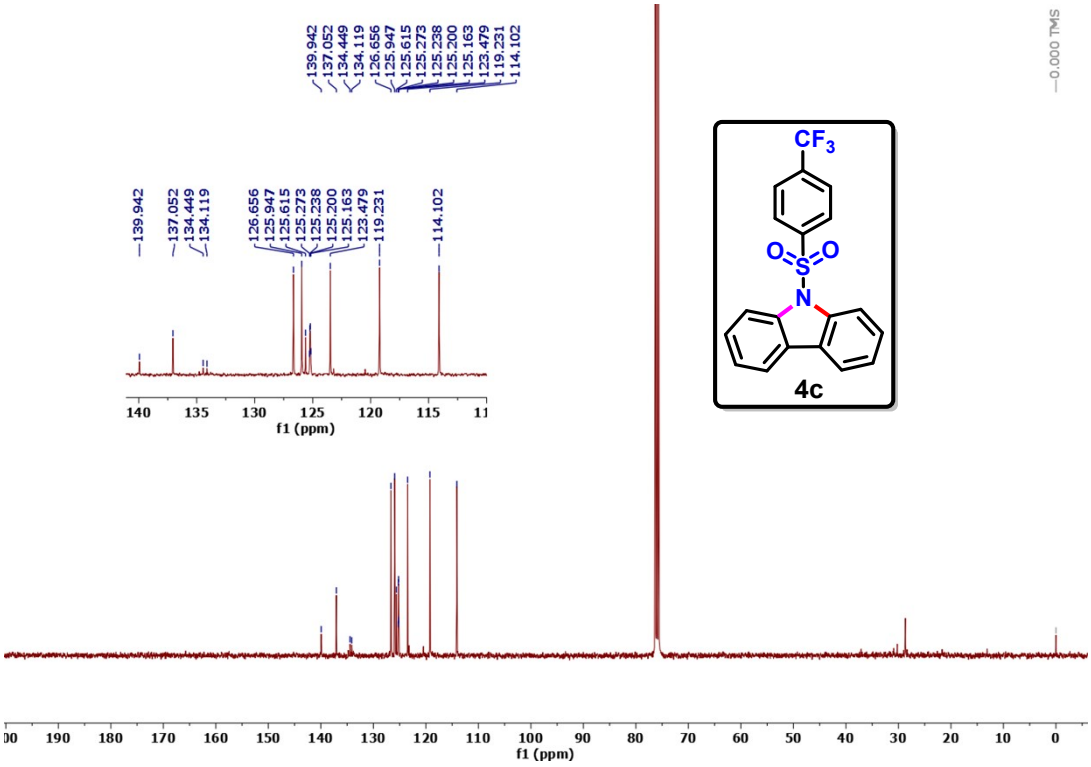

Fig. S61: $^{13}C\{1H\}$-NMR Spectrum of **4c** in $CDCl_3$ (101 MHz)

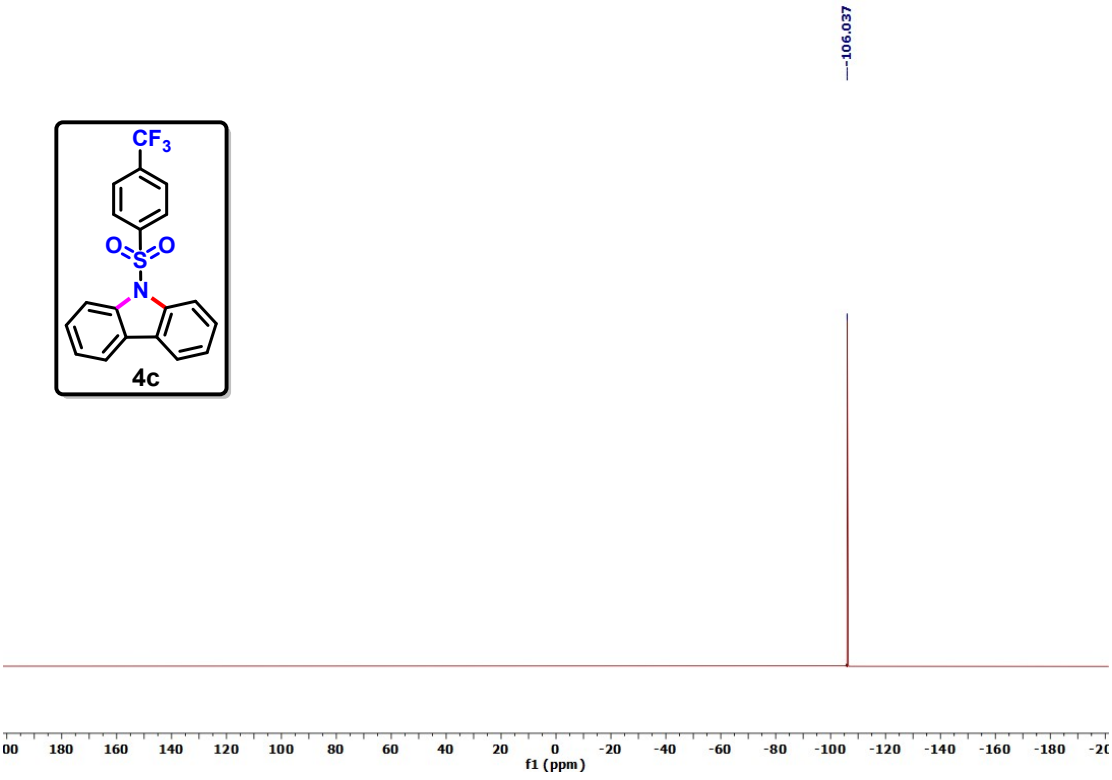

Fig. S62: ^{19}F-NMR Spectrum of **4c** in $CDCl_3$ (376 MHz)

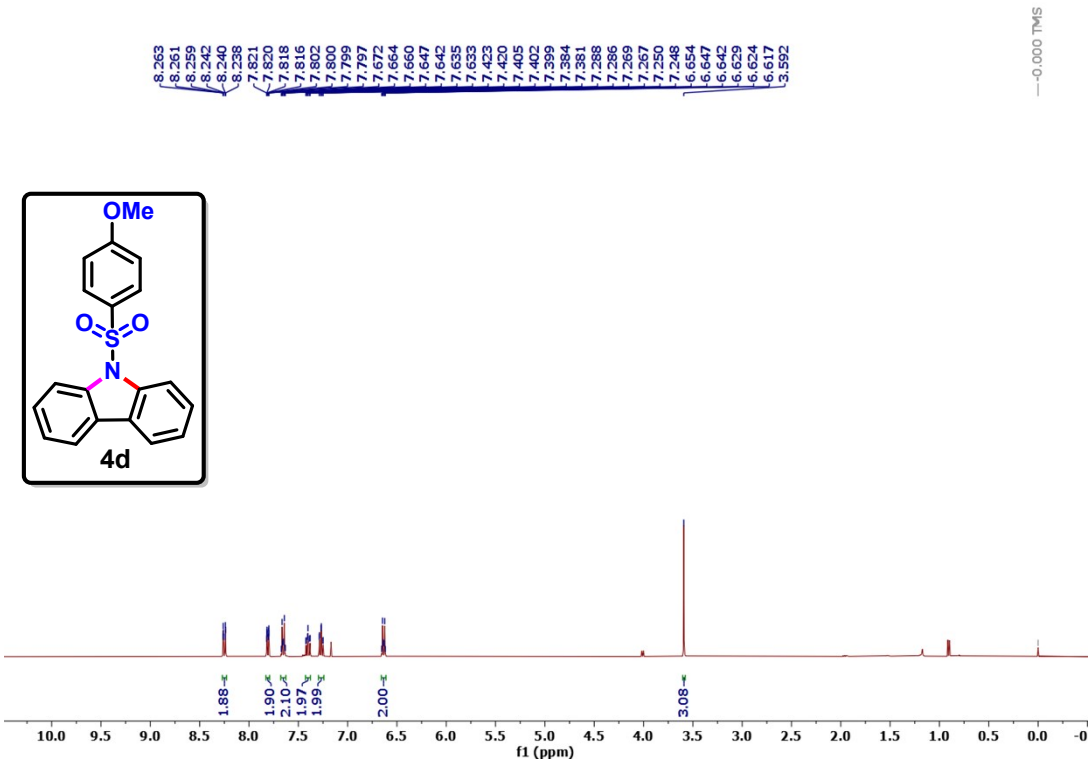

Fig. S63: ^{1}H-NMR Spectrum of **4d** in $CDCl_3$ (400 MHz)

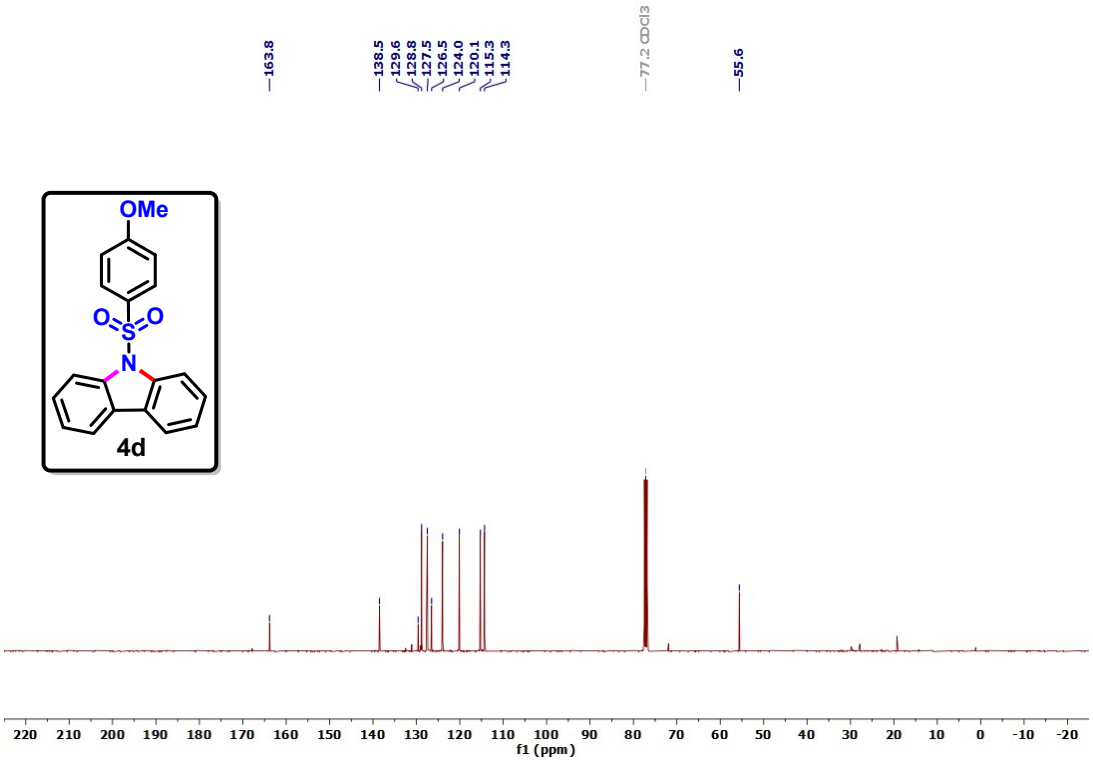

Fig. S64: $^{13}C\{^{1}H\}$-NMR Spectrum of **4d** in $CDCl_3$ (101 MHz)

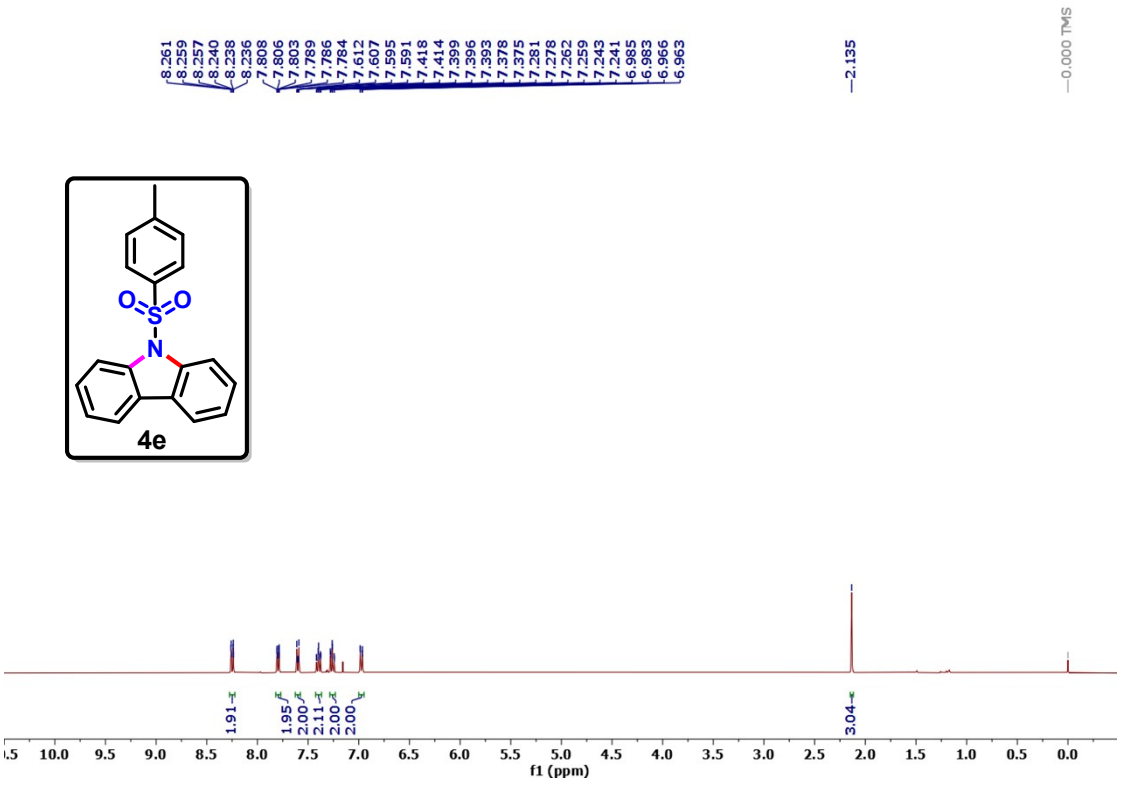

Fig. S65: ^{1}H-NMR Spectrum of **4e** in $CDCl_3$ (400 MHz)

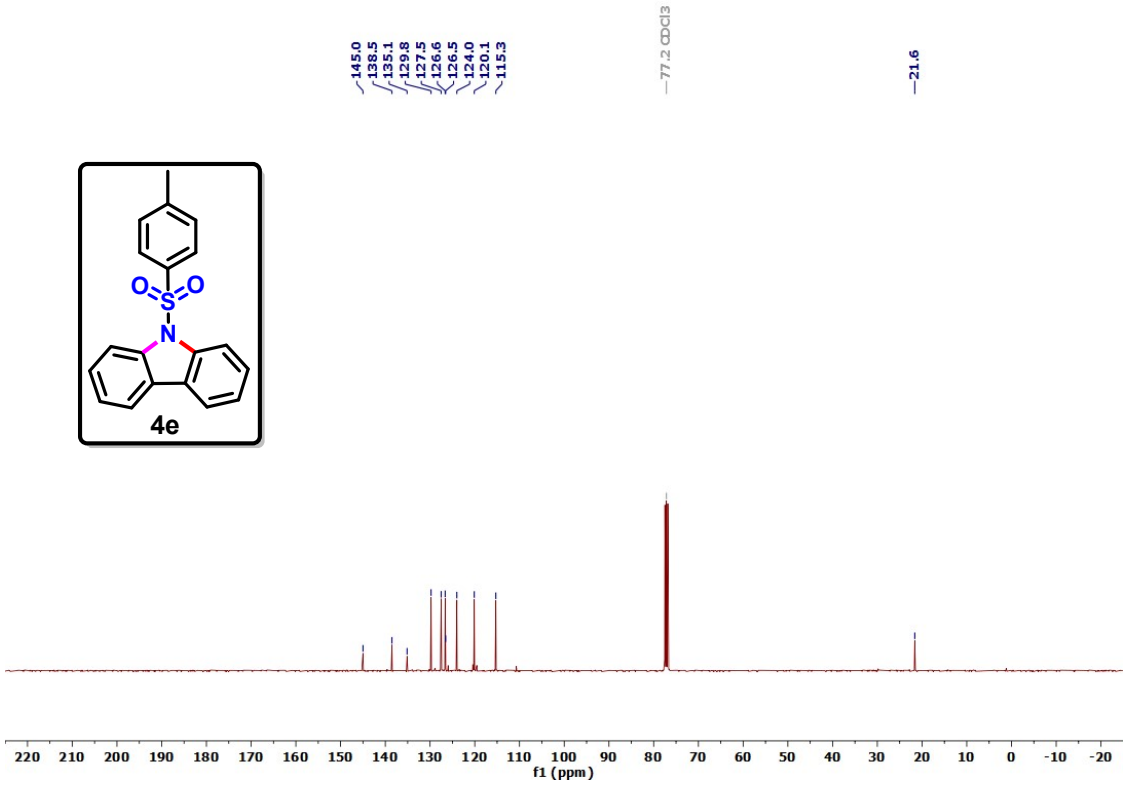

Fig. S66: $^{13}C\{^{1}H\}$-NMR Spectrum of **4e** in $CDCl_3$ (101 MHz)

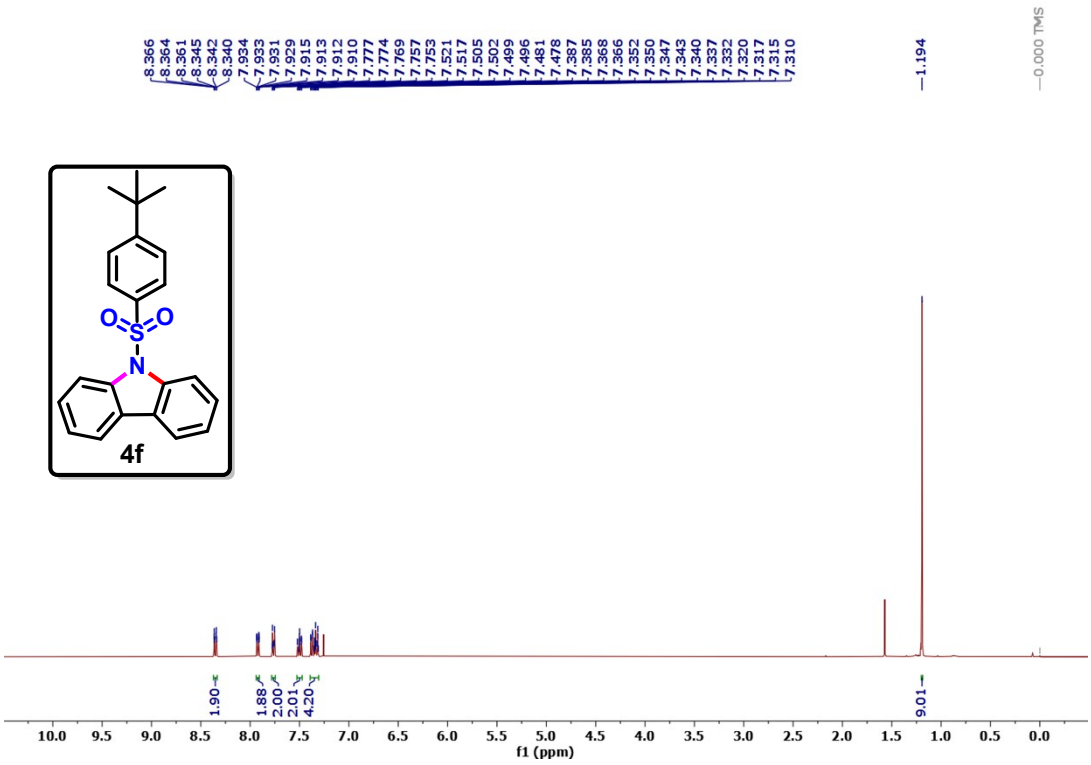

Fig. S67: ^{1}H-NMR Spectrum of **4f** in $CDCl_3$ (400 MHz)

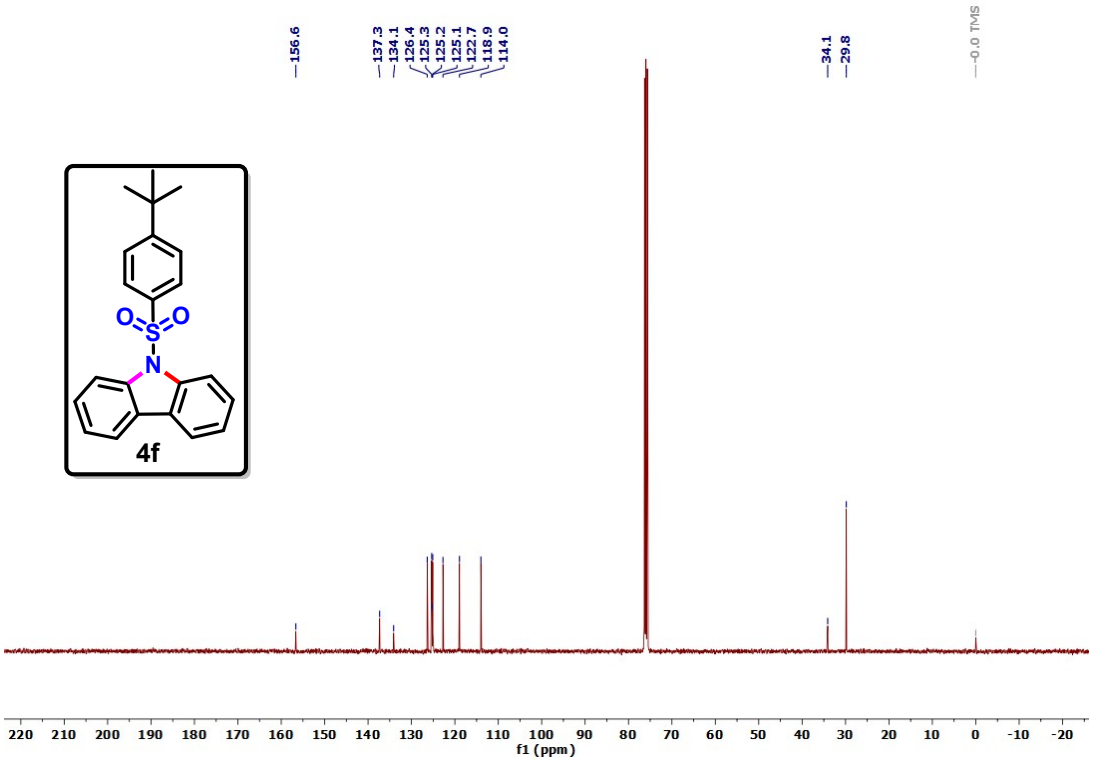

Fig. S68: $^{13}C\{^{1}H\}$-NMR Spectrum of **4f** in $CDCl_3$ (101 MHz)

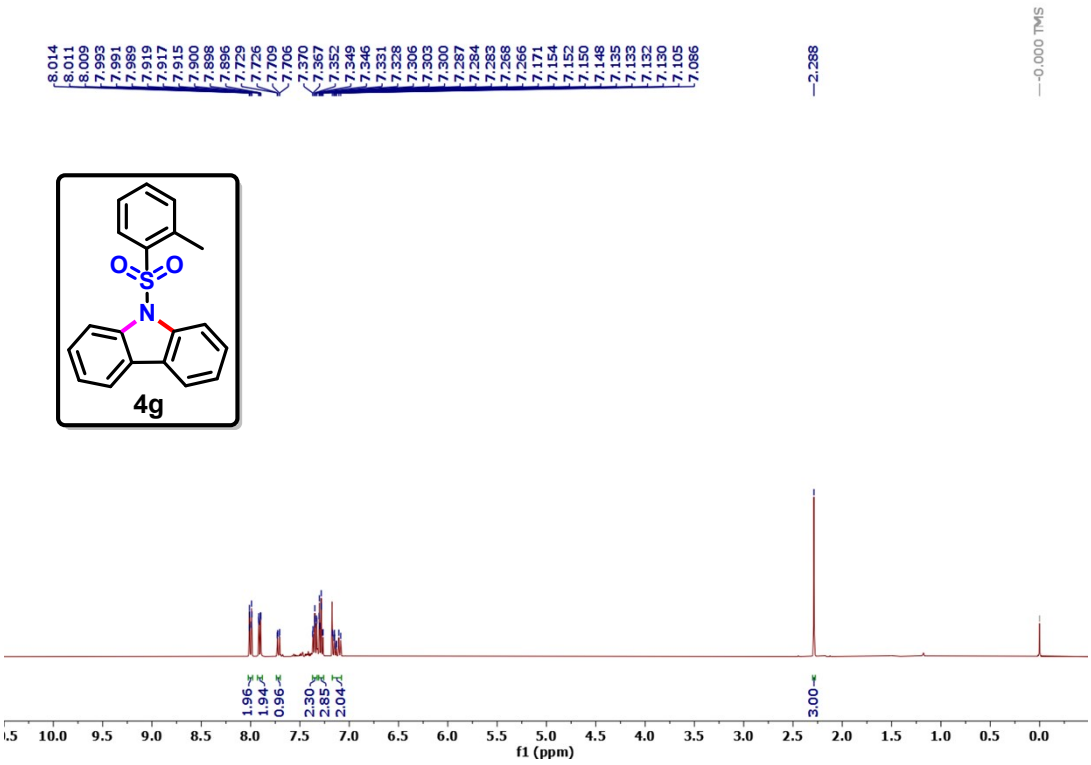

Fig. S69: ^{1}H-NMR Spectrum of **4g** in $CDCl_3$ (400 MHz)

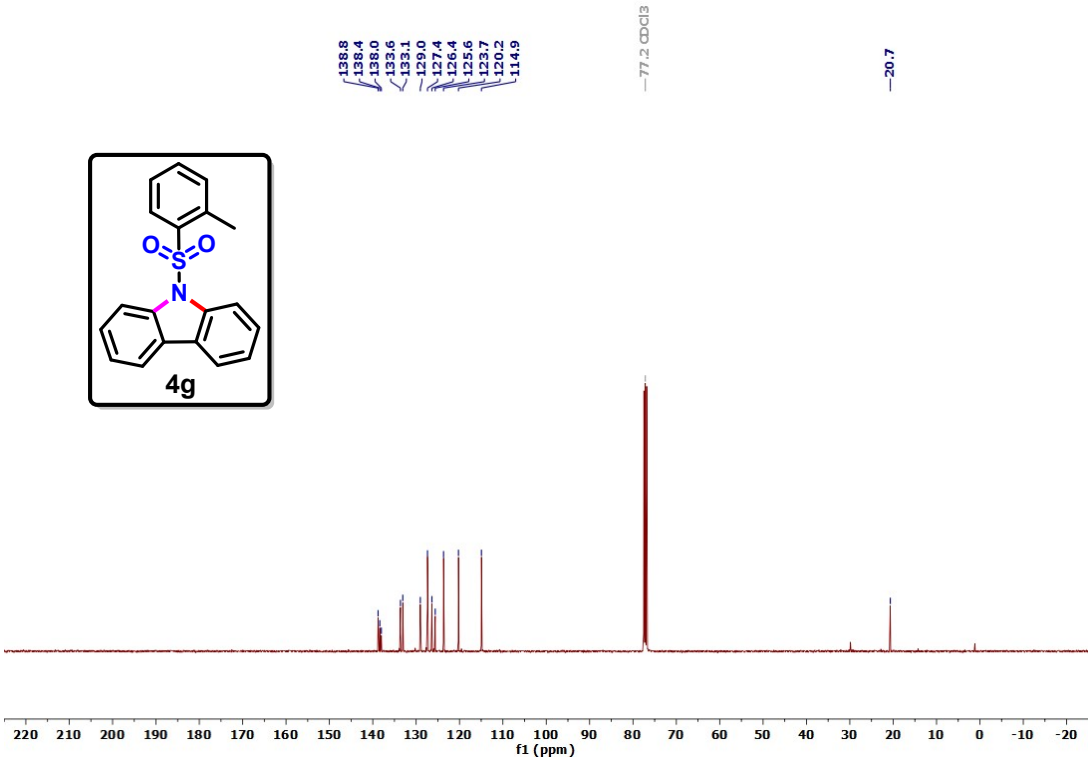

Fig. S70: $^{13}C\{^{1}H\}$-NMR Spectrum of **4g** in $CDCl_3$ (101 MHz)

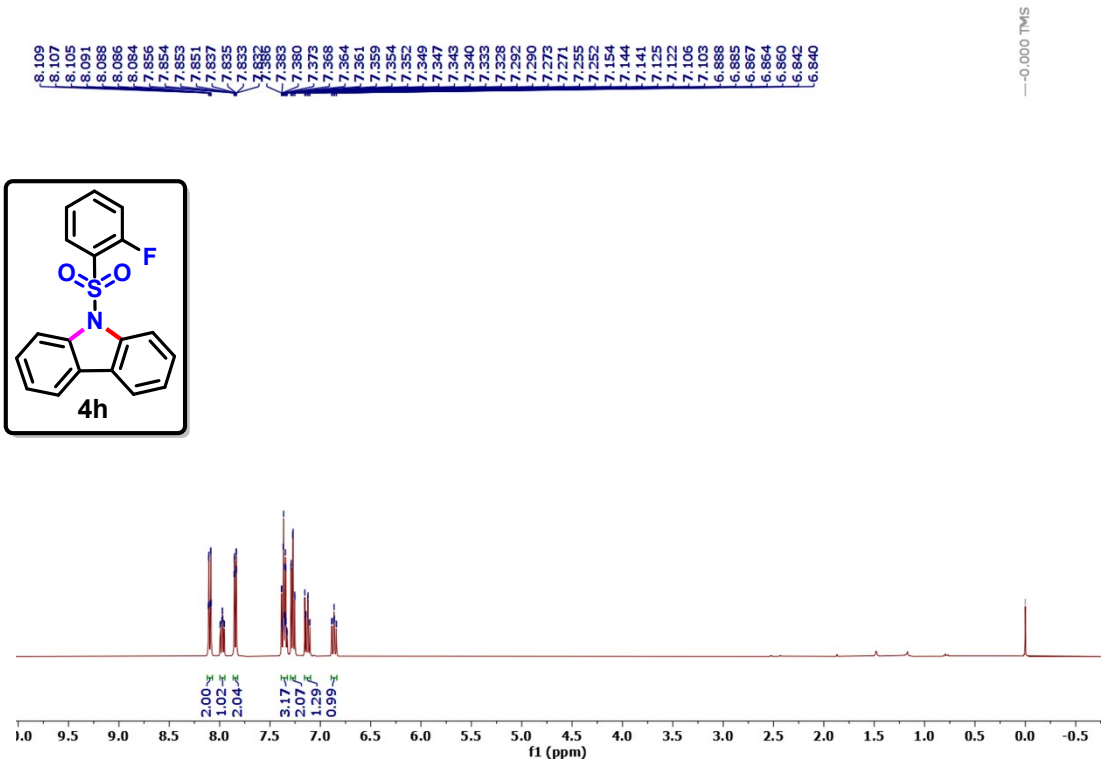

Fig. S71: ^{1}H-NMR Spectrum of **4h** in $CDCl_3$ (400 MHz)

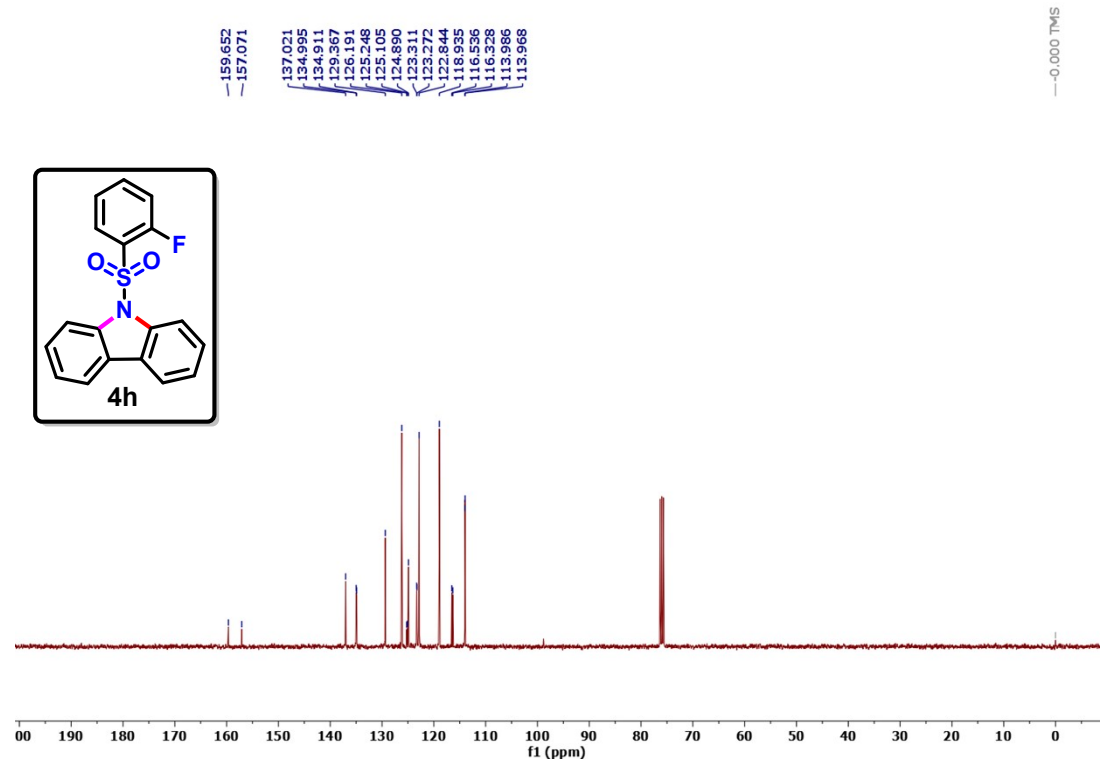

Fig. S72: $^{13}C\{^{1}H\}$-NMR Spectrum of **4h** in $CDCl_3$ (101 MHz)

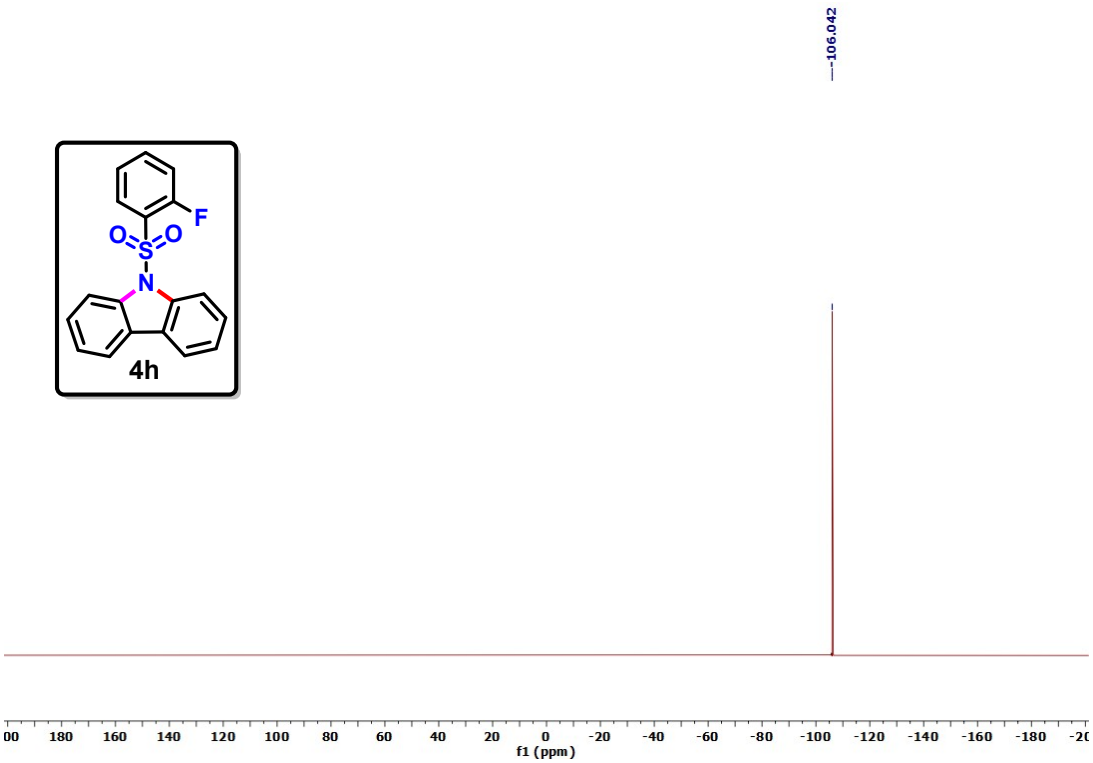

Fig. S73: ^{19}F-NMR Spectrum of **4h** in $CDCl_3$ (376 MHz)

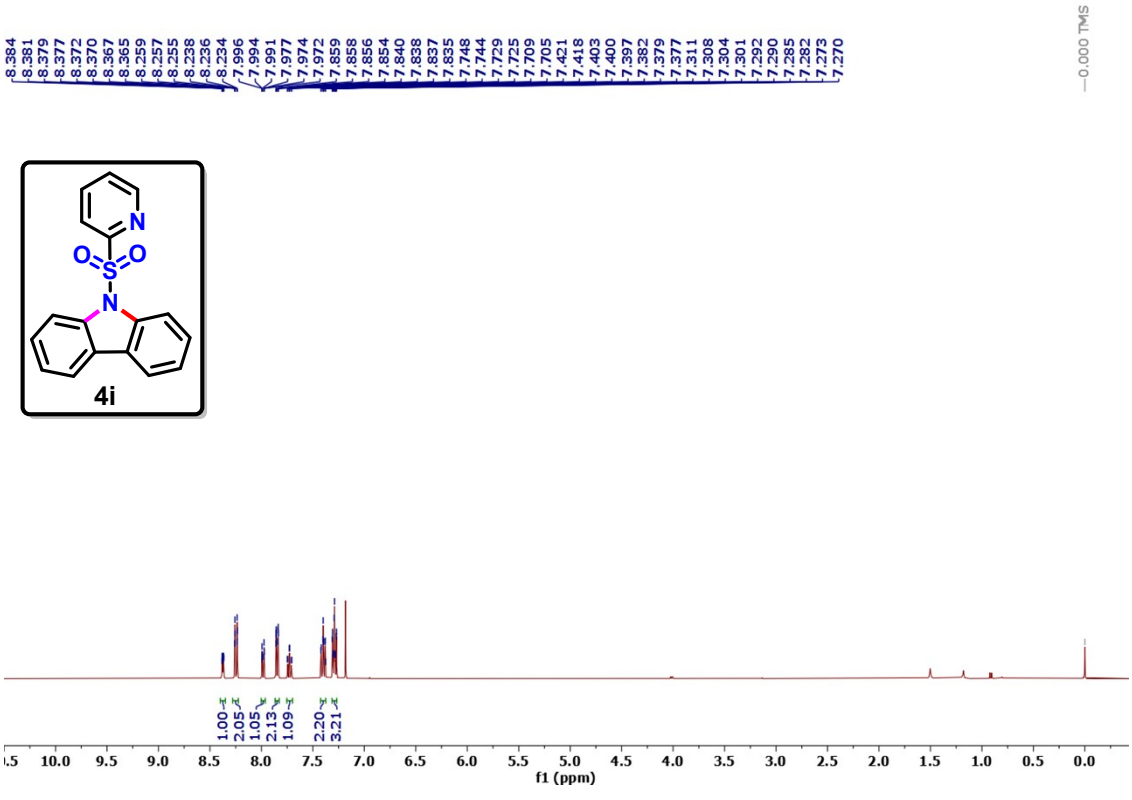

Fig. S74: ^{1}H-NMR Spectrum of **4i** in $CDCl_3$ (400 MHz)

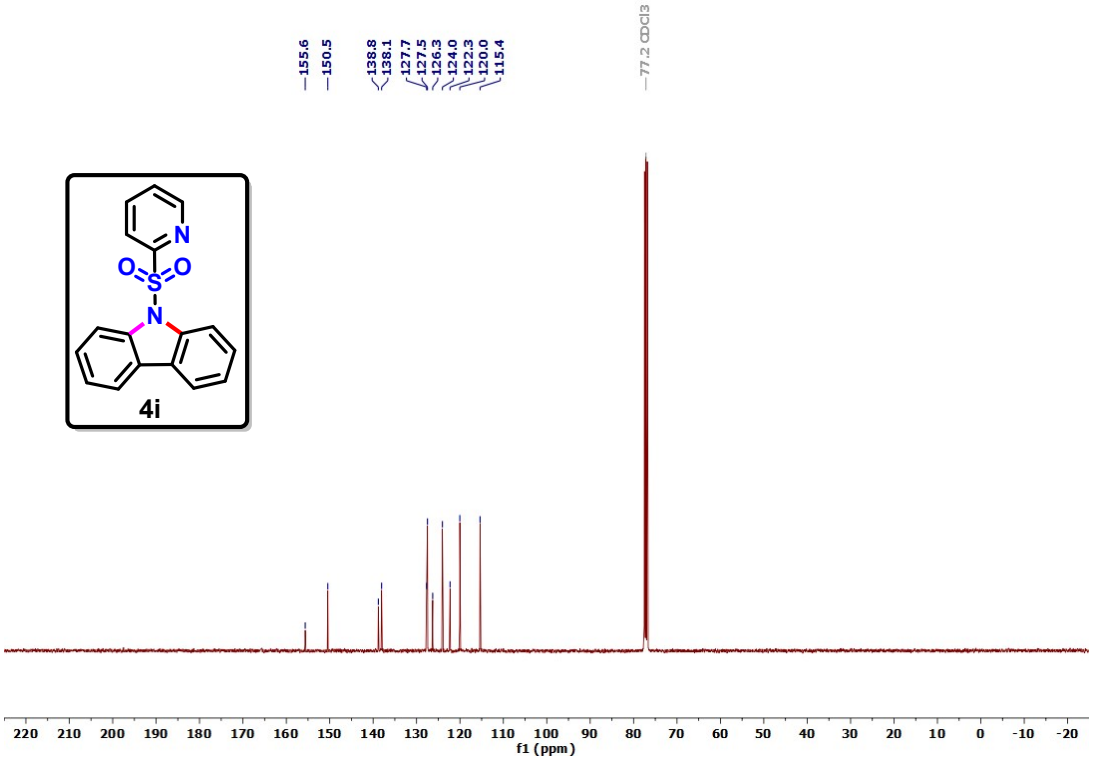

Fig. S75: $^{13}C\{^{1}H\}$-NMR Spectrum of **4i** in $CDCl_3$ (101 MHz)

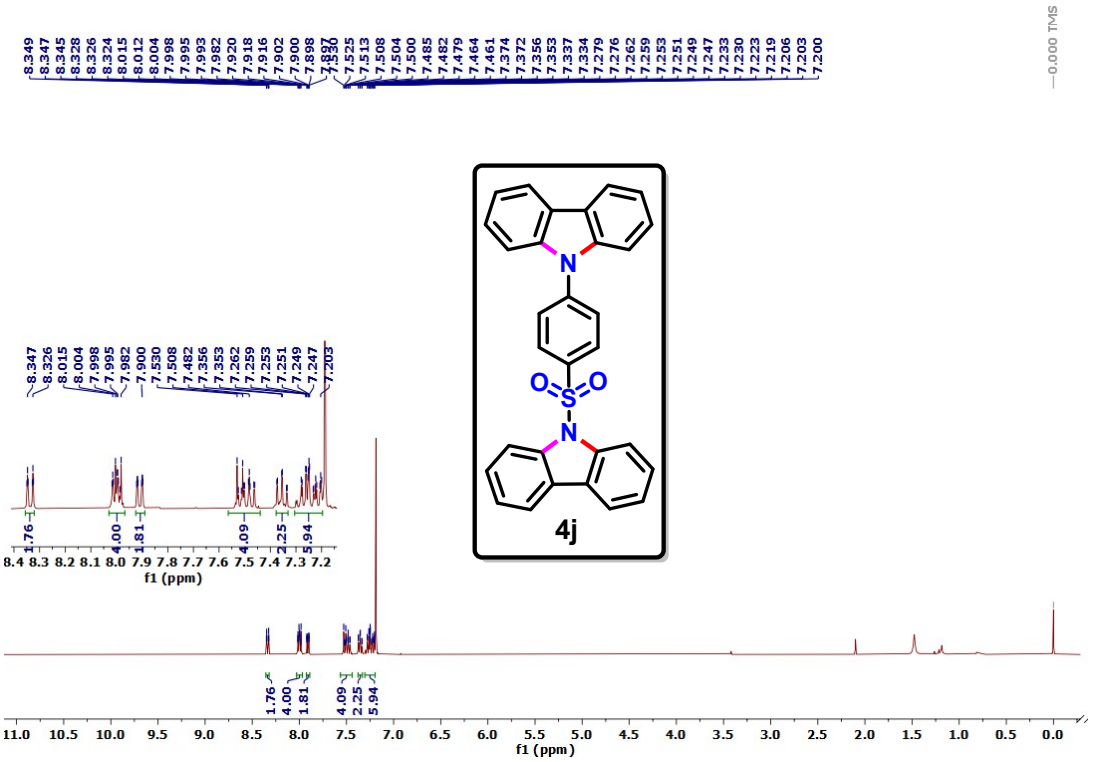

Fig. S76: ^{1}H-NMR Spectrum of **4j** in $CDCl_3$ (400 MHz)

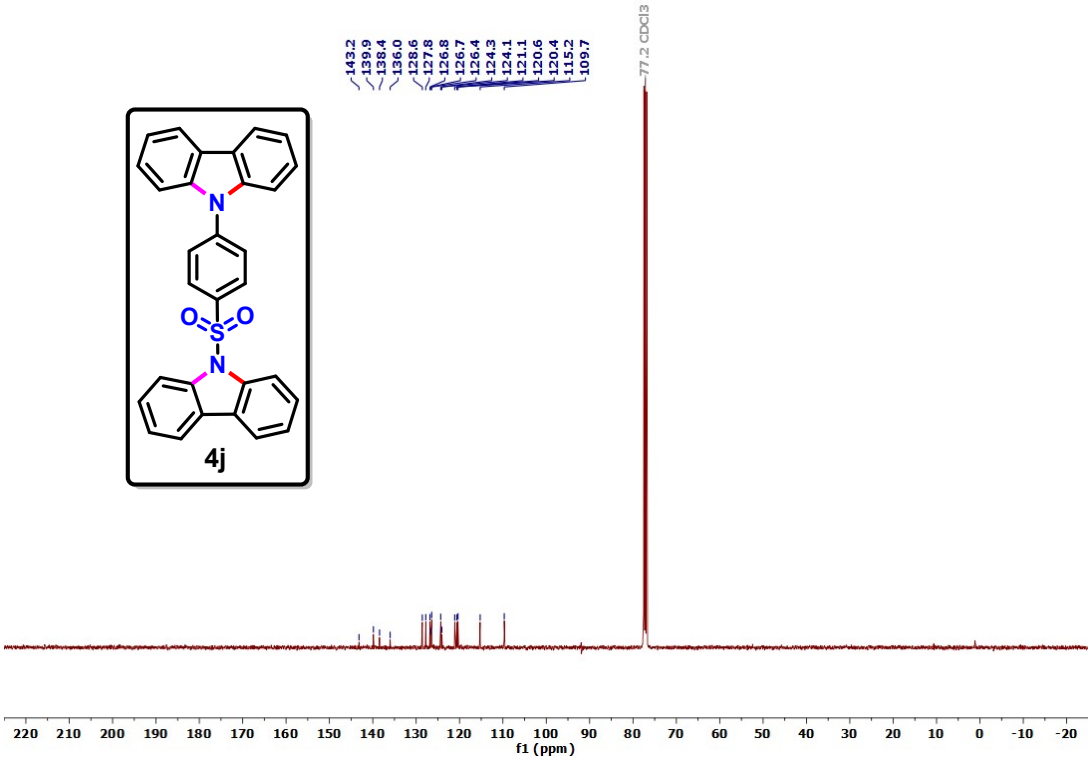

Fig. S77: $^{13}C\{^{1}H\}$-NMR Spectrum of **4j** in $CDCl_3$ (101 MHz)

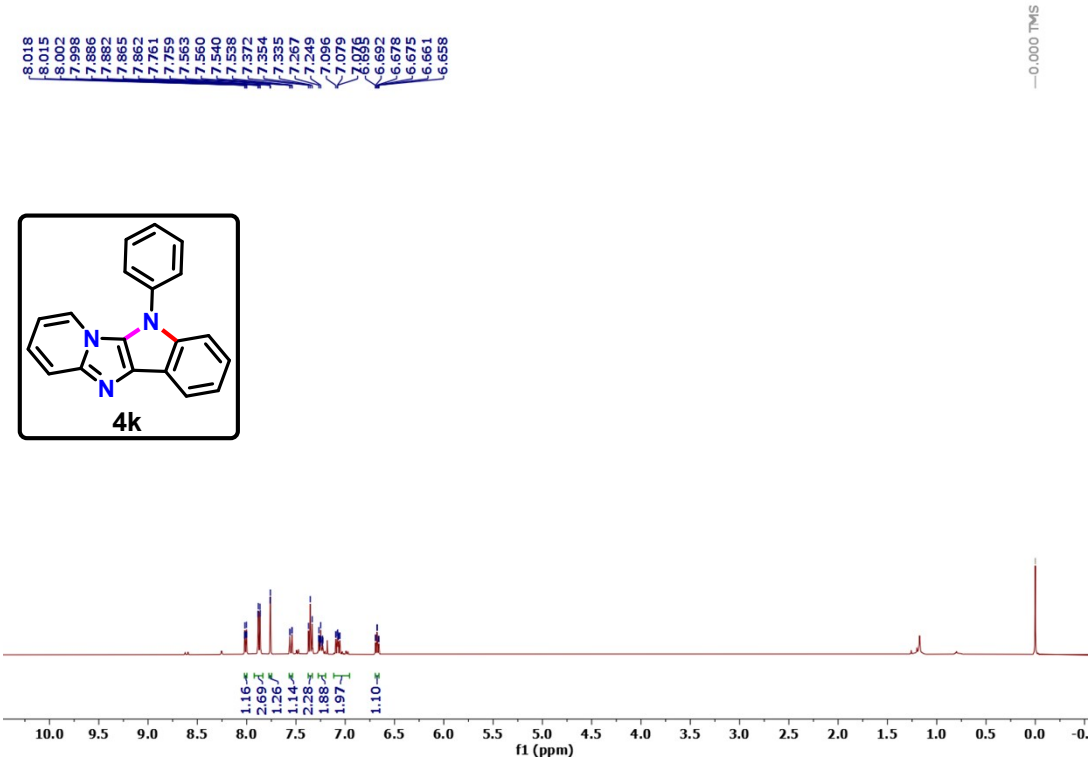

Fig. S78: ^{1}H-NMR Spectrum of **4k** in $CDCl_3$ (400 MHz)

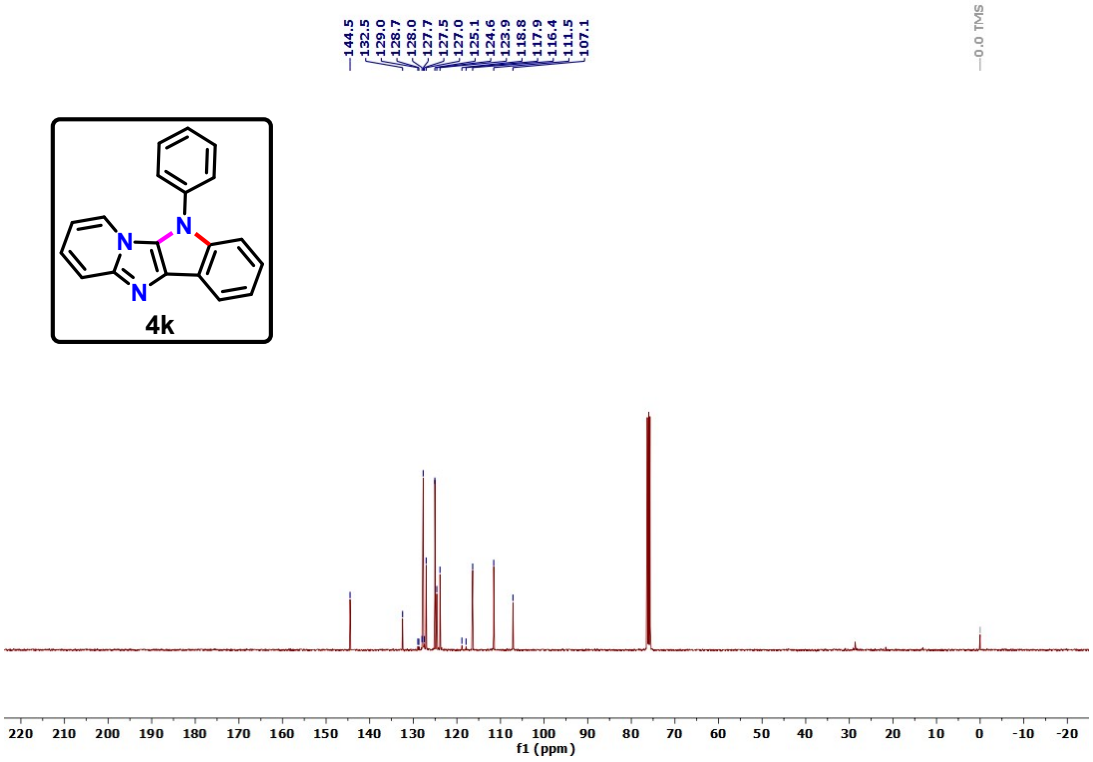

Fig. S79: $^{13}C\{^{1}H\}$-NMR Spectrum of **4k** in $CDCl_3$ (101 MHz)

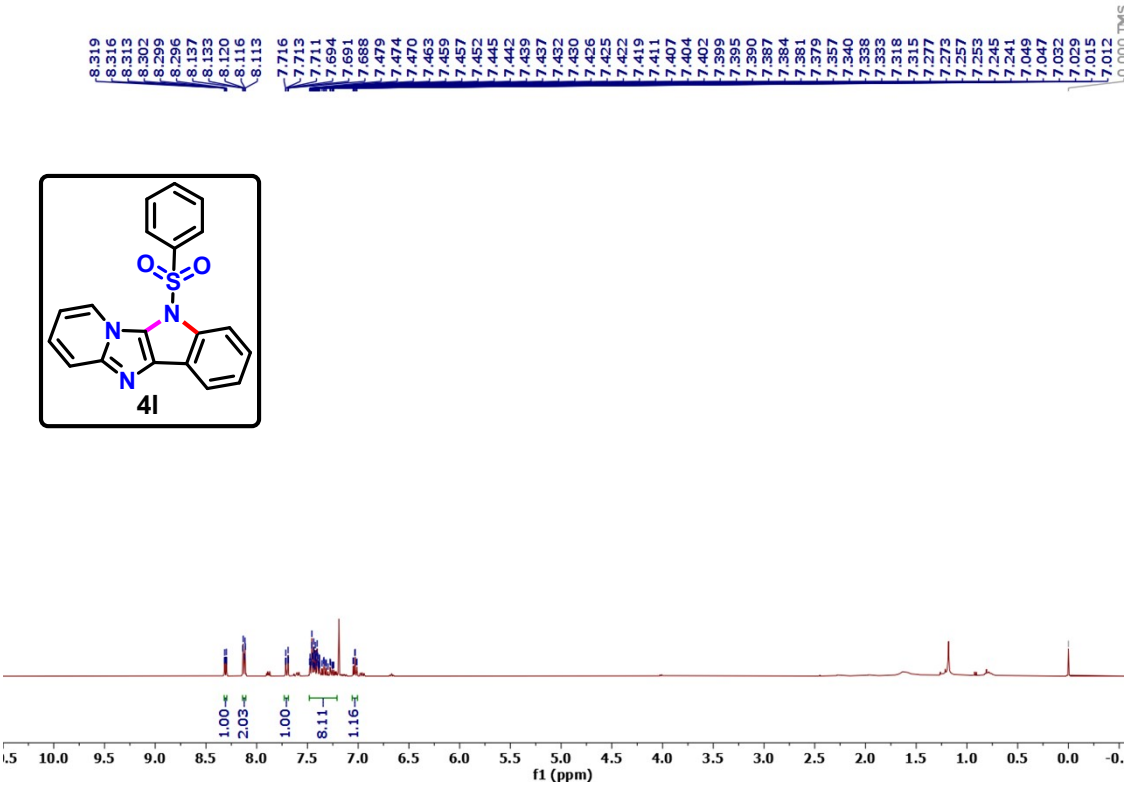

Fig. S80: ^{1}H-NMR Spectrum of **4l** in $CDCl_3$ (400 MHz)

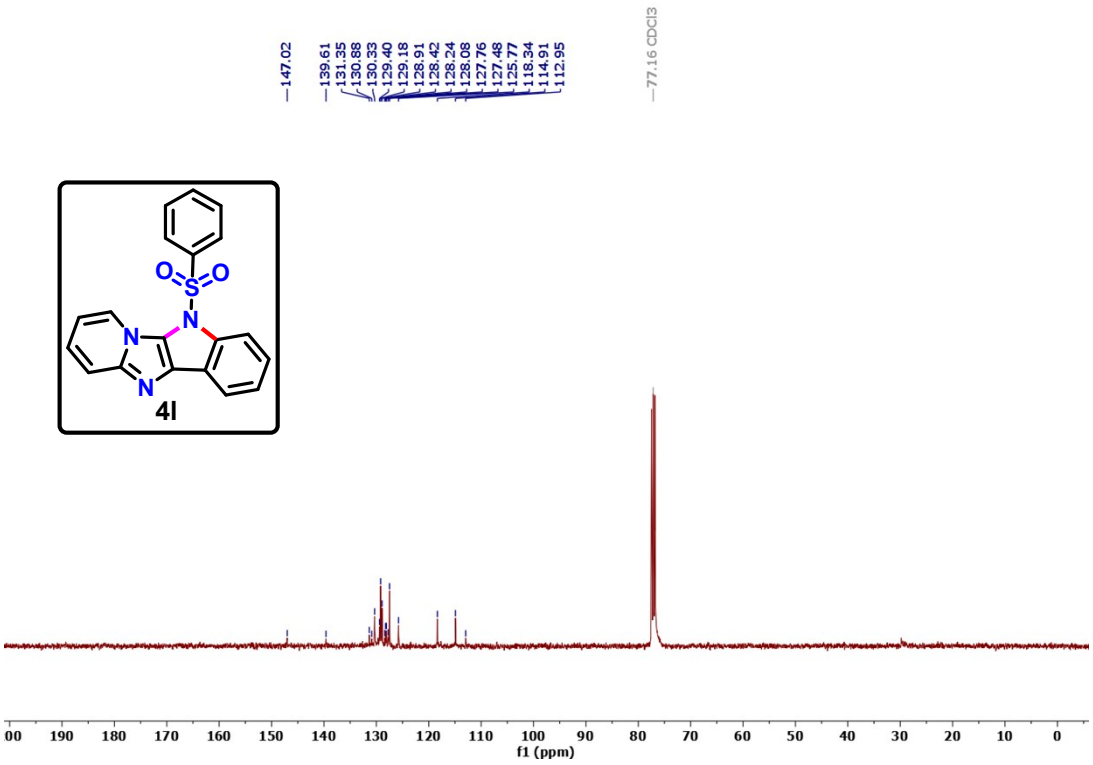

Fig. S81: $^{13}C\{^{1}H\}$-NMR Spectrum of **4l** in $CDCl_3$ (101 MHz)

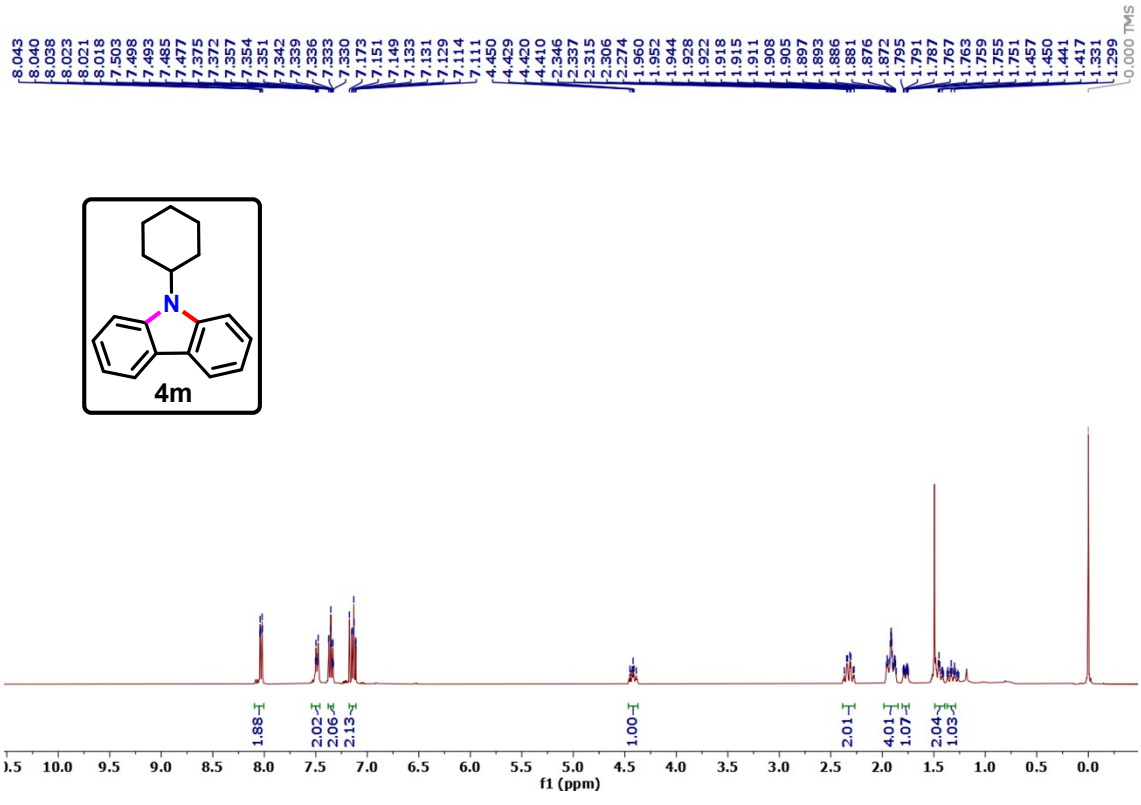

Fig. S82: ^{1}H-NMR Spectrum of **4m** in $CDCl_3$ (400 MHz)

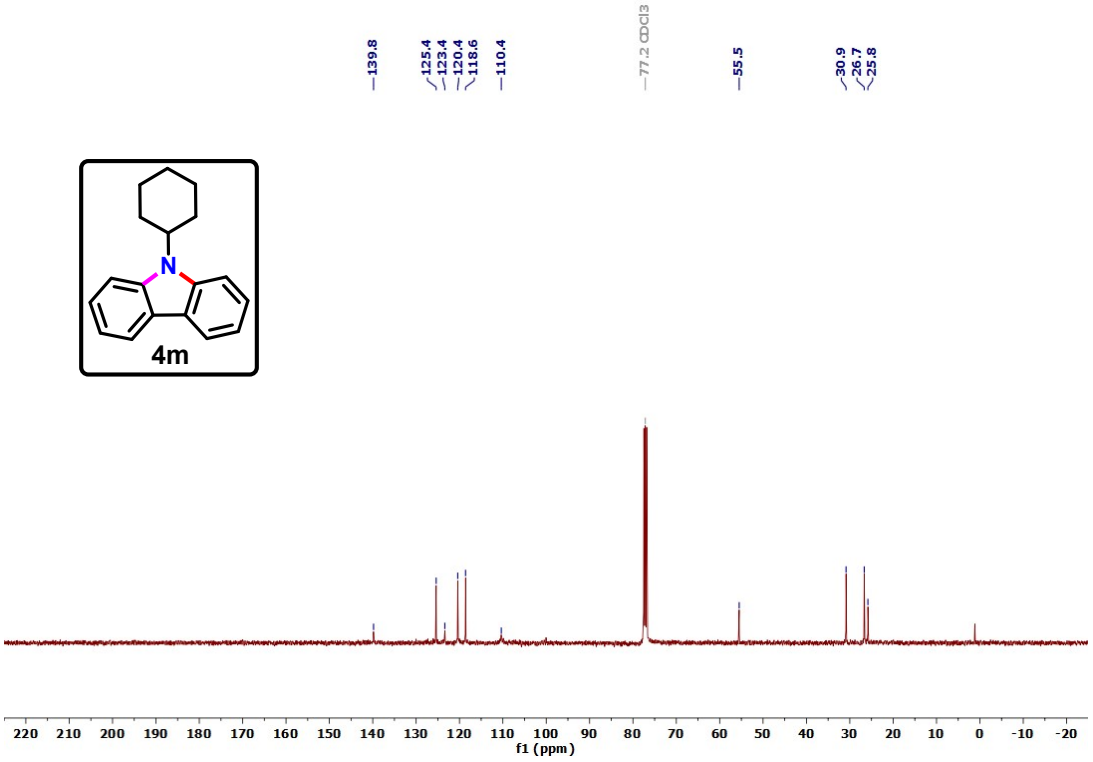

Fig. S83: $^{13}C\{^{1}H\}$-NMR Spectrum of **4m** in $CDCl_3$ (101 MHz)

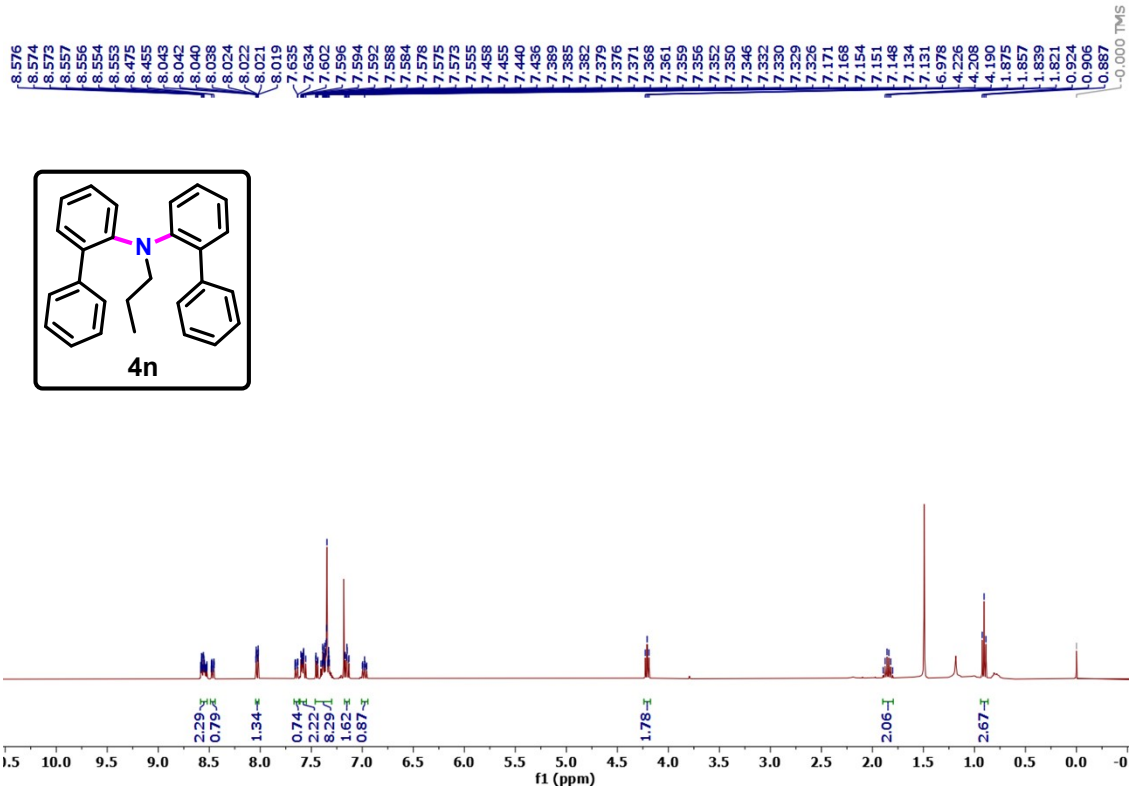

Fig. S84: ^{1}H-NMR Spectrum of **4n** in $CDCl_3$ (400 MHz)

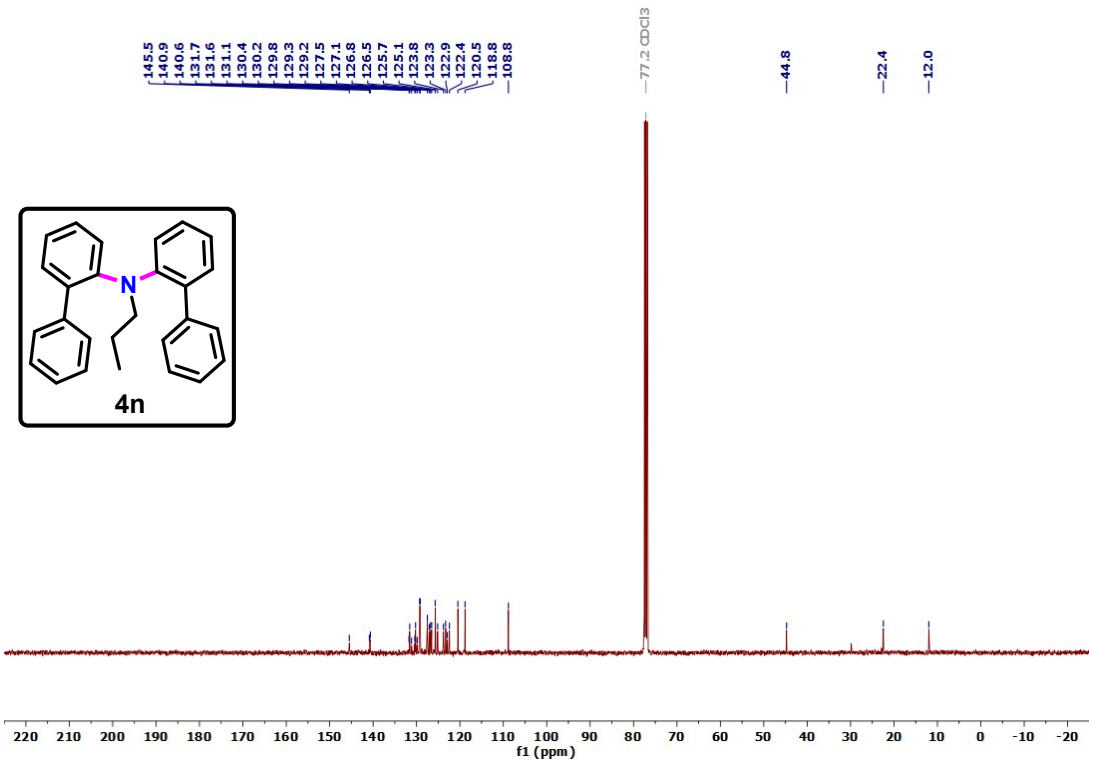

Fig. S85: $^{13}C\{^{1}H\}$-NMR Spectrum of **4n** in $CDCl_3$ (101 MHz)

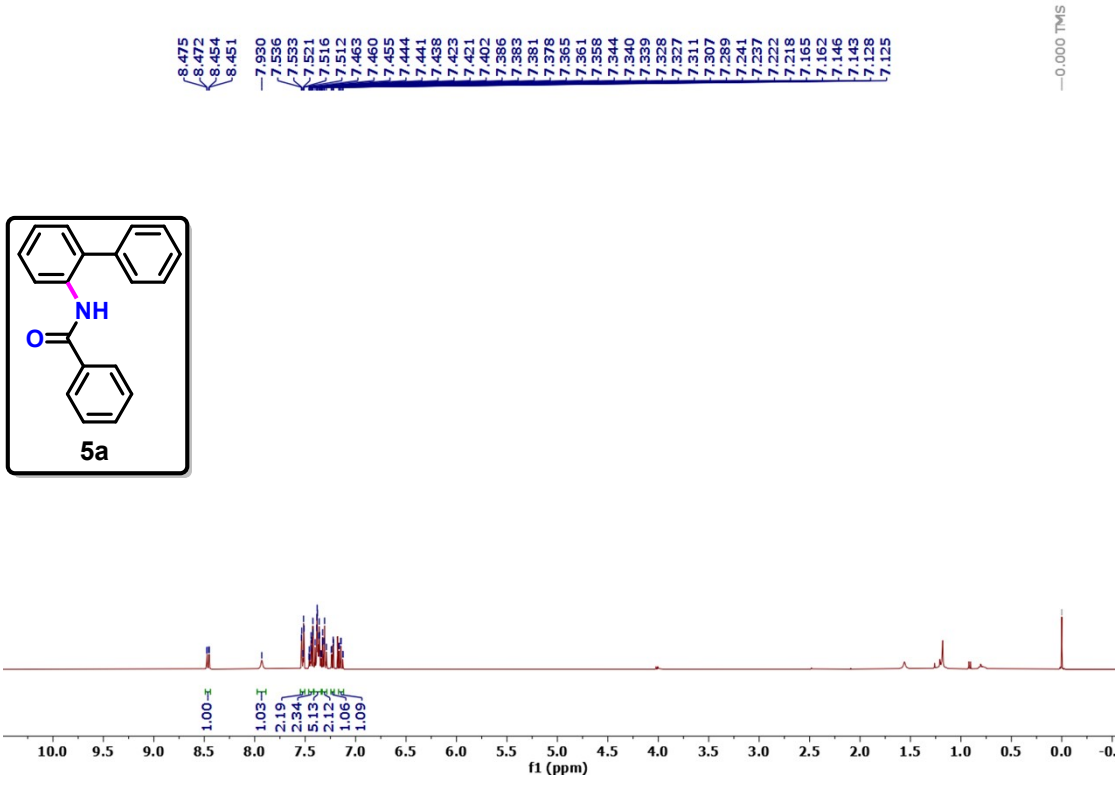

Fig. S86: ^{1}H-NMR Spectrum of **5a** in $CDCl_3$ (400 MHz)

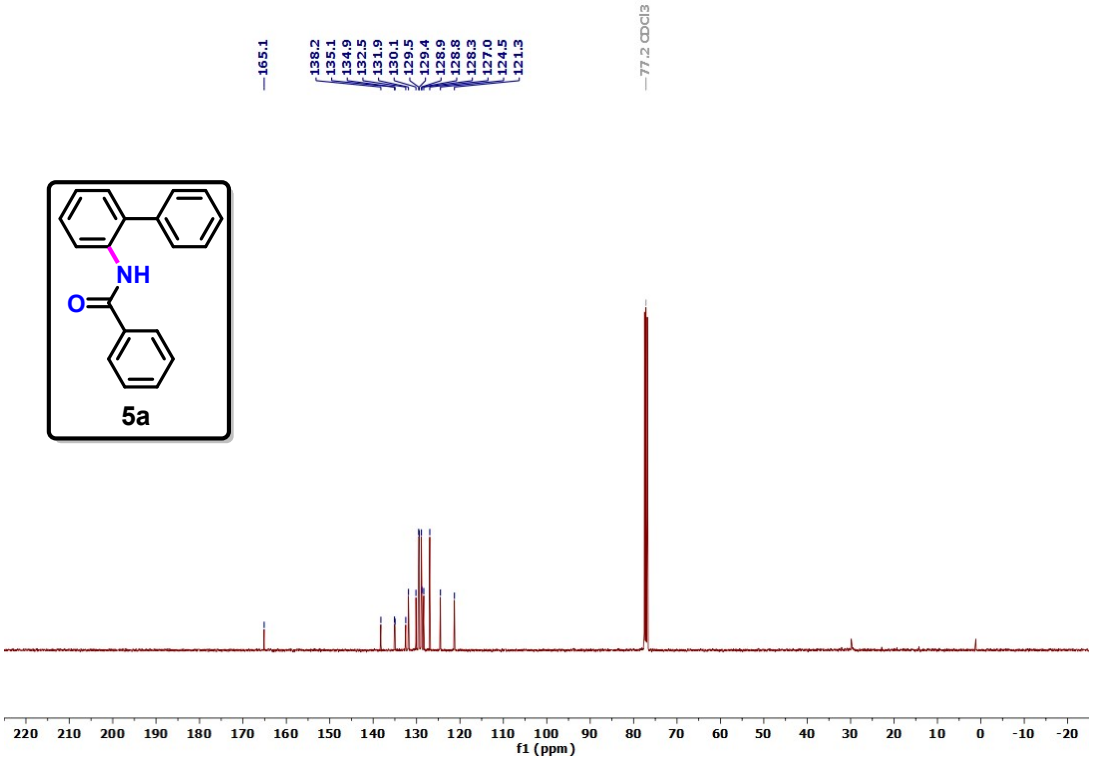

Fig. S87: $^{13}C\{^{1}H\}$-NMR Spectrum of **5a** in $CDCl_3$ (101 MHz)

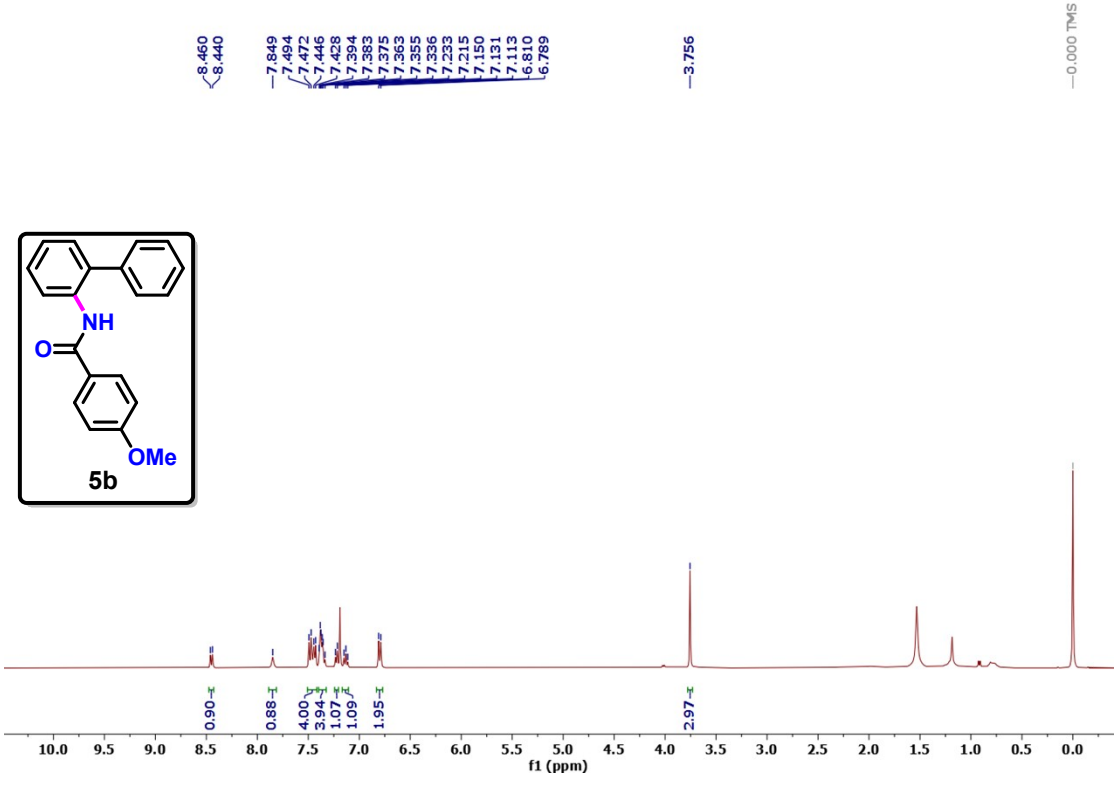

Fig. S88: ^{1}H-NMR Spectrum of **5b** in $CDCl_3$ (400 MHz)

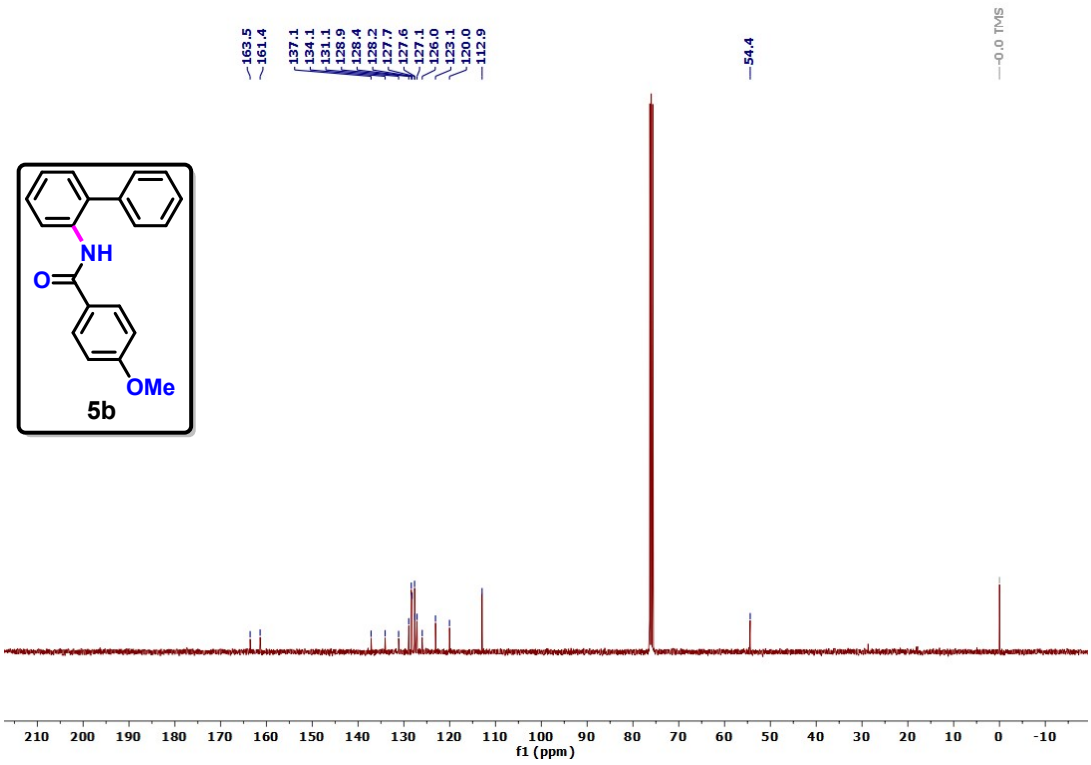

Fig. S89: $^{13}C\{^{1}H\}$-NMR Spectrum of **5b** in $CDCl_3$ (101 MHz)

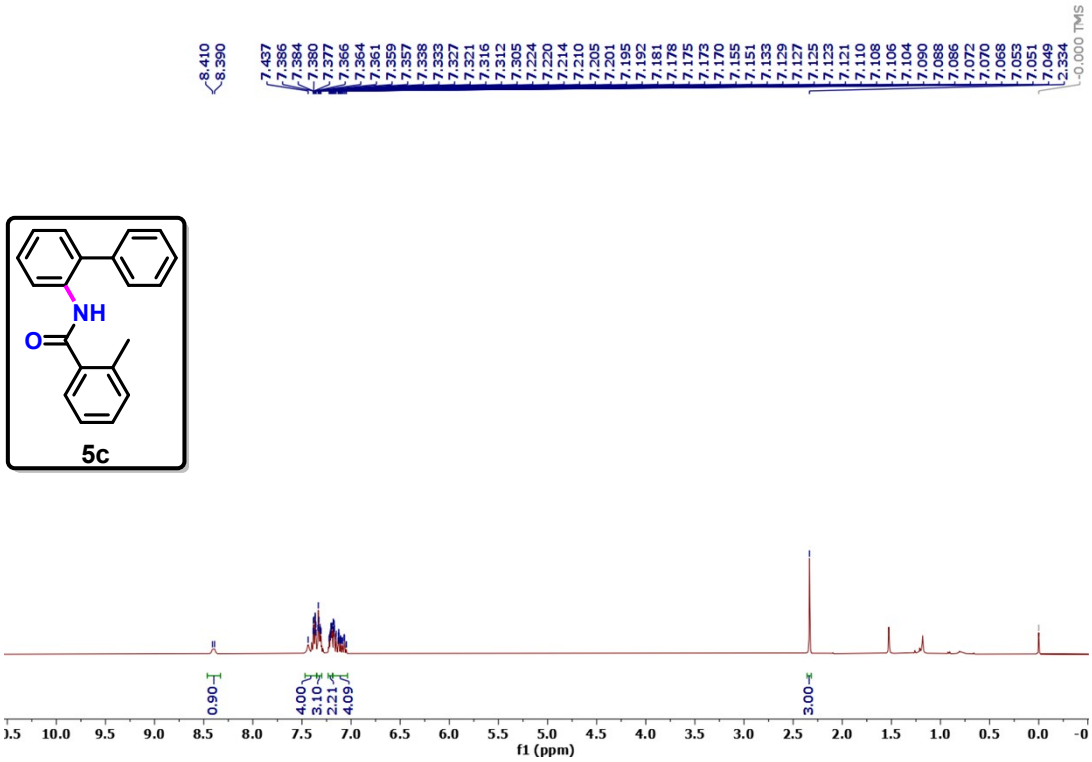

Fig. S90: ^{1}H-NMR Spectrum of **5c** in $CDCl_3$ (400 MHz)

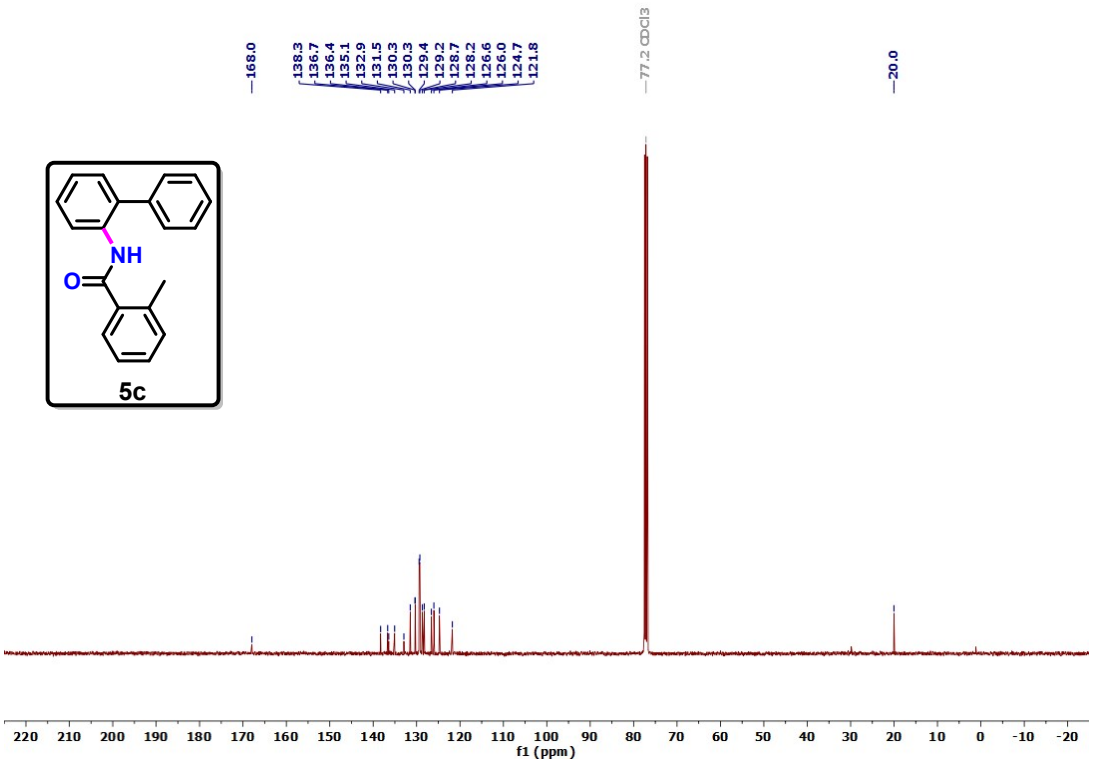

Fig. S91: $^{13}C\{^{1}H\}$-NMR Spectrum of **5c** in $CDCl_3$ (101 MHz)

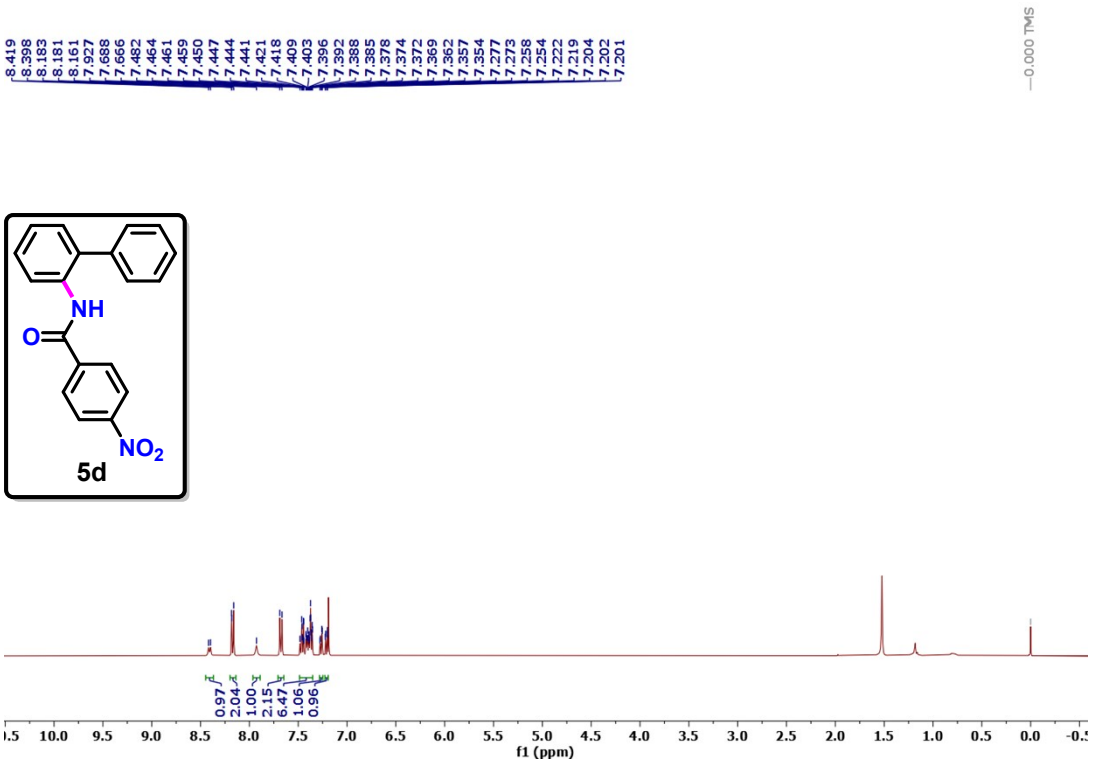

Fig. S92: ^{1}H-NMR Spectrum of **5d** in $CDCl_3$ (400 MHz)

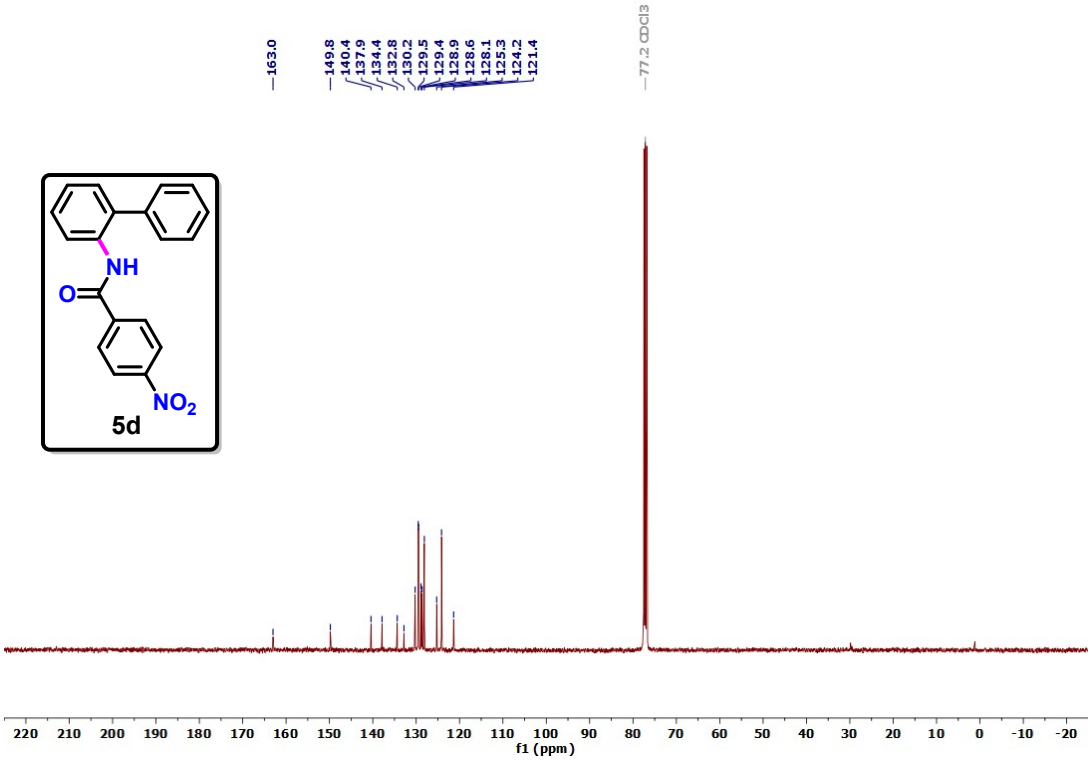

Fig. S93: $^{13}C\{^{1}H\}$-NMR Spectrum of **5d** in $CDCl_3$ (101 MHz)

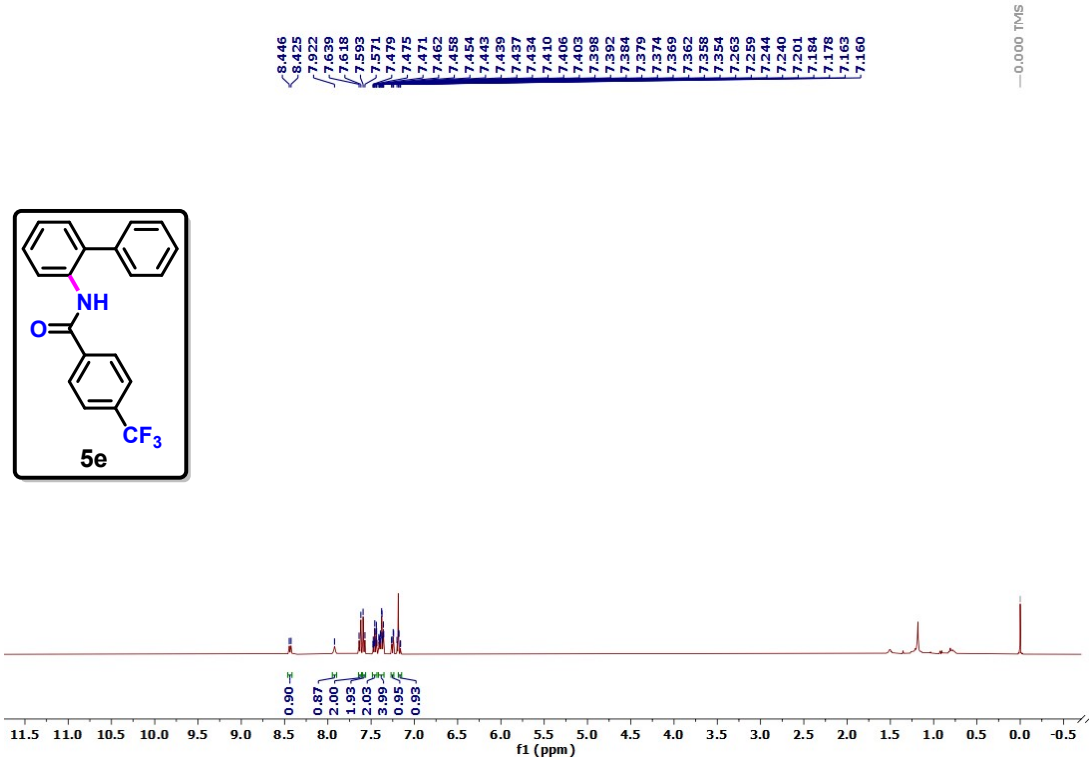

Fig. S94: ^{1}H-NMR Spectrum of **5e** in $CDCl_3$ (400 MHz)

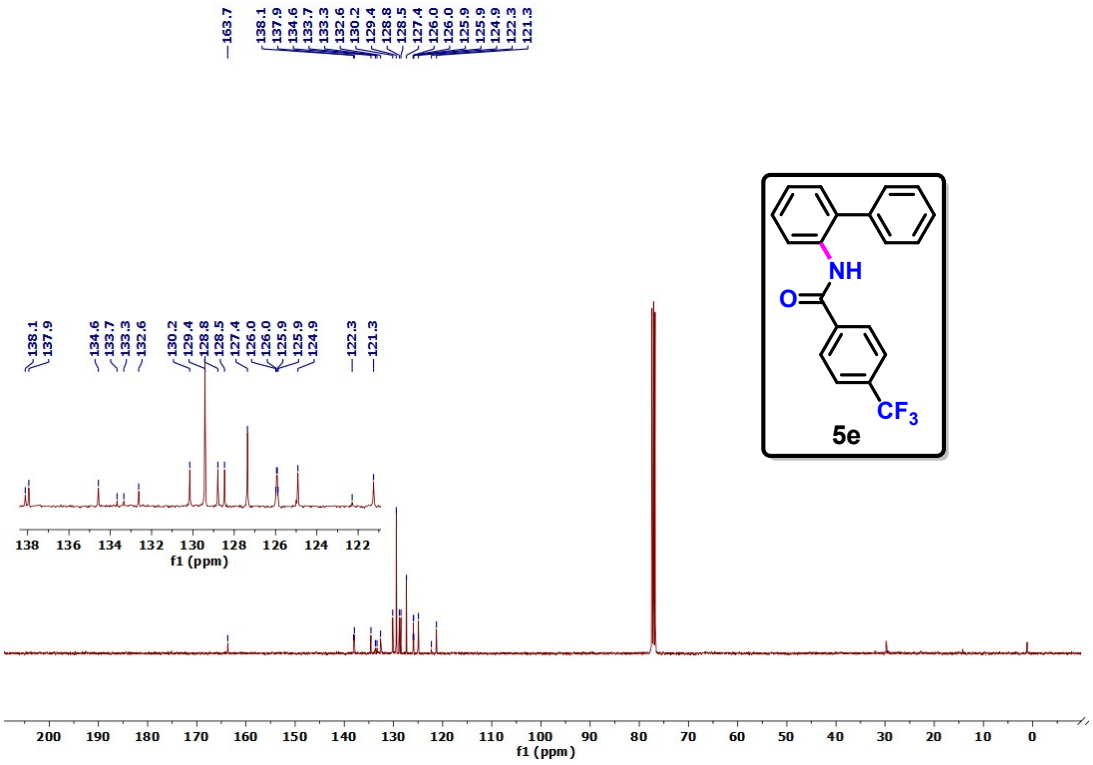

Fig. S95: $^{13}C\{^{1}H\}$-NMR Spectrum of **5e** in $CDCl_3$ (101 MHz)

8. HRMS data of N-substituted carbazoles

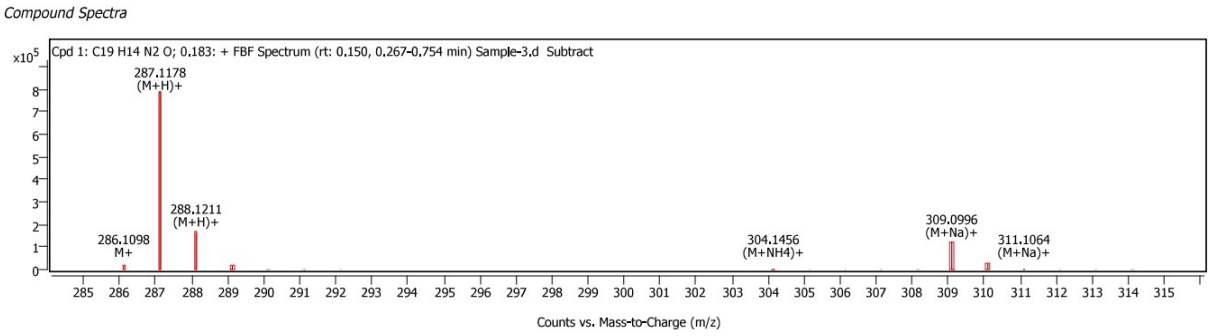

Fig S96: HRMS (ESI^+) of **3i** showing $[M+H]^+$ molecular ion peak.

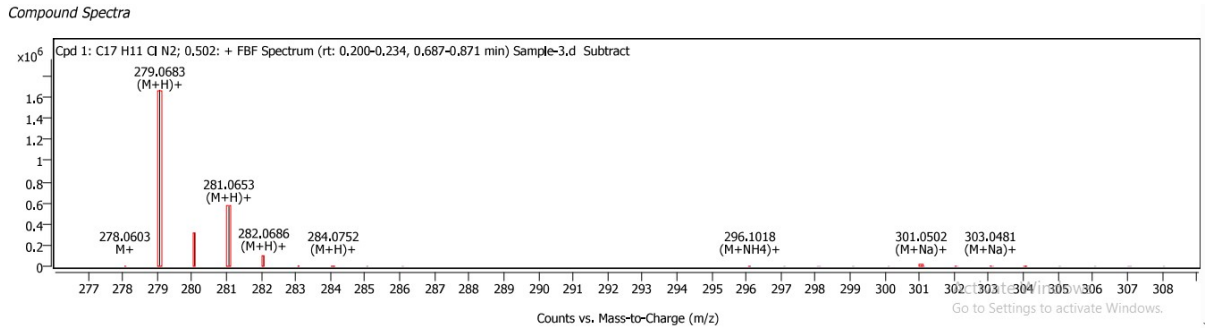

Fig S97: HRMS (ESI$^+$) of **3q** showing [M+H]$^+$ molecular ion peak.

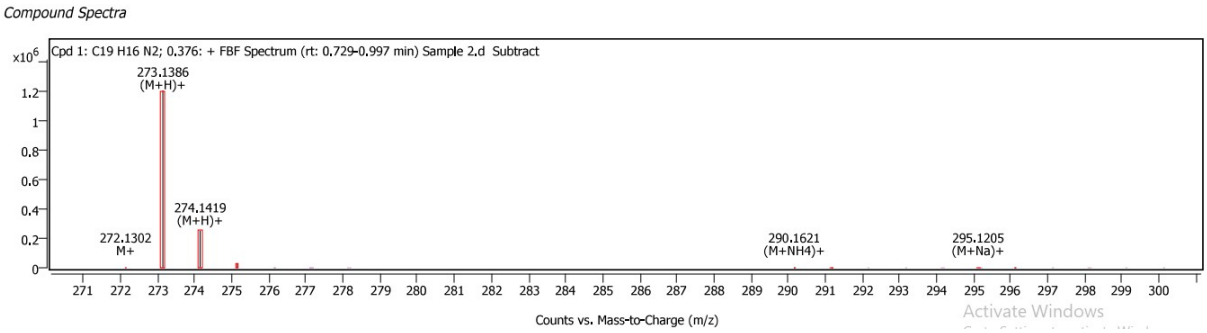

Fig S98: HRMS (ESI$^+$) of **3r** showing [M+H]$^+$ molecular ion peak.

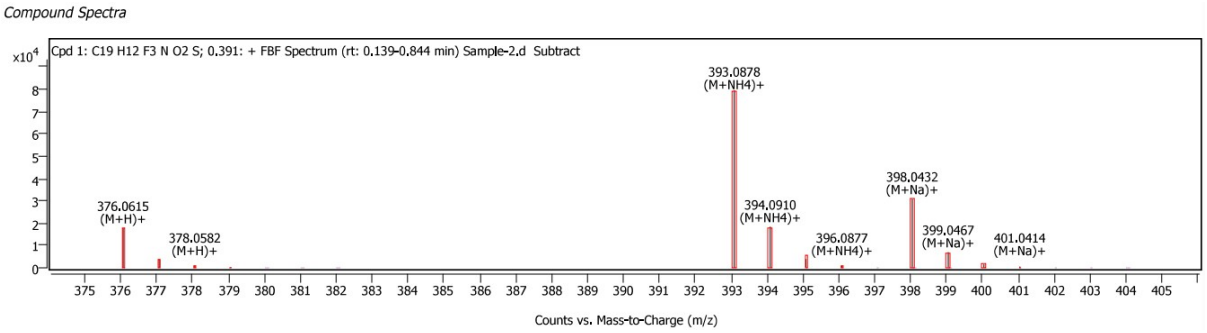

Fig S99: HRMS (ESI$^+$) of **4c** showing [M+H]$^+$ molecular ion peak.

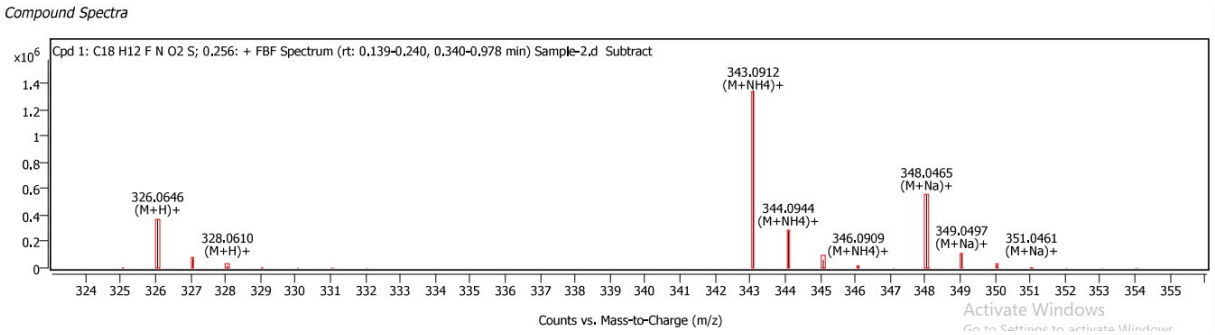

Fig S100: HRMS (ESI$^+$) of **4h** showing [M+H]$^+$ molecular ion peak.

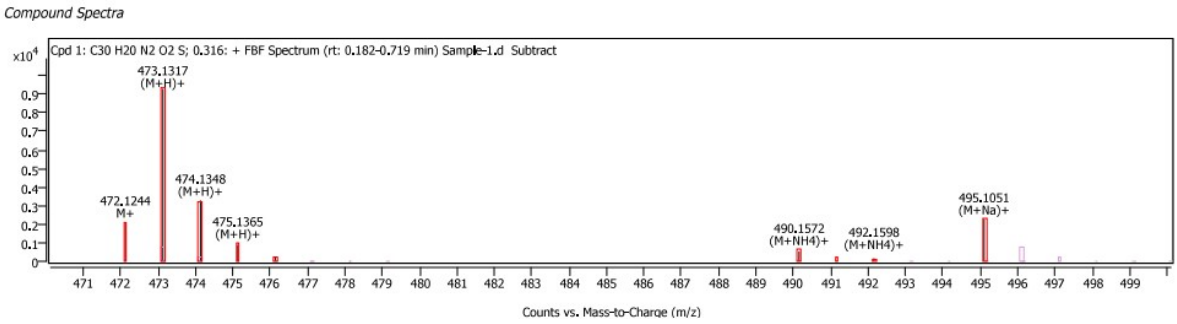

Fig S101: HRMS (ESI$^+$) of **4j** showing [M+H]$^+$ molecular ion peak.

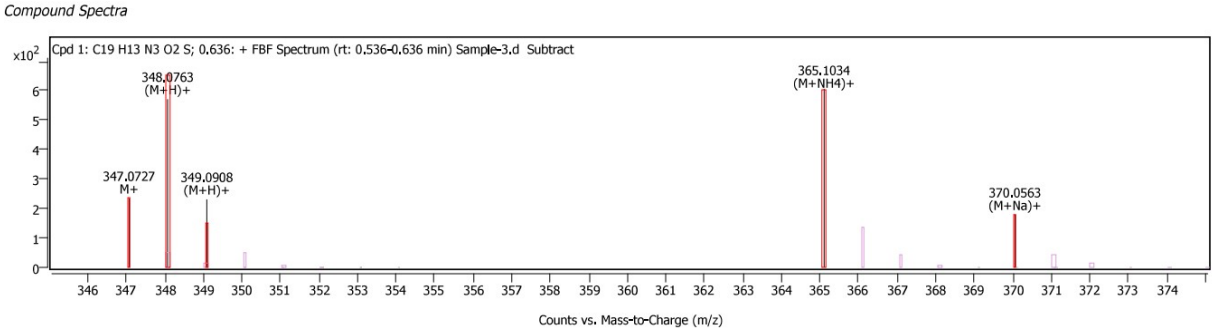

Fig S102: HRMS (ESI$^+$) of **4l** showing [M+H]$^+$ molecular ion peak.

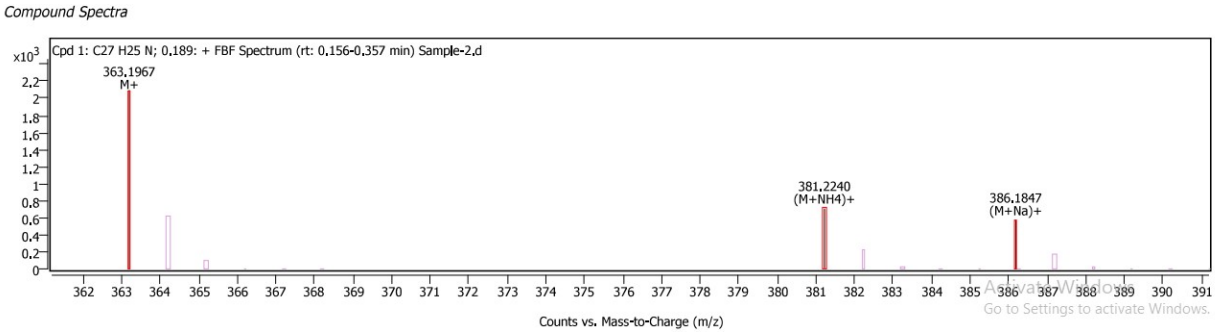

Fig S103: HRMS (ESI$^+$) of **4n** showing [M+H]$^+$ molecular ion peak.

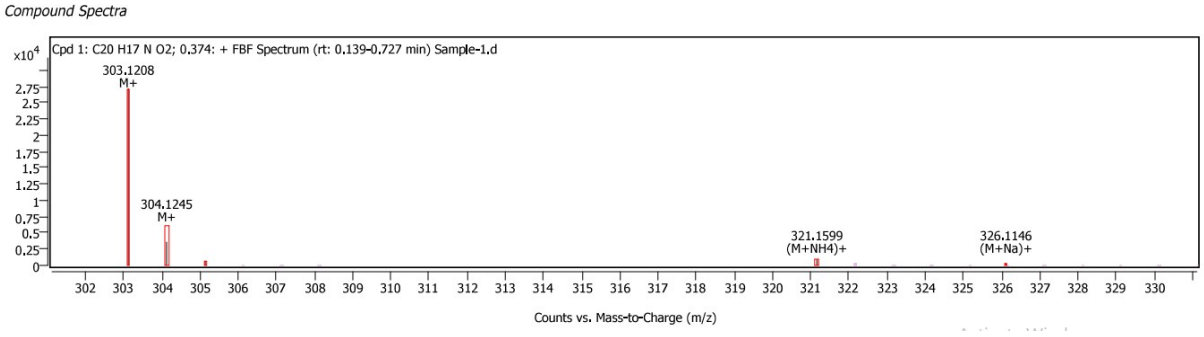

Fig S104: HRMS (ESI$^+$) of **5b** showing [M+H]$^+$ molecular ion peak.

9. References

1. S. Das, A. W. Ehlers, S. Patra, B. de Bruin and B. Chattopadhyay, *Journal of the American Chemical Society*, 2023, **145**, 14599-14607.
2. L. Wang, X. Yu, X. Feng and M. Bao, *The Journal of Organic Chemistry*, 2013, **78**, 1693-1698.
3. Y. Wu, X. Peng, B. Luo, F. Wu, B. Liu, F. Song, P. Huang and S. Wen, *Organic & Biomolecular Chemistry*, 2014, **12**, 9777-9780.
4. Z. Liang, J. Zhang, Z. Liu, K. Wang and Y. Zhang, *Tetrahedron*, 2013, **69**, 6519-6526.
5. X. Liu, H. Sheng, Y. Zhou and Q. Song, *Chemical Communications*, 2020, **56**, 1665-1668.
6. S. Mallick, K. Kollimalaian, P. Chetti and V. Parthasarathy, *Chemistry–A European Journal*, 2024, **30**, e202302876.
7. A. Hörner, D. Volz, T. Hagendorn, D. Fürniss, L. Greb, F. Rönicke, M. Nieger, U. Schepers and S. Bräse, *Rsc Advances*, 2014, **4**, 11528-11534.
8. A. s. Aguilar-Granda, M. C. García-González, S. Pérez-Estrada, A. Kozina and B. Rodríguez-Molina, *The Journal of Physical Chemistry C*, 2018, **122**, 27093-27099.
9. Y. Long, Y. Zheng, Y. Xia, L. Qu, Y. Yang, H. Xiang and X. Zhou, *ACS Catalysis*, 2022, **12**, 4688-4695.
10. F. Chen, N. Liu, E. Ji and B. Dai, *RSC Advances*, 2015, **5**, 51512-51523.
11. L. Wang, E. Ji, N. Liu and B. Dai, *Synthesis*, 2016, **48**, 737-750.
12. B. Li, Y. Gong, L. Wang, H. Lin, Q. Li, F. Guo, Z. Li, Q. Peng, Z. Shuai and L. Zhao, *The Journal of Physical Chemistry Letters*, 2019, **10**, 7141-7147.
13. J. K. Kwon, J. H. Cho, Y.-S. Ryu, S. H. Oh and E. K. Yum, *Tetrahedron*, 2011, **67**, 4820-4825.
14. X. Zhao, Y. She, K. Fang and G. Li, *The Journal of Organic Chemistry*, 2017, **82**, 1024-1033.
15. S. Choi, T. Chatterjee, W. J. Choi, Y. You and E. J. Cho, *ACS Catalysis*, 2015, **5**, 4796-4802.
16. T. Yuan, K. Fu and L. Shi, *Organic Chemistry Frontiers*, 2024, **11**, 4529-4538.
17. L. He and Y. Xu, *Advanced Synthesis & Catalysis*, 2022, **364**, 2352-2357.
18. Y. Huang, Z. Guo, H. Song, Y. Liu and Q. Wang, *Chemical Communications*, 2018, **54**, 7143-7146.
19. M. Abid, L. Teixeira and B. Török, *Tetrahedron letters*, 2007, **48**, 4047-4050.
20. B. Urones, R. G. Arrayás and J. C. Carretero, *Organic Letters*, 2013, **15**, 1120-1123.
21. T. Kitawaki, Y. Hayashi, A. Ueno and N. Chida, *Tetrahedron*, 2006, **62**, 6792-6801.
22. G. Li and M. Szostak, *Nature communications*, 2018, **9**, 4165.
23. R. Lu, L. Cao, H. Guan and L. Liu, *Journal of the American Chemical Society*, 2019, **141**, 6318-6324.
24. P. Kumar, P. Pathak and B. Kushwaha, *ORIENTAL JOURNAL OF CHEMISTRY*, 2005, **21**, 565.
25. E. Longhi, J. M. Fernandez-Hernandez, A. Iordache, R. Fröhlich, H.-P. Josel and L. De Cola, *Inorganic Chemistry*, 2020, **59**, 7435-7443.